โคพอลิเมอร์ไรเซชันของเอทิลีนกับแอลฟาโอลิฟินชนิดต่างๆด้วยตัวเร่งปฏิกิริยา Cp_2ZrCl_2/MAO บนตัวรองรับพอลิสไตรีนโคไดไวนิลเบนซีน

นายสมพงษ์ แซ่ต่าง

วิทยานิพนธ์นี้เป็นส่วนหนึ่งของการศึกษาตามหลักสูตรปริญญาวิศวกรรมศาสตรมหาบัณฑิต
สาขาวิชาวิศวกรรมเคมี ภาควิชาวิศวกรรมเคมี
คณะวิศวกรรมศาสตร์ จุฬาลงกรณ์มหาวิทยาลัย
ปีการศึกษา 2555

COPOLYMERIZATION OF ETHYLENE WITH DIFFERENT α–OLEFINS WITH POLY(STYRENE-CO-DIVINYLBENZENE)-SUPPORTED Cp_2ZrCl_2/MAO CATALYST

Mr. Sompong Saetang

A Thesis Submitted in Partial Fulfillment of the Requirements

for the Degree of Master of Engineering Program in Chemical Engineering

Department of Chemical Engineering

Faculty of Engineering

Chulalongkorn University

Academic Year 2012

Thesis Title	COPOLYMERIZATION OF ETHYLENE WITH DIFFERENT α–OLEFINS WITH POLY(STYRENE-CO-DIVINYLBENZENE)-SUPPORTED Cp_2ZrCl_2/MAO CATALYST
By	Ms. Sompong Saetang
Field of Study	Chemical Engineering
Thesis Advisor	Associate Professor Bunjerd Jongsomjit, Ph.D.

Accepted by the Faculty of Engineering, Chulalongkorn University in Partial Fulfillment of the Requirements for the Master's Degree

…… Dean of the Faculty of Engineering

(Associate Professor Boonsom Lerdhirunwong, Dr.Ing.)

THESIS COMMITTEE

…….. Chairman

(Assistant Professor Joongjai Panpranot, Ph.D.)

…….……. Thesis Advisor

(Associate Professor Bunjerd Jongsomjit, Ph.D.)

…….. Examiner

(Chutimon Satirapipathkul, Ph.D.)

…….. External Examiner

(Ekrachan Chaichana, Ph.D.)

สมพงษ์ แซ่ต่าง : โคพอลิเมอร์ไรเซชันของเอทิลีนกับแอลฟาโอลิฟินชนิดต่างๆด้วยตัวเร่งปฏิกิริยา Cp_2ZrCl_2/MAO บนตัวรองรับพอลิสไตรีนโคไดไวนิลเบนซีน (COPOLYMERIZATION OF ETHYLENE WITH DIFFERENT α–OLEFINS WITH POLY(STYRENE-CO-DIVINYLBENZENE)-SUPPORTED Cp_2ZrCl_2/MAO CATALYST) อ. ที่ปรึกษาวิทยานิพนธ์หลัก : รศ.ดร.บรรเจิด จงสมจิตร, 88 หน้า

ศึกษาการใช้พอลิสไตรีนโคไดไวนิลเบนซีนเป็นตัวรองรับสำหรับตัวเร่งปฏิกิริยา Cp_2ZrCl_2/MAO เพื่อโคพอลิเมอร์ไรเซชันของเอทิลีน/แอลฟา-โอลิฟิน โดยมีวัตถุประสงค์เพื่อหาผลความยาวโซ่ของโคมอนอเมอร์และอัตราส่วนระหว่างเอทิลีน/แอลฟา-โอลิฟินที่มีผลต่อความว่องไวของตัวเร่งปฏิกิริยาและคุณสมบัติของพอลิเมอร์ที่ได้ ปฏิกิริยาโคพอลิเมอร์ไรเซชันของเอทิลีน/แอลฟา-โอลิฟินจะถูกสังเคราะห์ในถังปฏิกรณ์เซมิแบทที่เป็นโลหะเหล็กกล้าไร้สนิทขนาด 100 มิลิลิตรซึ่งถูกกระตุ้นด้วยตัวเร่งปฏิกิริยาร่วม MAO ที่อุณหภูมิ 70 องศาเซลเซียลและทำการป้อนเอทิลีนที่ความดัน 6 ปอนด์ต่อตารางนิ้วที่มีชนิดและความเข้มข้นของโคมอนอเมอร์แตกต่างกัน ผลจากการวิเคราะห์ด้วยการสแกนนิงอิเล็กตรอนไมโครสโคปี พบว่าชนิดของตัวว่องไวจะอยู่บนพื้นผิวและกระจายตัวสม่ำเสมอตลอดทั่วอนุภาค ความว่องไวของเอทิลีน/แอลฟา-โอลิฟินโคพอลิเมอร์ไรเซชันเพิ่มขึ้นเมื่อความเข้มข้นของโคมอนอเมอร์เพิ่งสูงขึ้นจนกระทั่งถึงจุดสูงสุดและจากนั้นก็เริ่มลดลงเมื่อเพิ่มความเข้มข้นของโคมอนอเมอร์ อย่างไรก็ตามมีความยาวโซ่ของโคมอนอเมอร์และอัตราส่วนระหว่างเอทิลีน/แอลฟา-โอลิฟินมีผลกระทบต่อความว่องไวและโปร์ไฟล์ความว่องไวของโคพอลิเมอร์ไรชันเพียงเล็กน้อย คุณสมบัติของโคพอลิเมอร์ที่ผลิตได้ถูกตรวจสอบโดยใช้สแกนนิงอิเล็กตรอนไมโครสโคปี นิวเคลียร์แมกเนติกเรโซแนนซ์และดิฟเฟอร์เรนเชียลสแกนนิงคาลอรีเมทรี จากผลของนิวเคลียร์แมกเนติกเรโซแนนซ์และดิฟเฟอร์เรนเชียลสแกนนิงคาลอรีเมทรี พบว่าโคพอลิเมอร์ทั้งหมดมีการกระจายตัวเหมือนกันโดยส่วนใหญ่จะเป็นแบบ [EEE] และความเป็นผลึกของโคพอลิเมอร์จะลดลงเมื่อความเข้มข้นของโคมอนอเมอร์เพิ่มขึ้น

ภาควิชา วิศวกรรมเคมี ลายมือชื่อนิสิต .....

สาขาวิชา วิศวกรรมเคมี ลายมือชื่อ อ.ที่ปรึกษาวิทยานิพนธ์หลัก .....

ปีการศึกษา 2555

5370661021 : MAJOR CHEMICAL ENGINEERING

KEYWORDS : ETHYLENE COPOLYMERIZATION/ METALLOCENE CATALYST/POLY(STYRENE-CO-DIVINYLBENZENE)

SOMPONG SAETANG : COPOLYMERIZATION OF ETHYLENE WITHDIFFERENT α-OLEFINS WITH POLY(STYRENE-CO-DIVINYLBENZENE)-SUPPORTED Cp_2ZrCl_2/MAO CATALYST

ADVISOR : ASSOC. PROF. BUNJERD JONGSOMJIT, Ph.D., 88 pp.

The study reveals the use of poly(styrene-co-divinylbenzene) as a support for Cp_2ZrCl_2/MAO catalyst for copolymerization of ethylene/α-olefins. It was aimed to determine the effect of comonomer chain length and ethylene/α-olefin ratios on the catalytic activity and properties of the polymer. Ethylene/α-olefins copolymerization reactions were carried out in a 100 mL semi-batch stainless steel autoclave reactor, activated by MAO cocatalyst at 70 °C and 6 psi of ethylene pressure at various initial comonomer type and comonomer concentrations. From the analysis of the resulting support particles by SEM, it was found that the active species are located on the particle surface and they have uniformly distributed throughout the particles. The activities of ethylene/α-olefin copolymerization increased with the increase of the comonomer concentration until the maximum was reached and then started to decrease with further increase of comonomer concentration. Moreover, The length of the chain of the comonomer and comonomer concentration had little effect on activities and activity profiles of copolymerization. The properties of copolymers produced were characterized by means of SEM, ^{13}C NMR and DSC. Based on ^{13}C NMR and DSC, all copolymer exhibited the similar distribution having the majority for the triad of EEE and melting temperature decreased slightly with increasing comonomer concentration.

Department : Chemical Engineering Student's Signature .....

Field of Study : Chemical Engineering Advisor's Signature .....

Academic Year : 2012

ACKNOWLEDGEMENTS

The author would like to express my greatest gratitude and appreciation to Associate Professor Dr. Bunjerd Jongsomjit, my thesis advisor, for his invaluable suggestions, guidance, and useful discussions throughout this research. His advices are always worthwhile and without him this work could not be possible.

I would like to thank Associate Professor Dr. Joongjai Panpranot, as the chairman, Dr. Ekrachan Chaichana as the external examiner, Dr. Chutimon Satirapipathkul as the examiner of the thesis for their valuable guidance and revision throughout my thesis.

I would like to thank Ms.Mingkwan Wannaborworn, Ms.Sasiradee Jantasee, Ms. Arunrat Kitchareon, and Mr. Therdthai Therdjittoam for their helpful suggestions and patience to correct my thesis and paper manuscript writings.

I wish to thank the member of the Center of Excellence on Catalysis and Catalytic Reaction Engineering, Department of Chemical Engineering, Faculty of Engineering, Chulalongkorn University for their assistance and encouragement.

Finally, I would like to extremely express my highest gratitude to my parents for their unconditional love and their support throughout my study.

CONTENTS

Page

ABSTRACT (THAI) iv

ABSTRACT (ENGLISH) v

ACKNOWLEDGEMENTS vi

CONTENTS vii

LIST OF TABLES ix

LIST OF FIGURES x

CHAPTER I : INTRODUCTION 1

CHAPTER II : **THEORY AND LITERATURE REVIEWS** 4

2.1 Classification of polyethylene 4

2.2 Metallocene catalyst 5

2.3 Heterogeneous metallocenec catalyst 8

2.4 Copolymerization 11

2.5 Polystyrene 13

CHAPTER III : EXPERIMENTAL 17

3.1 Objectives of This Thesis 17

3.2 Scopes of This Thesis 17

3.3 Benefits 17

3.4 Research Methodology 18

3.5 Chemicals 19

3.6 Equipments 20

3.7 Preparation of supported MAO 24

3.8 Copolymerization of ethylene/α-olefin 24

3.9 Characterization 25

CHAPTER IV : RESULTS AND DISCUSSION 27

4.1 Characterization of support 27

4.1.1 Characterization of support with SEM and EDX 27

Page

4.1.1 Characterization of support with TGA 29
4.2 Characteristic and catalytic properties of ethylene/α-olefin copolymerization 30
4.2.1 Characterization The effect of various α-olefins and ratios between ethylene/α-olefin on the catalytic activity 30
4.2.2 Characterization The effect of various α-olefins and ratios between ethylene/α-olefin on the catalytic activity profile 32
4.2.3 Characterization The effect of various α-olefins on morphologies of copolymers 33
4.2.4 Characterization The effect of various α-olefins and ratios between ethylene/α-olefin on incorporation of copolymers 36
4.2.5 Characterization The effect of various ratios between ethylene/α-olefin on melting temperatures of copolymers 37
CHAPTER V : CONCLUSIONS AND RECOMMENDATION 39
5.1 Conclusions 39
5.2 Recommendation 40
REFERENCES 41
APPENDICES 48
APPENDIX A 49
APPENDIX B 52
APPENDIX C 68
APPENDIX D 86
VITAE 88

LIST OF TABLES

Page

Table 3.1 Chemicals will be used in experiments……..…..…19

Table 4.1 Copolymerization activity of ethylene/α-olefin……..…….30

Table 4.2 ^{13}C-NMR analysis of ethylene/ α-olefin copolymer……..……..36

Table 4.3 Melting temperature of copolymers obtained upon different α-olefin……..……37

LIST OF FIGURES

Page

Figure.1 Structures structures of different types of polyethylene 5

Figure.2 Structure of metallocene used for olefin polymerization 6

Figure.3 Mechanism formation of the active center for Cp_2ZrCl_2/MAO catalyst system 8

Figure 3.1 Glove box schematic diagram 20

Figure 3.2 Schlenk line 21

Figure 3.3 Schlenk tube 22

Figure 3.4 Vacuum pump 22

Figure.3.5 Inert gas purification 23

Figure 3.6 Slurry phase polymerization diagram 24

Figure 4.1 SEM/EDX of MAO supported onto PS 28

Figure 4.2 A typical spectrum of the supported MAO from EDX analysis used to measure $Al_{[MAO]}$ concentration on PS supports 28

Figure 4.3 TGA profile of MAO on PS support 39

Figure 4.4 Activity profiles for various α-olefins with ratio between ethylene/α-olefin 1:0.5 in copolymerization 33

Figure 4.5 Activity profiles for various ratios between ethylene/1-hexene in copolymerization 33

Figure 4.6 SEM micrographs of copolymers obtained from various ethylene/α-olefin 35

Figure A-1 Activity profiles for various ratios between ethylene/1-octene incopolymerization 50

Figure A-2 Activity profiles for various ratios between ethylene/1-dodecene incopolymerization 50

Figure A-3 Activity profiles for various ratios between ethylene/1-tetradecene incopolymerization 51

Figure A-4 Activity profiles for various ratios between ethylene/1-octadecene incopolymerization 51

Page

Figure B-1 ^{13}NMR spectra of ethylene/1-hexene copolymer at ratio 1:0.25……...……53
Figure B-2 ^{13}NMR spectra of ethylene/1-hexene copolymer at ratio 1:0.50……...54
Figure B-3 ^{13}NMR spectra of ethylene/1-hexene copolymer at ratio 1:0.75……...55
Figure B-4 ^{13}NMR spectra of ethylene/1-octene copolymer at ratio 1:0.25……...……56
Figure B-5 ^{13}NMR spectra of ethylene/1-octene copolymer at ratio 1:0.50……...57
Figure B-6 ^{13}NMR spectra of ethylene/1-octene copolymer at ratio 1:0.75……...58
Figure B-7 ^{13}NMR spectra of ethylene/1-dodecene copolymer at ratio 1:0.25……...59
Figure B-8 ^{13}NMR spectra of ethylene/1-dodecene copolymer at ratio 1:0.55……...60
Figure B-9 ^{13}NMR spectra of ethylene/1-dodecene copolymer at ratio 1:0.75……...61
Figure B-10 ^{13}NMR spectra of ethylene/1-tetradecne copolymer at ratio 1:0.25……...62
Figure B-11 ^{13}NMR spectra of ethylene/1-tetradecne copolymer at ratio 1:0.50……...63
Figure B-12 ^{13}NMR spectra of ethylene/1-tetradecne copolymer at ratio 1:0.75……...64
Figure B-13 ^{13}NMR spectra of ethylene/1-octadecne copolymer at ratio 1:0.25……...65
Figure B-14 ^{13}NMR spectra of ethylene/1-octadecne copolymer at ratio 1:0.50……...66
Figure B-15 ^{13}NMR spectra of ethylene/1-octadecne copolymer at ratio 1:0.75……...67

Page

Figure C-1 DSC curve of polyethylene no comonomer 69
Figure C-2 DSC curve of ethylene/1-hexene copolymer at ratio 1:0.25 70
Figure C-3 DSC curve of ethylene/1-hexene copolymer at ratio 1:0.50 71
Figure C-4 DSC curve of ethylene/1-hexene copolymer at ratio 1:0.75 72
Figure C-5 DSC curve of ethylene/1-octene copolymer at ratio 1:0.25 73
Figure C-6 DSC curve of ethylene/1-octene copolymer at ratio 1:0.50 74
Figure C-7 DSC curve of ethylene/1-octene copolymer at ratio 1:0.75 75
Figure C-8 DSC curve of ethylene/1-dodecene copolymer at ratio 1:0.25 76
Figure C-9 DSC curve of ethylene/1-dodecene copolymer at ratio 1:0.50 77
Figure C-10 DSC curve of ethylene/1-dodecene copolymer at ratio 1:0.75 78
Figure C-11 DSC curve of ethylene/1-tetradecene copolymer at ratio 1:0.25 79
Figure C-12 DSC curve of ethylene/1-tetradecene copolymer at ratio 1:0.50 80
Figure C-13 DSC curve of ethylene/1-tetradecene copolymer at ratio 1:0.75 81
Figure C-14 DSC curve of ethylene/1-octadecene copolymer at ratio 1:0.25 82
Figure C-15 DSC curve of ethylene/1-octadecene copolymer at ratio 1:0.50 83
Figure C-16 DSC curve of ethylene/1-octadecene copolymer at ratio 1:0.75 84

CHAPTER I

INTRODUCTION

Polyolefin is synthetic polymeric materials, which rule the market. It is estimated that approximately 65 million tons of polyethylene (PE) and 40 million tons of polypropylene (PP) are produced annually worldwide. The success of polyolefin is logically explained as this polymer family is found in the majority of industrial domains including films, packaging, machinery parts, electrical insulators, inks, petroleum additives, and hot melt adhesives to name but a few, since one can mention their low cost, chemical inertness, mechanical properties, absence of potential toxicity, and processability. Polyolefins can replace more expensive materials, include materials that are associated with health and environmental risks. The growth of polyolefin may be expected to continue at a rate of around 5% in the near few years, because only a few materials can match their versatility and economy [1].

Nowadays, polymers play a significant role in many applications, especially linear low-density polyethylene (LLDPE). The LLDPE has been used to produce many products such as shopping bags, food packaging film, plastic pipe and house appliances, etc. Therefore, it has many properties such as low density, good mechanical and easy fabrication and recycling. [2-4]. When compared LLDPE with the other polymer, it is very desirable. For the production of LLDPE to better activity for the catalyst system, the polymer can be synthesized by the copolymerization of ethylene and short chain 1-olefins (comonomer), namely 1-hexene, 1-octene and 1-decene. A low pressure slurry process, the gas phase process and the solution-phase process [5] can be produced for LLDPE. The main of LLDPE are produced extensive using the metallocene catalyst system, since many types of comonomer can incorporate with that catalysts. Moreover, it can give a narrow molecular weight distribution. Thus, there has been an increase in research and development on the synthesis of the LLDPE using metallocene catalysts [6,7].

The polyolefin field has undergone with the development of single-site catalysts referred to metallocenes, followed by post-metallocenes, which helping to improved the synthesis of polyolefin-based materials. Metallocene catalysts have been and are still the topic of significant research in industries. However, the cost and the use of methylaluminoxane (MAO) as the main co-catalyst of metallocenes and post-metallocenes in large excess relative to the catalyst ([MAO]/[Cat] > 1000 under homogeneous conditions) are limitations to the development of these catalysts at an industrial scale.

Therefore, metallocenes need to be supported to fulfill the existing industrial production process of polyolefins. This heterogenization enables control of the morphology of the polyolefins. Controlling particle growth eliminates reactor fouling and produces polymer particles with shapes as well as the catalyst particles.In this way, it has been shown that ratio of MAO can be extremely reduced compared to homogeneous system in order to optimize the performance of the catalyst. Hence, supported catalyst should keep the characteristics of single-sites under homogeneous conditions. The distribution of active sites at the interior and the surface of the support is another important parameter. Indeed, support fragmentation occurring during polymerization gives access to new active sites [8].

There have been reported about single-site catalyst in heterogenization system. They mainly consider the use of inorganic-based supports such as silica, alumina or magnesium chloride [9–11]. However, these supports meet several drawbacks, including the need for complex chemical treatments to get the appropriate particle morphology and the presence of residual inorganic fragments within the produced polyolefins that may affect their mechanical and optical properties. Nowadays, more and more attention is paid to the design and the use of organic supports [12]. Organic supports have significant advantages over their inorganic supports: they do not require fastidious preparation and pre-treatment, and can be easily functionalized to accommodate the metallocene catalyst. Unlike inorganic supports, the organic residues should not significantly affect the final polyolefin properties.

Organic supports for metallocenes are mainly based on polystyrene (PS) because of its well defined structure, ready availability, and incorporation into the product polymer [13]. As solid beads crosslinked with divinylbenzene (DVB), however, PS is often hindered in fragmentation. It is therefore necessary for PS to be improved to meet the requirements for metallocene supports [14]. Modified poly(styrene-co-divinylbenzene) beads have been used widely as organic carriers for immobilizing metallocene catalysts. The metallocene immobilized on the crosslinked polystyrene exhibited good activity, and a polyolefin with the desired morphology was obtained. The reversibly crosslinked networks of polystyrene facilitate carrier fragmentation during polymerization [15].

In this work, the effects of comonomer chain length and ratio of ethylene/comonomer on polymerization activity and properties of the resulting copolymer were investigated. The synthesis of the PE was performed by copolymerization of ethylene with different α–olefins via poly(styrene-co-divinylbenzene) supported Cp_2ZrCl_2/MAO catalyst.

CHAPTER II

THEORY AND LITERATURE REVIEWS

2.1 Classification of Polyethylene

Polyolefins dominate the market of synthetic polymeric materials. It is estimated that approximately 65 million tons of polyethylene (PE) is produced annually worldwide. The success of polyolefins is logically explained as this polymer family is found in the majority of industrial domains including films, packaging, machinery parts, electrical insulators, inks, petroleum additives, and hot melt adhesives to name but a few. Among the reasons for the important utilization of these materials, one can mention their low cost, chemical inertness, mechanical properties, absence of potential toxicity, and processability. Polyolefins can replace more expensive materials, as well as materials that are associated with health and environmental risks. Their growth is expected to continue at a rate of around 5% in the near future, because only a few materials can match their versatility and economy.

Polyethylene is categorized based primary on their density and branching structure. In addition, depending on the polymerization method used in polymerization of ethylene, several types of polyethylene with different properties can be obtained. Furthermore, the mechanical properties depend upon various variables such as the extent and type of branching, crystal structure and molecular weight. Also, the melting point and glass transition temperature depend on these variables and vary significantly with the type of polyethylene. There are different types of polyethylene and the most important types are LLDPE, HDPE and LLDPE. These different types are based on the structure of the Polyethylene molecule, which affects its density and the name. The structures of different types of polyethylene are shown in Figure 1.

In LDPE some of the carbon atoms are attached to three carbon atoms instead of two, this causes a branch on which other polyethylene chains are attached. These branches are long and link with other polyethylene molecules. LDPE has long molecules with a lot of molecules attached to the origin one.

HDPE is a more linear molecule where there are fewer branches, and these branches are usually short compared to LDPE. If the previous molecules are changed, it would introduce variety of properties that are intermediate between LDPE and HDPE. It has a large number of branches; however these branches are shorter. The operation conditions can control and vary the mechanical, chemical, electrical and thermal properties

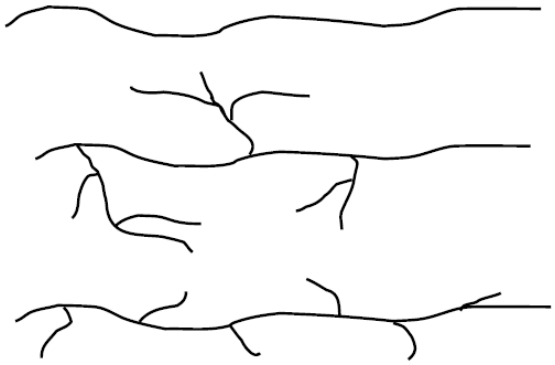

Figure.1 Structures structures of different types of polyethylene: (a) HDPE, (b) LDPE, (c) LLDPE [16].

The polymer commonly known as LLDPE is a copolymer produced by copolymerization ethylene with α-olefin such as propylene, 1-butene, 1-hexene and 4methy-1-pentene. LLDPE possesses a linear molecular structure with SCB distributed nonuniformly along the backbone of polyethylene chain. The amount and distribution of SCB has a profound effect on the thermal, physical, and mechanical properties of LLDPE. The diversity of various LLDPE grades is primarily a result of variations in distribution of molar mass and short chain branches.

2.2 Metallocene catalyst

Metallocene catalysts are discrete molecules that have two cyclic ligands bonded to a central transition metal atom. These compounds have been named “sandwich complexes”, if organometallic compounds bearing only one Cp-ligand are known as “half sandwich complexes”. The term metallocene called “single site catalyst” (one type of active site) often used for olefin polymerization.The

single site catalyst mean catalyst produce polymers with narrow molar mass distribution [17]. The structure of metallocene is show by Figure 2.

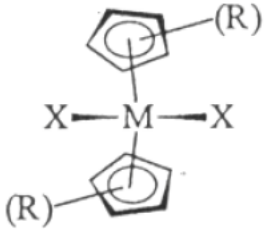

When

M is group 4, 5, 6 transition metal (normally Ti, Zr and Hf).

X is chlorine or other halogens from group 7 or an alkyl group.

R is hydrocarbyl substituents or fused ring sytems.

Figure.2 Structure of metallocene used for olefin polymerization [18].

Metallocene complexes are become an important class of polymerization catalyst in research and industail area since it have many advantage in polymerization such as [19]

- The homogeneous nature of catalyst provides the active sites that have the great number of activity in olefin polymerization. Comparison to conventional Ziegler-Natta catalyst or Philips catalyst, it was found that metalocene complex gave the higher activity about 100 times.
- Metallocene catalysts have ability to control the stereoregurarity (isotactic, atactic, syndiotactic and hemitactic polypropylene) of the polymer produced from prochiral olefins, such as propylene.
- According from the narrow molecular weight distribution of polymer about 1-2,we can call metallocene catalyst as single site catalyst.
- Their potential for producing polyolefin with regularly distributed short and long chain branches in the polymer chain. These parameter determine the properties of new materials for applications i.e. LLDPE and thus generate new markets.

- Heterogeneous catalyst provide the different active sites than those in solution and can have an enormous effect on catalyst activity and the properties of the produce polyolefin in term of molecular weights, branching and stereospecificity.

Cp_2ZrCl_2 and its derivatives are excellent Ziegler–Natta catalysts having high potential in practical applications [20-21] to produce polyolefin with defined microstructures and narrow molecular weight distributions [22]. Three challenges are foci for development of new metallocene catalysts [23]: (i) increasing productivity to lower the catalyst cost, (ii) fitting catalyst systems and compositions to existing polymerization processes (gas phase, slurry or solution) by way of heterogenization (for the first two cases), and (iii) developing a wider range of polymers and copolymers with improved physical properties (e.g., processability, mechanical, and optical properties) to control molecular weight, molecular weight distribution, and the incorporation of co-monomer and molecular polymer chain architecture. Therefore, it is necessary to modify metallocene catalysts in order to produce polyolefins with wider molecular weight distributions and avoid blending polyolefins for better performance [24].

Metallocene catalysts have to be activated by a cocatalyst such as alkylaluminums including methylaluminoxane (MAO), triethylaluminum (TMA), triethylaluminum (TEA), triisobutylaluminum (TIBA), and cation forming agents [25]. Among these, MAO is a very effective cocatalyst for metallocene. It is generally assumed that the function of MAO is firstly to undergo a fast ligand exchange reaction with the metallocene dichloride, thus, rendering the metallocene methyl and dimethylaluminum compounds [26-28]. The primary reaction step for the formation of active center is methylation of the transition metal compound by MAO show by Figure 3.

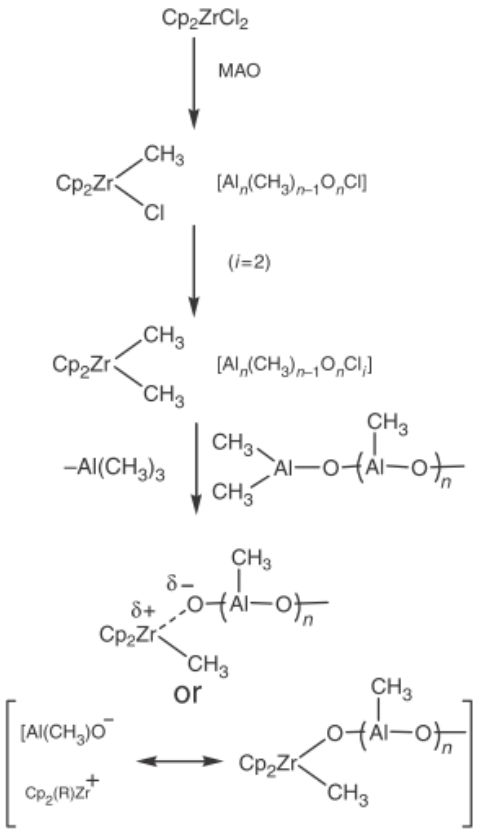

Figure.3 Mechanism formation of the active center for Cp_2ZrCl_2/MAO catalyst system [29].

2.3 Heterogeneous metallocene catalyst

Due to the fact,metallocene catalyst are not suitable for industrial olefin polymerization system. Support metallocene catalysts are developed to overcome this disadvantage. Most of the supported metallocenes have exhibited lower catalytic activities in comparison to the homogenous system [30]. The reduction of catalytic activity has been attributed to three reasons:

- The metallocene complexes are deactivated during the impregnating process.
- The metallocene complexes inadequate react to the cocatalyst (MAO) and hindering its activation.

- The monomers are restricted approach to the active site, there by disappearing the chain propagation.

Although supported catalysts are generally less active than non-supported catalysts, they can be practically used for the existing slurry and gas phase polymerization process. Without using a heterogeneous system, high bulk density and narrow size distribution of polymer particles cannot be achived [31]. The advantages of supported catalytic include improved polymer morphology, avoiding reactor fouling, lower Al/metal mole ratios required to obtain the maximum activities in some cases the elimination of the use of MAO, and improved stability of the catalyst due to much slower deactivation by bimolecular catalyst interaction. In order to heterogenize metallocene the most commonly employ an innocuous carrier for catalyst such as silica, alumina and magnesium chloride. And many supporting materials have been on the research are zeolite, nanocomposite or other organic support.

The main preparatory routes reported in the literature for metallocene immobilization on these supports can be classified according to three main methodologies, as follows [32]:

- The first method involves direct impregnation of metallocene on the support

  (modified by previous treatment or not). This can be done either (a) with mild impregnation conditions or (b) at high temperatures and long impregnation times (refined route).
- The second method involves immobilization of MAO on the support followed by reaction with the metallocene compound. A modified version of this method involves the replacement of MAO by an aluminum alkyl.
- The third method involves immobilization of aryl ligands on the support followed by addition of a metal salt such as zirconium halide; recently, titanium and neodymium halides have also been used to form the attached metallocene.

A large number of studies have been devote to the transformation of soluble metallocene complexes into heterogeneous catalysts by supporting then on inorganic or organic carriers [33-34]. Surface modification of the support can also be applied to improve the catalyst's performances. Modification may include reaction of the support with organometallic compounds as well as thermal treatments; the nature of support and the technique used for supporting the metallocene have a crucial influence on the resulting catalytic behavior and polymer properties.

Steinmetz et al. [35] examined the particle growth of polypropylene made with a supported metallocene catalyst using scanning electron microscopy (SEM).They noticed formation of a polymer layer only on the outer surface of catalyst particles during the initial induction period. As the polymerization continued, the whole particle was filled with polymer. Particle fragmentation pattern depended on the type of supported metallocene.

The fragmentation of three different supports has been investigated in the presence of the catalyst $Me_2Si(2MeBenzInd)_2ZrCl_2$: PS beads with hydroxymethyl groups, commercially available (100 μm) and prepared (~80 nm) by mini-emulsion, and nanoporous silica beads (50–60 μm) [36]. After treatment with the MAO/metallocene catalytic system, aggregation of the nanometric PS support took place, producing beads with an average size of 80–100 μm. Ethylene polymerization performed in the presence of these different supports revealed that the micrometric PS support was the least active (activity = 320 kg PE/(mol Zr h bar)). The highest activity was observed with the one supported on nanometric PS particles (activity = 1500 kg PE/(mol Zr h bar)). In line with the order of activity, no fragmentation took place with the micrometric PS particles, whereas fragmentation of the nanometric PS supports occurred right from the beginning of the polymerization. Fragmentation of the silica support also takes place going from the bead surface to the core.

2.4 Copolymerization

The enhancement of the rate in copolymerization of ethylene with α-olefin has been observed in both homogeneous and heterogeneous catalyst systems. Introducing small amounts of α-olefin, such as 1-hexene and propylene, may increase activity by 50-100% in ethylene polymerization with Cp_2ZrCl_2/MAO catalyst [37]. The comonomer can affected the overall crystallinity, melting point, softening rang, transparency and also structure, thermochemical, and rheological properties of the formed polymer. Copolymer can also be used to enhance mechanical properties by improving the miscibility in polymer blending. This comonomer effect is sometimes linked to the reduction of diffusion limitations by producing a lower crystallinity polymer or to the activation of catalytic site by the comonomer. The polymer molecular weight often decreases with comonomer addition, possibly because of a transfer to comonomer reactions. Heterogenenous polymerization tends to be less sensitive to changes in the aluminum/transition metal ratio. Chain transfer to aluminum is also favored at high aluminum concentrations. This increase in chain transfer would presumably produce a lower molecular weight polymer. In addition, some researcher observed the decrease, and some observed no change in the molecular weight with increasing aluminum concentration [38]

Copolymer based on ethylene with different incorporation of 1-hexene, 1-octene, and 1-decene were investigated by Quijada [39]. The type and the concentration of the comonomer in feed do not have a strong influence on the catalyst activity of the system,but the presence of the comonomer increases the activity compared with that in the absence of it. From ^{13}C-NMR it was found that the size of the lateral chain influences the percentage of comonomer incorporated, 1-hexene being the highest one incorporated. The molecular weight of the copolymers obtained was found to be dependent on the comonomer concentration in the feed, showing that there is a transfer reaction with the comonomer. The polydispersity (Mw/Mn) of the copolymer is rather narrow and dependent on the concentration of the comonomer incorporated.

Soga et al. [40] noted that some metallocene catalysts produce two different type of copolymer in term of crystallinity. They copolymerized ethylene and 1-alkenes using 6 different catalysts such as Cp_2ZrCl_2, Cp_2TiCl_2, Cp_2HfCl_2, $Cp_2Zr(CH_3)_2$, $Et(IndH_4)_2ZrCl_2$ and iPr(Cp)(Flu)$ZrCl_2$. Polymers with bimodal crystallinity distribution (as measured by TREF-GPC analysis) were produced with some catalytic systems. Only Cp_2TiCl_2-MAO and $Et(IndH_4)_2ZrCl_2$-MAO produced polymers that have unimodal crystallinity distribution. The results seem to indicate that more than one active site type are persenet in some of these catalysts. However, it is also possible that unsteady-state polymerization time were very short (5 minutes for most cases).

Marques et al. [41] investigated copolymerization of ethylene and 1-octene by using homogeneous catalyst system based on $Et(Flu)_2ZrCl_2$/MAO. A study was performed to compare this system with that of Cp_2ZrCl_2/MAO. The influence of different support materials for the Cp_2ZrCl_2 was also evaluated, using silica, MgCl2, and the zeolite sodic mordenite NaM. The copolymer produced by the $Et(Ind)_2ZrCl_2$/MAO system showed higher weight and narrow molecular weight distribution, compared with that produced by Cp_2ZrCl_2/MAO system. Because of the extremely congested environment of the fluorenyl rings surrounding chain transference. Moreover, the most active catalyst was the one supported on SiO_2, whereas the zeolite sodic mordenite support resulted in a catalyst that produced copolymer with higher molecular weight and narrower molecular weight distribution. Both homogeneous catalystic system showed the comonomer effect, considering that a significant increase was observed in the activity with the addition of a larger comonomer in the reaction medium.

Soares et al. [42] investigated copolymerization of ethylene and 1-hexene with different catalyst: homogeneous $Et(Ind)_2ZrCl_2$, Cp_2HfCl_2 and $[(C_5Me_4)SiMe_2N(tert\text{-}Bu)]TiCl_2$, the corresponding in situ supported metallocene and combine in-situ support metallocene catalyst (mixture of $Et(Ind)_2ZrCl_2$ and Cp_2HfCl_2 and mixture of $[(C_5Me_4)SiMe_2N(tert\text{-}Bu)]TiCl_2$). They studied properties of copolymers by using ^{13}C-NMR, gel permeation chromatography (GPC) and crystallization analysis fractionation (CRYSTAF) and compared with

the corresponding homogeneous metallocene. The in-situ supported metallocene produced polymers having different 1-hexene fraction, SCBD and MWD. It was also demonstrated that polymers with broader MWD and SCBD can be produced by combining two different in-situ supported metallocenes.

In addition, Soares et al. [43] studied copolymerization of ethylene and 1-hexene with an in-situ supported metallocene catalysts. Copolymer was produced with alkyaluminum activator and effect on MWD and SCBD was examined. They found that TMA exhibited the highest activity while TEA and TIBA had significantly lower activities. Molecular weight distribution of copolymer produced by using the different activator types were unimodal and narrow, however, shot chain branching distributions were very different. Each activator exhibited unique comonomer incorporation characteristic that can produce bimodal SCBD with the use of the single activator. They used individual and mixed activator system for controlling the SCBD of the resulting copolymer while maintaining narrow MWDs.

2.5 Polystyrene

Polystyrene (PS) is the parent polymer of a family of styrene-based plastics which are used for the manufacture of items ranging from furniture and electrical goods, to toys, house wares and a wide variety of packaging. The principal comonomer which is coupled with styrene to form plastics with enhanced physical properties suitable for food packaging is 1,3-butadiene. The resultant plastics are known as the high impact polystyrenes (HIPS). Polystyrene homopolymer, also known commercially as crystal polystyrene, is an amorphous polymer and has the particular properties of high clarity, colourless, hard, but rather brittle with low impact strength. The amorphous nature and other properties, which arise from the aromatic chemical structure and glass transition temperature (Tg) of around 100 °C, differ markedly from those of the polyolefin plastics, such as polyethylene, which are based on aliphatic hydrocarbons and have below ambient glass transition temperatures [44].

The unique physical and chemical properties of polystyrene are responsible for its use in a wide range of applications. Polystyrene is hard and brittle and has a density of 1.050 g/cm^3. It is represented by the chemical formula, C_8H_8. It is made up of three chemical elements, carbon, hydrogen and oxygen. Most of the polystyrene properties are as a result of the unique properties of carbon. It is highly flammable and burns with an orange yellow flame, giving off soot, as a characteristic of all aromatic hydrocarbons. Polystyrene, on oxidation, produces only carbon dioxide and water vapor [44].

Considerable attention has been paid to the immobilization of the catalyst or the co-catalyst on PS-based supports, which has led to the development of numerous preparative routes. Interest in PS is motivated by the low cost of this polymer and to its neutrality during the olefin polymerization process, providing to the active species a polymerization microenvironment close to the one existing under homogeneous conditions. In addition, functionalization of PS supports is rather simple and their molecular architecture can be controlled. To this aim, styrene can either be copolymerized with a functional monomer or the PS backbone can undergo chemical post modifications [8].

Three main methods have been followed to immobilize single-site catalysts, either inside or at the surface of linear or cross-linked polymers, generally polystyrene (PS) or polysiloxane-based organic supports: (i) In-situ synthesis of the catalyst onto the support, (ii) Immobilization of the catalyst on the support chemically modified by an aluminic derivatives (MAO or alkylaluminum derivatives) or another co-catalysts, (iii) Encapsulation of the catalytic system inside the support.

Stork et al. [45] reported the preparation of polystyrene supported zirconocene catalysts and their use in the polymerization of ethylene on Cp_2ZrCl_2/MAO catalyst system. Part of the latter reacts with $CpZrCl_3$ to form Cp_2ZrCl_2 covalently bound to PS and the remaining cyclopentadiene moieties lead to insoluble beads crosslinked by Diels–Alder reaction. They found polyethylene exhibited a high molecular weight in excess of 600,000 for M_w, a relatively

narrow molecular weight distribution (M_w/M_n 2.9-3.4) and morphology of product is isolated as nearly spherical beads.

Copolymerization of ethylene with different incorporation of 1-hexene and 1-dodecene by using polystyrene supported Cp_2ZrCl_2/MAO catalyst were investigated by Wang et al. [46] They observed catalytic activity increase with the Al/Zr ratio up to 2000 for homopolymerization of ethylene. The crosslinked polystyrene-supported metallocene was converted to noncrosslinked species because of the retro-Diels–Alder reaction via MAO. Moreover, the reversible crosslinking of this catalyst system accommodate supports fragmentation during polymerization. Copolymerization of ethylene with α-olefins in the presence of the same PS supported system [47] gives higher catalytic activities higher the ethylene homopolymerization, the positive " comonomer effect" was pappened.

Hong et al. [48] supported rac-$Ph_2Si(Ind)_2ZrCl_2$ catalyst on PS beads using a phenyl group as a spacer and tested by polymerization of ethylene. The catalytic activity in ethylene polymerization increased with temperature at 40°C to 150°C but the spherical shape of polymer disappeared due to the melting in solvent. From the analysis of the resulting polyethylene particles by SEM and EPMA, indicated that active species were located on the surface layer of catalyst particles and uniformly distributed throughout the polymer particle, suggesting that the PS beads also followed the fragmentation process during the polymerization. [50]

A spacer-modified polystyrene support with alcohol functionality was prepared by Barrett and De Miguel [51-52], which using solid-phase organic reaction. The p-nitrosulfonate function was then converted into a peralkylated cyclopentadienyl ligand and reacted with $CpTiCl_3$ to form a metallocene bound to the support via the spacer. This PS-bound titanocene complex showed quite low catalytic activities, but the molecular weight and dispersity are similar to those obtained with soluble titanocene dichloride catalyst. Concerning the morphology, the PE obtained did not copy the spherical shape of the support, but rather, noodle-like PE chain structures were observed. The authors attributed this phenomenon to the presence of very active catalytic centers. The high local

activity of these centers on the PS beads could be due to site-isolation of the active species.

Chan et al. [53] and Gibson and Reed [54] studied effect of amino-functionalised polystyrene supports on imidovanadium for ethylene polymerization catalysts. It can be described here on a model vanadium catalyst system highlight a strategy for covalently attaching transition metal procatalysts to an inert polystyrene support and demonstrate that improved kineticprofiles for the polymerisation of ethylene relative to their unsupported analogues can be obtained. Moreover, the use of MAO instead of DEAC did not lead to a significant increase. Although catalyst deactivation was observed at elevated temperatures, immobilizing the vanadium catalyst on such supports increased the stability of the catalyst with respect to the unsupported complex.

CHAPTER III
EXPERIMENTAL

3.1 Objective of the Thesis

The objective of this work is to investigate the copolymerization of ethylene and various α-olefins and study the effect of comonomer chain length on the catalytic activity and properties of the polymer in the poly(styrene-co-divinylbenzene)-supported Cp_2ZrCl_2/MAO catalyst system.

3.2 Scope of the Thesis

1. Preparation of poly(styrene-co-divinylbenzene) (PS) by impregnation with methylaluminoxane (MAO) cocatalyst.

2. Characterization of PS/MAO supports using SEM/EDX and TGA measurement.

3. Copolymerization of ethylene/α-olefin with different α–olefins over PS supported Cp_2ZrCl_2/MAO catalyst.

4. Copolymerization of ethylene/α-olefin with different molar ratios of ethylene/comonomer via poly(styrene-co-divinylbenzene) supported Cp_2ZrCl_2/MAO catalyst.

5. Characterization of polymer using SEM, DSC and ^{13}C NMR measurement.

3.3 Benefits

1. Poly(styrene-co-divinylbenzene)-supported Cp_2ZrCl_2/MAO catalyst system can be change and improve activities of copolymerization.

2. Understand how the effect of comonomer on catalyst activity and polymer characteristion.

3. This information will be used as a reference for polymer industries and commercial application.

3.4 Research methodology

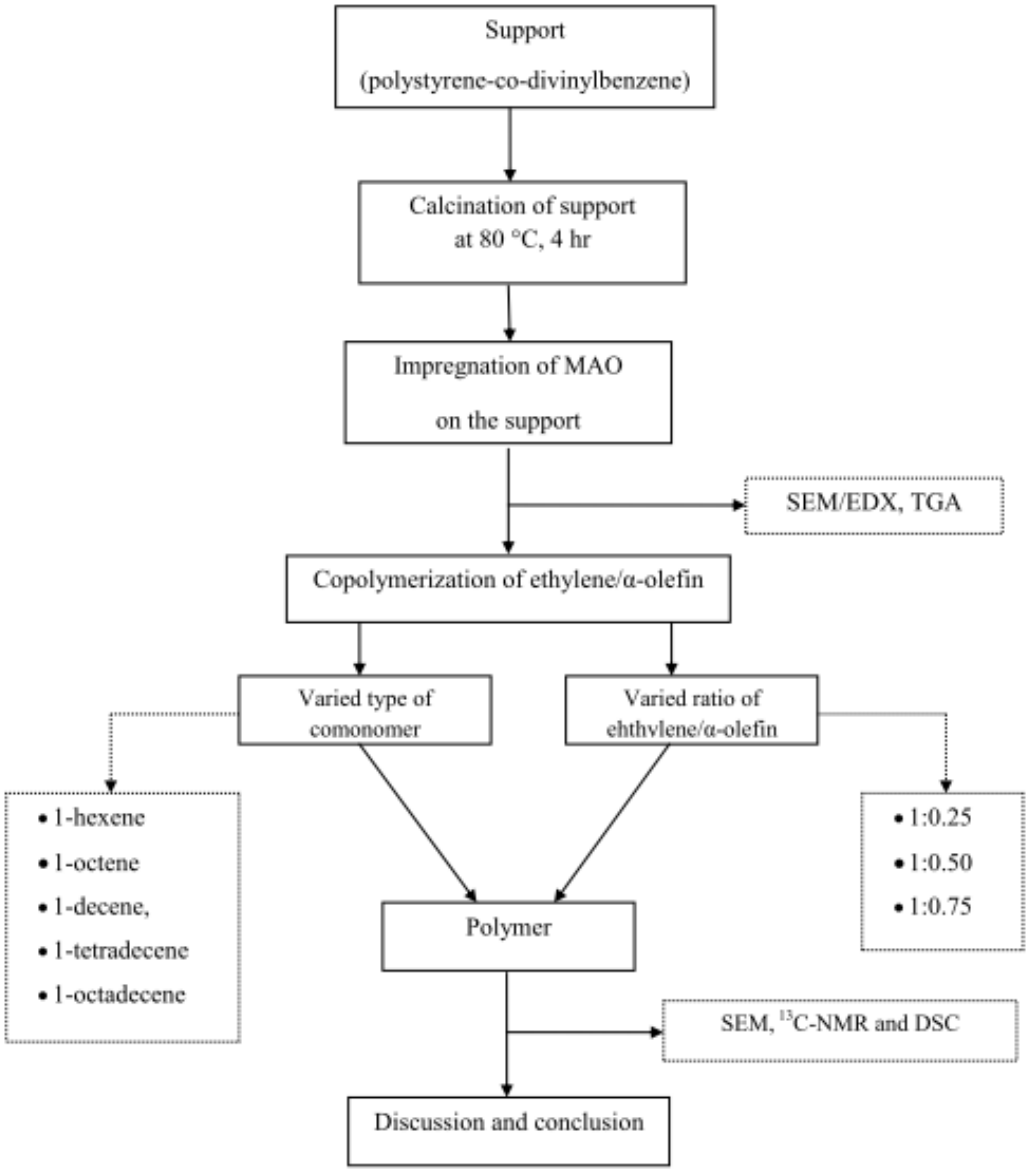

3.5 Chemicals

The chemicals used in these experiments will be employed in this proposed are listed in **Table 3.1** as follows:

Table 3.1 Chemicals will be used in experiments.

No.	Chemicals	**Supplier**	**Details**
1	Ethylene gas	Thai Polyethylene Co., Ltd.	99.9%
2	Bis(cyclopentadienyl) zirconium dichloride	Alrich Chemical Company, Inc.	-
3	Methylaluminoxane	Tosoh Akso, Japan	10% in toluene
4	Poly(styrene-co-divinylbenzene)	Alrich Chemical Company, Inc.	98% styrene – 2% DVB
5	Toluene	EXXON Chemical Ltd., Thailand.	-
6	Argon	Thai Polyethylene Co., Ltd.	99.999%
7	Hydrochloric acid	SR lab	Fuming 36.7%
8	Methanol	SR Lab	commercial grade
9	1-hexene, 1-octene, 1-dodecene,1-tetradecene and 1-octadecene	Alrich Chemical Company, Inc.	99+%

3.6 Equipments

All kinds of equipments were used in the experiments are listed below:

3.6.1 Glove Box

Glove Box System 30905C from Vacuum Atmospheres Company of United States of America was used for preparation of catalyst in order to prevent catalyst deactivation.

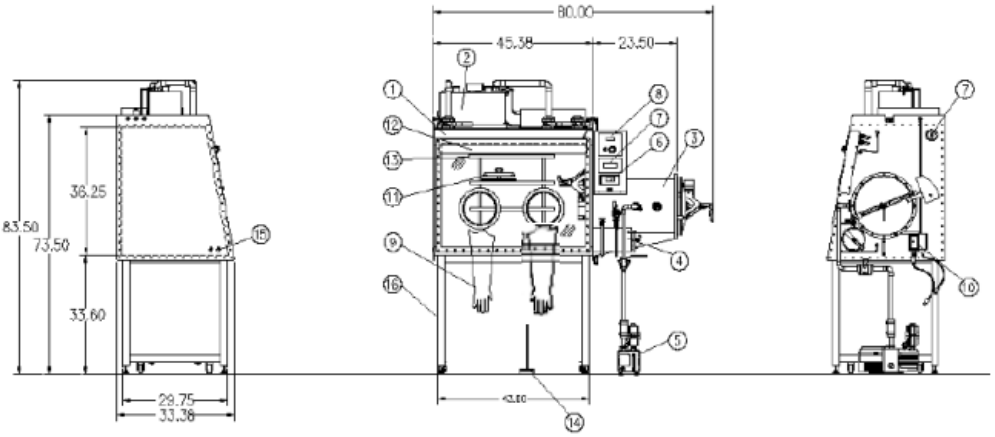

Figure 3.1 Glove box schematic diagram

1. Omni vac chamber
2. Purification unit
3. 15”diax24”lg. antechamber
4. 6”dizx12”lg. mini antechamber
5. Vacuum pump, 4.1cfm
6. Control panel
7. Moisture analysis (Optional)
8. Oxygen analysis (Optional)
9. Butyl rubber glove
10. Electrical J-Box
11. Glove port cover
12. Fluorescent light
13. Shelves
14. Foot switch
15. Feedthru, ¼” NPT, 2 PL
16. Support frame

3.6.2 Schlenk line

Schlenk line composts of two parts, the first part is attached to vacuum system and another part is attached to purified inert gas such as Argon. Vacuum system part is connected with solvent trap in order to trap solvent before pass through vacuum pump. The Argon system is connected with glass tubing contained quartz wool and sodium hydroxide (NaOH), which increase pressure drop before release to atmosphere through oil bubble.

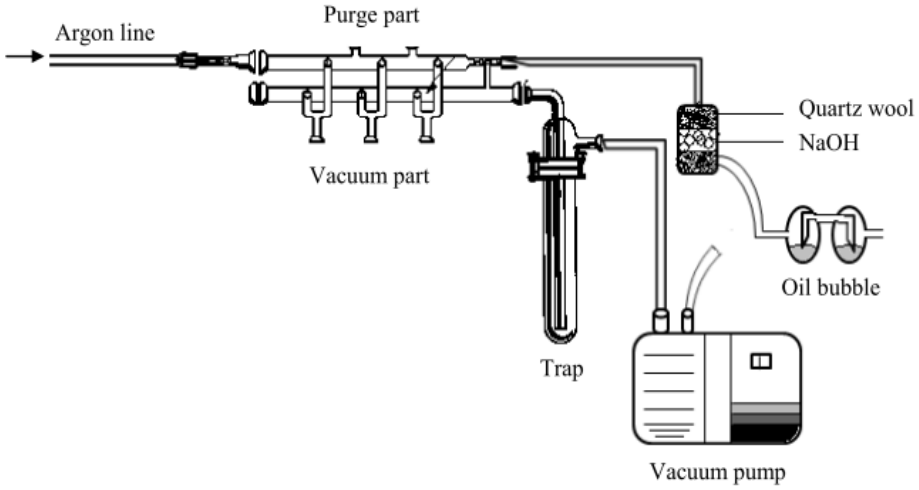

Figure 3.2 Schlenk line

3.6.3 Reactor

Polymerization was carried out in a 100 mL semi-batch stainless steel autoclave reactor equipped with a magnetic stirrer.

3.6.4 Magnetic stirrer and hot plate

Magnetic stirrer and hot plate moded RCT Basic from IKA Labortechnik is used to prepare catalyst solution and mix reactants for polymerization.

3.6.5 Cooling system

Cooling system was used for condense the recently evaporated solvent in distillation system.

3.6.6 Schlenk tube

Schlenk tube consists of ground glass joint connected with side arm. Side arm is three-way glass valve. The sizes of shlenk tube are 50, 100 and 200 ml which used to calcine nanoclay and keep chemicals which are sensitive to oxygen and moisture.

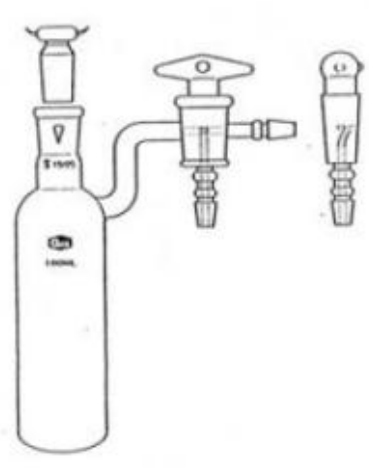

Figure 3.3 Schlenk tube

3.6.7 Vacuum pump

Vacuum pump model 195 from Labconco Coporation was effective 10^{-4}–10^{-3} mmHg pressure. The range of this pressure was enough for vacuum supply to the vacuum line in the schlenk line. Suction port is connected to the chamber or piping to be vacuum-pumped.

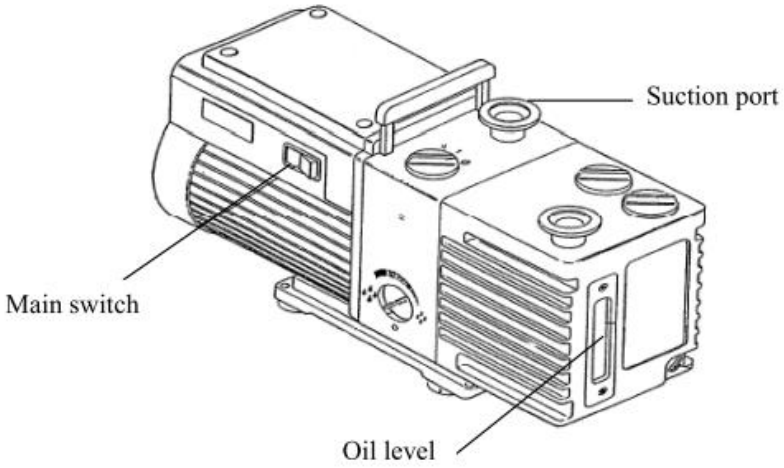

Figure 3.4 Vacuum pump

3.6.8 Inert gas purification system

Argon (Ar) was used in the experiment as inert gas. It was used for preparation of catalyst and polymerization. Argon purification system composts of molecular sieve, columns of BASF catalyst R3-11G, and dehumidify unit.

Molecular sieve was used to remove moisture. BASF catalyst acts as scavenger to remove oxygen contamination in the argon before preparation of catalyst and polymerization, due to high reactivity of catalyst and cocatalyst with oxygen. Dehumidify unit composts of two glasswares which are packed with sodium hydroxide (NaOH) compound and phosphorus pentoxide (P_2O_5) compound, respectively. For the purpose of moisture elimination, it can reduce catalyst deactivation.

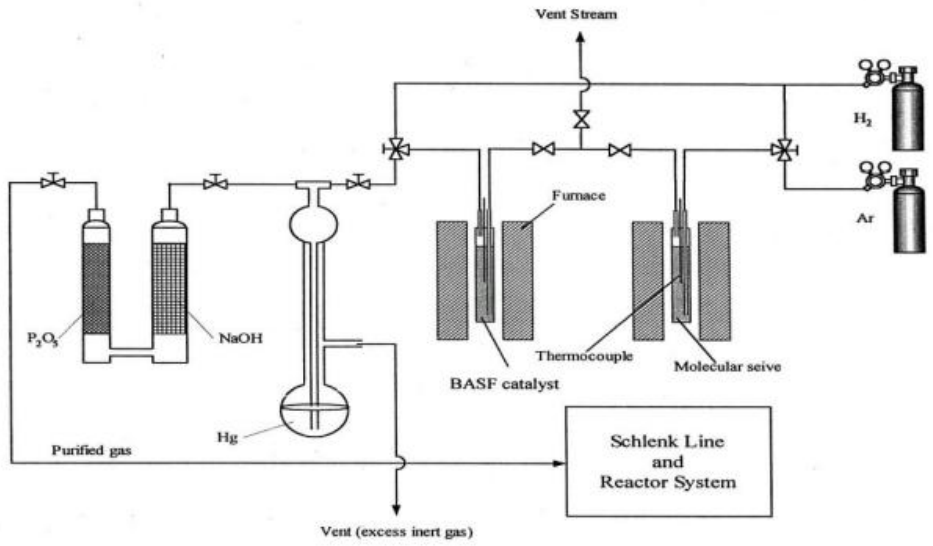

Figure 3.5 Inert gas purification system

3.6.9 Polymerization line

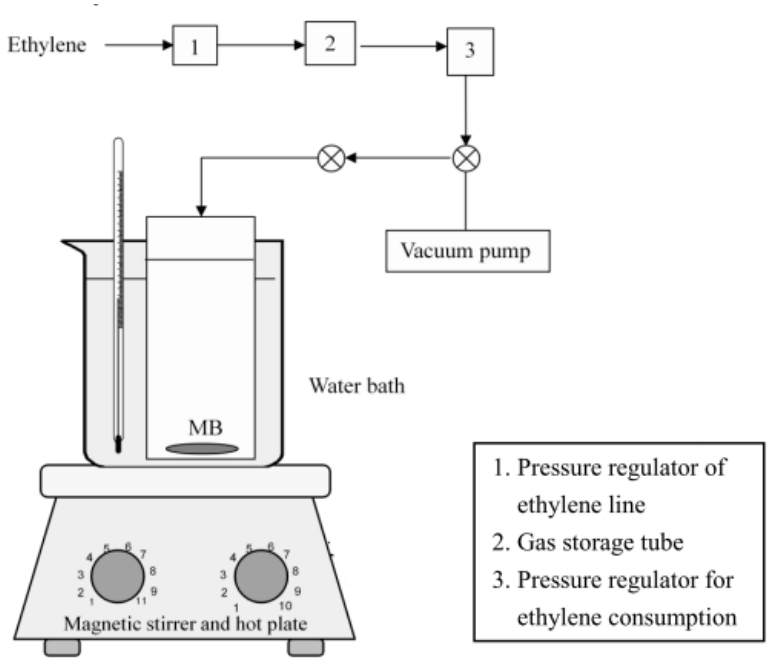

Figure 3.6 Slurry phase polymerization diagram

3.7 Preparation of supported MAO

Commercial poly(styrene-co-divinylbenzene) (PS) heated under vacuum at 80 °C for 4 hr. After that MAO 10 mL impregnated onto PS 1 g in schlenk tube by inject 10 ml of toluene and stirred for 5 hr. Solid part washed 5 times with toluene 10 ml and removed the toluene by drying under vacuum at room temperature to obtain power of supported MAO (PS /MAO).

3.8 Copolymerization of ethylene/α-olefin

The ethylene/α-olefin copolymerization reactions carried out in a 100 mL semi-batch stainless steel autoclave reactor equipped with a magnetic stirrer. At first, the desired amounts of the supported MAO and the toluene [needed to make the total volume of 30 mL] were introduced into the reactor. The desired amount Cp_2ZrCl_2 (5×10^{-5} M) and MAO ($[Al]_{MAO}$ /$[Zr]_{cat}$ = 5200).Then, the reactor was immersed in liquid nitrogen. The followed by addition of the α-olefin into the

frozen reactor. The reactor was heated up to the polymerization temperature at 323 K. By feeding a fixed amount of ethylene (0.018 mole ~ 6 psi) into the reaction mixture, the ethylene consumption can be observed corresponding to the ethylene pressure drop. The reaction of polymerization was terminated by addition of acidic methanol. The time of reaction was recorded for purpose of calculating the activity. The precipitated polymer was washed with methanol and dried at room temperature.

3.9 Characterization

3.9.1 Scanning electron microscopy (SEM) and energy dispersive X-ray spectroscopy (EDX)

SEM and EDX were observe the morphology of copolymer and elemental distribution of $Al_{[MAO]}$ throughout the support particles. The sample will must be conductive to prevent charging by coating with gold particle by ion sputtering device. Sample will be analyzed by JEOL JSM-6400 scanning electron microscopy and energy dispersive X-ray spectroscopy will be analyzed by Link ISIS Series 300 program at Scientific and Technological Research Equipment Center (STREC), Chulalongkorn University.

3.9.2 Differential scanning calorimetry (DSC)

DSC was to determine the thermal properties especially melting temperature (T_m) in term of heat flows associated as a function of time and temperature. Prepare sample about 10-15 mg prior to use. The heating cycle will be run twice. In the first scan, sample will be heated in oder to premelt prior to first used and cooled to room temperature. Then, the sample will be reheated in the second scan. The melting temperature will be determined by a Perkin-Elmer diamond DSC from MEKTEC, at Center of Excellence on Catalysis and Catalytic Reaction Engineering, Chulalongkorn University. The analyses will be proceeded at the heating rate of 20 °C/min in the temperature range of 50-150 °C.

3.9.3 Thermo Gravimetric Analysis (TGA)

TGA was to determine thermal stablility in term of percent weight in sample as a function of temperature. Sample preparation consists of weighing a crucible, loading the sample about 2 to 3 mg into the crucible, weighing the full crucible, and setting it on a tray.Sample will be analyzed by thermo gravimetric, PerkinElmer Thermal Analysis Diamond TG/DTA at Center of Excellence on Catalysis and Catalytic Reaction Engineering, Chulalongkorn University. The analysis will be proceeded under nitrogen atmosphere gas at gas flow rate of 100 mL/min. The sample will be heated form 25°C to 700°C at a constant rate of 10°C/min, and then cooled naturally.

3.9.4 Nuclear Megnetic Resonance (^{13}C NMR)

^{13}C NMR was to evaluated percent insertion of comonomer in polymer. For sample preparation, the comonomer must be solution, in which prepared by using 1,2,4-trichlorobenzene as solvent and chloroform-d for internal lock, then heat until ensure it will be solution. The ^{13}C NMR spectra will be recorded at 110°C using JEOL JNM-A500 operating at 400 MHz.

CHAPTER IV

RESULTS AND DISCUSSION

4.1 Characteristics of support

4.1.1 Characteristics of support with scanning electron microscopy (SEM) and energy dispersive X-ray spectroscopy (EDX)

The morphologies and aluminium (Al) distributions of the supports after impregnation with MAO were determined using SEM and EDX, respectively. The distribution of Al can be identified using the EDX mapping as shown in **Figure 4.1 (a1., a2.),** indicating that Al element representing the active species was distributed on the surface layer uniformly throughout the PS beads. The SEM of the PS supported MAO is shown in **Figure 4.1(b.)** showing that the spherical shape of supports was mainly observed. The typical measurement curve for the quantitative analysis using EDX is shown in **Figure 4.2,** evaluating average Al concentration on PS supports.

The PS beads used in the present study can be justified as microporous PS beads. Good solvents may create micropores, but removal of solvent or non-solvent should collapse the pores. The active species are located on the surface layer of catalyst particles, and uniformly distributed throughout the polymer particles, whereas the cores of PS beads lack a potential active species, were not disintegrated during polymerization. Since the content of divinylbenzene in PS beads was very low (2%), the mechanical strength of catalyst particles was not so high. As a result, some polymer and catalyst particles were fractured during the preparation of sample for SEM analysis.[53]

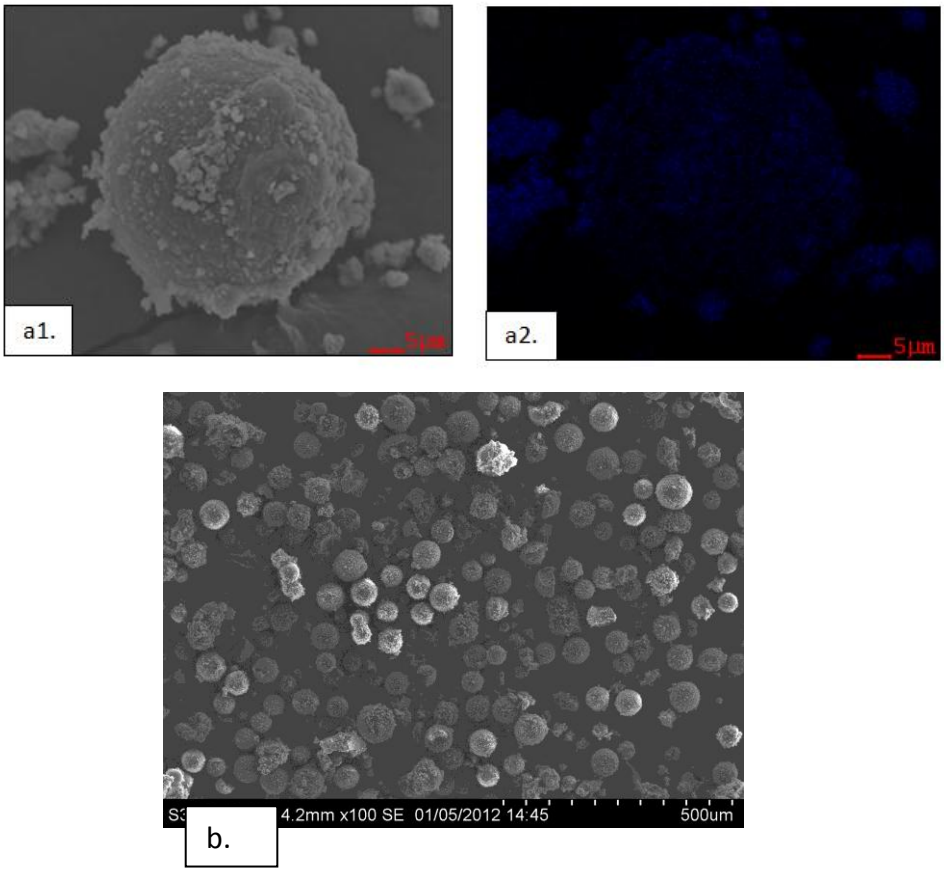

Figure 4.1 SEM/EDX of MAO supported onto PS: (a1., a2.) EDX mapping for Al
distribution on PS, and (b.) SEM of PS supported-MAO particles

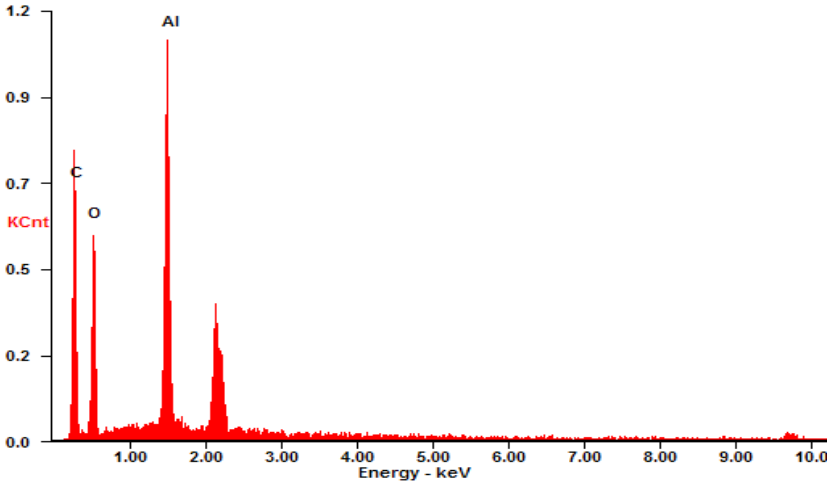

Figure 4.2 A typical spectrum of the supported MAO from EDX analysis used to measure the average $Al_{[MAO]}$ concentration on PS supports

4.1.2 Characteristics of support with thermo gravimetric analysis (TGA)

In this study, MAO was dispersed by impregnation onto the PS support. The degree of interaction between the support and cocatalyst (MAO) can be determined by the TGA measurement. The TGA provides information on the degree of interaction for MAO bound to the PS support in term of weight loss and removal temperature. The TGA profile is shown in **Figure 4.3**. It was observed the weight loss of $[Al]_{MAO}$ present on PS support in left hand. The decomposition temperatures at 10% weight loss (T_d 10%) of $[Al]_{MAO}$ on PS support was 250 °C. The weight loss was converted into the derivative weight from prior to plot with temperature as also seen in **Figure 4.3**. It can be observed that the first peak of humidity is located 110-120 °C, the second peak of MAO decomposition is located 290-300 °C, and the highest peak of polystyrene decomposition is located 450 °C. Therefore, it can be concluded that the decomposition temperatures of $[Al]_{MAO}$ on PS support was 290-300 °C.

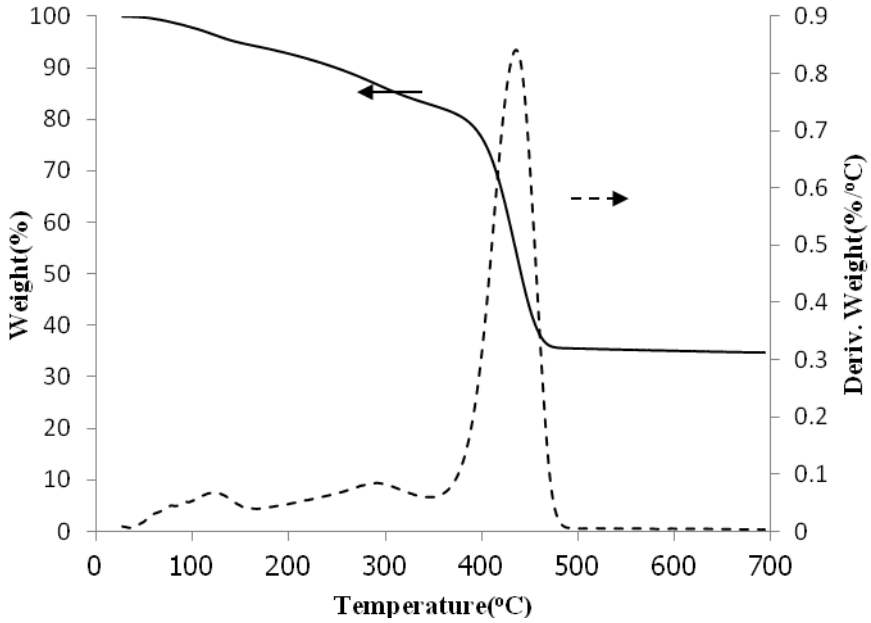

Figure 4.3 TGA profile of MAO on PS support

4.2 Characteristic and catalytic properties of ethylene/α-olefin copolymerization

4.2.1 The effect of various α-olefins and ratios between ethylene/α-olefin on the catalytic activity

The catalyst activities via various α-olefin and ratio between ethylene/ α-olefin in the heterogeneous system are listed in **Table 4.1**.

Table 4.1 Copolymerization activity of ethylene/α-olefin[a]

Run	α-olefin	Mole ethylene/monomer	Yield (g)	Activity (kgPE/molZr h)
1	-	-	0.67	8,729
2	1-hexene	1:0.25	0.70	19,858
3	1-hexene	1:0.50	0.80	23,357
4	1-hexene	1:0.75	0.81	25,714
5	1-octene	1:0.25	0.71	19,320
6	1-octene	1:0.50	0.87	22,378
7	1-octene	1:0.75	0.90	22,641
8	1-dodecene	1:0.25	0.84	28,717
9	1-dodecene	1:0.50	0.90	30,508
10	1-dodecene	1:0.75	1.04	29,296
11	1-tetradecene	1:0.25	0.89	22,390
12	1-tetradecene	1:0.50	1.02	25,987
13	1-tetradecene	1:0.75	1.12	21,960
14	1-octadecene	1:0.25	1.17	19,914
15	1-octadecene	1:0.50	2.11	24,463
16	1-octadecene	1:0.75	2.46	18,358

[a] Copolymerization conditions: [Al]/[Zr] = 5200, Temperature = 70 °C, 50 psi of ethylene pressure was applied.

The result of ethylene/α-olefin copolymerization is shown in **Table 4.1**. The activities of ethylene/α-olefin copolymerization (run2-16) were higher than that of ethylene homopolymerization (run1). Obviously, the positive "comonomer effect" was happened. Several authors have observed this effect when comparing the results obtained with ethylene homopolymerization. The phenomena were attributed to increase in the polymer solubility because an increase in monomer diffusion through the reaction medium would increase its concentration around the active centers. Furthermore, the presence of the comonomer in the polyethylene chain would make difficult the formation of a crystalline shell of polyethylene around the active sites.[50] The activities ethylene/1-hexcene and 1-octene copolymerization increased with increasing of the comonomer concentration until the maximum was reached, but the activities of ethylene/1-dodecene, 1-tetradecene and 1-octadecene copolymerization increased with the increase of ratio between ethylene/ α-olefin from 1:0.25 until the maximum value that is 1:0.50, and then started to decrease with further increase of ratio between ethylene/ α-olefin.

Generally, high comomer concentration (ratio of ethylene/ α-olefin from 1:0.75), the anticipated activity can not be attained. This is because high execess of α-olefin obstructed active sites of catalyst from reacting with ethylene monomer, and consequently reduce rate of ethylene insertion into the chain of growing polymer.[55] The length of the chain of the comonomer had only little effect on the activity of copolymerization. Here, the activities of 1-dodecene were the highest when comparing with other α-olefins (1-hexcene, 1-octene, 1-tetradecene and 1-octadecene).

In the olefin polymerization, the networks were swollen by a solvent, such as toluene, first, and then MAO and olefin monomers penetrated the network and came into contact with zirconocene. Without a chemical bond between the zirconocene and carrier, each network provided a homogeneous polymerization microenvironment for zirconocene. That is, the heterogeneous catalyst allowed microscopic homogeneous polymerization inside the networks. In the olefin

polymerization, the chains of the polyolefin grew inside the network originally, and subsequently the crosslinked network fragmented and allowed further permeation of the solvent and monomer into the inner part of the carrier.[56]

4.2.2 The effect of various α-olefins and ratios between ethylene/ α-olefin on catalyst activity profile.

The rate of ethylene consumption with various α-olefins and ratios between ethylene/ α-olefin are shown in **Figures 4.4** and **4.5.** There were found that the induction period of the catalyst was also observed at the beginning of polymerization. The consumption rate went to a maximum between 4-5 min, then decreased due to catalyst deactivation. The influence of the type of comonomer on rate of ethylene/ α-olefin copolymerization is shown in **Figure 4.4**. It can be explained that the type of comonomer had only little effect on the activity profile of copolymerization, where the rate of ethylene consumption of ethylene/1-dodecene in the first period was the highest. In addition, the influence of the comonomer concentration on rate of ethylene/1-hexene copolymerization is shown in **Figure 4.5,** where the profile of rate of ethylene consumption is similar to that of **Figure 4.4,** indicating that the comonomer concentration had little effect on the activity profile of copolymerization as well as the influence of the type of comonomer. The activity profiles of all experiment are shown in **Appendix A**. For the high [Al]/[Zr] molar ratio greater than 3000, the rate of polymerization increased and reached the maximum in a few minutes, then decayed slowly. Moreover, the influence of the comonomer concentration on the rate of ethylene/1-hexene and ethylene/1-dodecene copolymerization increased in the first reaction period, and then remained stable. The stable polymerization process implied that the fragmentation of carrier had great influence on the copolymerization kinetic. The fragmentation of carrier, active species were exposed gradually to comonomer, which led to slight deactivation of copolymerization.[50]

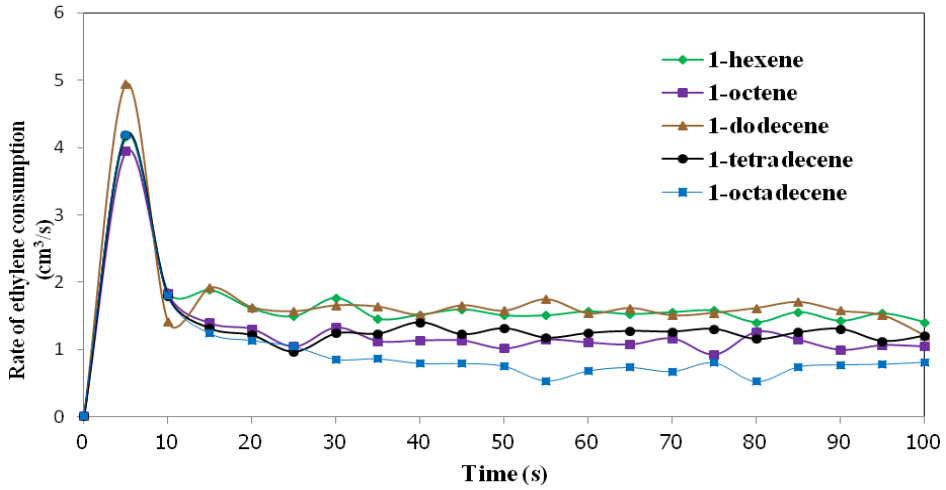

Figure 4.4 Activity profiles for various α-olefins with ratio between ethylene/α-olefin 1:0.5 in copolymerization

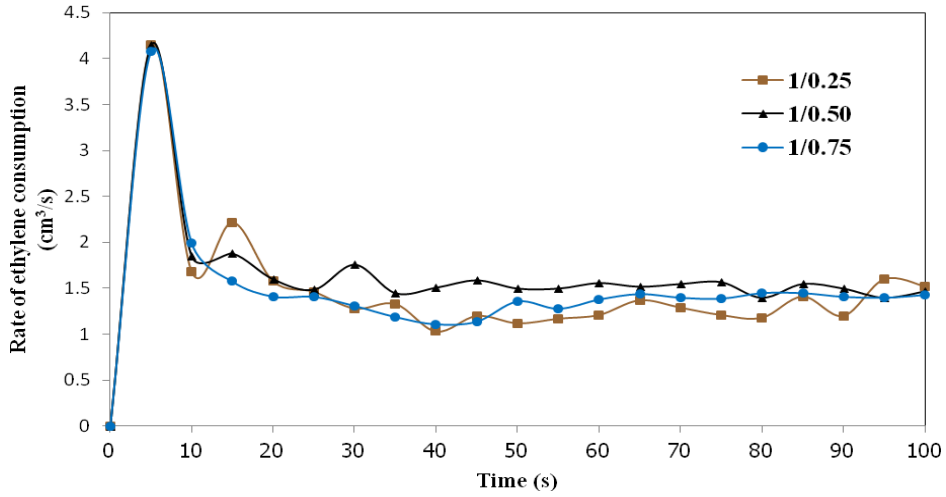

Figure 4.5 Activity profiles for various ratios between ethylene/1-hexene in copolymerization

4.2.3 The effect of various α-olefins on morphologies of copolymers

The morphologies of polymer produced were observed using scanning electron microscopy (SEM) technique. SEM micrographs of copolymer are shown in **Figure 4.6** indicating the morphologies of ratio of ethylene/α-olefins 1:0.50 obtained from the different type of comonomer. It is suggested that the use of higher length of the chain of the comonomer seemed to increase the degree of

agglomerate. The product without comonomers is isolated as nearly spherical beads and a larger magnification a cauliflower-like morphology of the polymer particles where polymer fragments seem to be held together by a threadlike polymer structure.[49]

Generally, it is accepted that the catalyst breaks up into small fragments, since the onset of polymerization and the fragments keep uniformly dispersed in the polymer particle throughout the whole growth process. This process can assure a uniform polymerization rate throughout the particle and finally leads to a perfect shape replication. Unfortunately, a detailed knowledge of the particle growth mechanism in case of PS beads supported catalyst is not clear yet. Actually, the mechanical strength of PS beads themselves is not so high due to low (2%) divinylbenzene content. Some PS beads are broken into parts even during the preparation of the catalysts.[52]

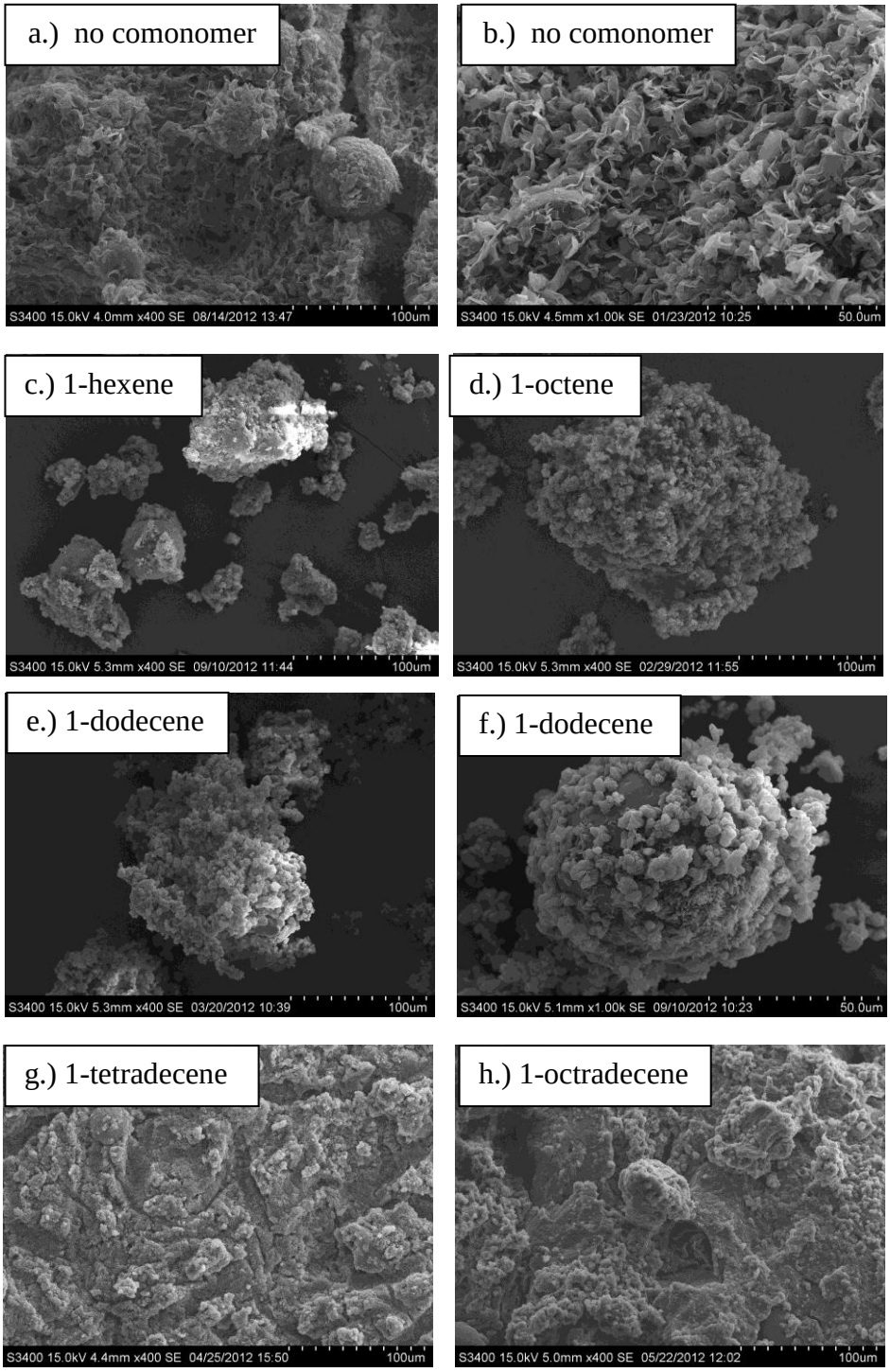

Figure 4.6 SEM micrographs of copolymers obtained from various ethylene/α-olefins; (a.,b.) no conomomer, (c.) 1-hexene, (d.) 1-octene, (e.,f..) 1-dodeccene, (g.) 1-tetradecene, (h.) 1-octradeccene.

4.2.4 The effect of various α-olefins and ratios between ethylene/α-olefin on incorporation of copolymers

^{13}C-NMR spectroscopy was used to determine comonomer incorporation and polymer microstructure. The quantitative analysis of triad distribution for all copolymers was calculated. The triad distributions of all copolymers from various α-olefins and ratios of ethylene/ α-olefin are shown in **Table 4.2.** The ^{13}C-NMR spectra of the copolymer are also shown in **Appendix B.** For copolymers all synthesized copolymer from each type of α-olefin exhibited similar triad distribution having the majority of [EEE]. Because the comonomer has a bigger size than the ethylene, which reaction of comonomer occurs harder than usual. Moreover, it can be observed that the comonomer incorporation increased with the longer chain of α-olefin and higher of ratio between ethylene/ α-olefin.

Table 4.2 ^{13}C-NMR analysis of ethylene/ α-olefin copolymer

Run	Comonomer type	Mole ratio	Triad distribution					
			[EEE]	[XEE]	[EXE]	[XEX]	[EXX]	[XXX]
2	1-hexene	1:0.25	0.943	0.015	0.028	0.014	0.000	0.000
3	1-hexene	1:0.50	0.926	0.034	0.029	0.012	0.000	0.000
4	1-hexene	1:0.75	0.906	0.045	0.033	0.010	0.000	0.005
5	1-octene	1:0.25	0.938	0.000	0.005	0.050	0.007	0.000
6	1-octene	1:0.50	0.924	0.016	0.016	0.028	0.016	0.000
7	1-octene	1:0.75	0.869	0.079	0.035	0.005	0.011	0.000
8	1-dodecene	1:0.25	0.932	0.036	0.026	0.000	0.006	0.000
9	1-dodecene	1:0.50	0.903	0.066	0.027	0.000	0.04	0.000
10	1-dodecene	1:0.75	0.840	0.096	0.047	0.007	0.010	0.000
11	1-tetradecene	1:0.25	0.911	0.049	0.022	0.005	0.014	0.000
12	1-tetradecene	1:0.50	0.905	0.050	0.024	0.005	0.016	0.000
13	1-tetradecene	1:0.75	0.815	0.093	0.043	0.029	0.020	0.000
14	1-octadecene	1:0.25	0.854	0.080	0.037	0.009	0.020	0.000
15	1-octadecene	1:0.50	0.815	0.082	0.048	0.016	0.040	0.000
16	1-octadecene	1:0.75	0.776	0.077	0.048	0.053	0.046	0.000

4.2.5 The effect of ratio between ethylene/α-olefin on melting temperatures of copolymers

The melting temperatures (T_m) of copolymer evaluated by the differential scanning calorimeter (DSC) are shown on **Table 4.3.** DSC curves of the copolymer are also shown in **Appendix C.**

Table 4.3 Melting temperature of copolymers obtained upon different α-olefin

Run	α-olefin	Mole ethylene/monomer	T_m (°C)
1	-	-	135
2	1-hexene	1:0.25	117
3	1-hexene	1:0.50	109
4	1-hexene	1:0.75	102
5	1-octene	1:0.25	121
6	1-octene	1:0.50	113
7	1-octene	1:0.75	110
8	1-dodecene	1:0.25	116
9	1-dodecene	1:0.50	114
10	1-dodecene	1:0.75	110
11	1-tetradecene	1:0.25	116
12	1-tetradecene	1:0.50	110
13	1-tetradecene	1:0.75	106
14	1-octadecene	1:0.25	110
15	1-octadecene	1:0.50	105
16	1-octadecene	1:0.75	102

The homopolymerization system (run1) produced polymer with high melting temperature (T_m) ~135 °C. In addition, from the characterization of copolymer, it can be seen also in **Table 4.3** that the effects of increasing α-olefin concentration include a decrease in the melting temperatures of copolymers and the continuous decrease in the crystallinity of the copolymer.

Meting points and degree of crystallinities of ethylene/α-olefin copolymers decrease as more α-olefin is incorporated into the polymer chain. Moreover, higher α-olefins give lower melting points and crystallinities than lower α-olefins.[58] A small amount of comonomer incorporation of 1-hexene or 1-octene leads to linear low density polyethylene (LLDPE), a product of great industrial interest. One effect of the monomer incorporation is a decrease in crystallinity. As result, polymer with a lower melting point and density, and an increased flexibility and processibility are obtained.[35]

CHAPTER V
CONCLUSIONS & RECOMMENDATION

5.1 Conclusions

In this thesis, we have reported the synthesis of polyethylene from copolymerization of ethylene/1-tetradecene via poly(styrene-co-divinylbenzene)-supported Cp_2ZrCl_2/MAO catalyst by varying chain length and comonomer concentration of α-olefins on the catalytic activity and properties of polymer. A number of conclusions may be summarized as follows:

1. The active species are located on the particle surface and they have uniformly distributed throughout the particles.
2. The activities of ethylene/α-olefin copolymerization were higher than that of ethylene homopolymerization.
3. The activities of ethylene/-olefin copolymerization increased with the increase of the comonomer concentration until the maximum value was reached, and then started to decrease with further increase of comonomer concentration.
4. The length of the chain of the comonomer had little effect on the activity of copolymerization.
5. The system providing to the species close to the homogeneous.
6. The comonomer concentration had little effect on the activity profile of copolymerization as well as the influence of the type of comonomer.
7. A all synthesized copolymers from each type of α-olefin exhibited similar triad distribution having the majority of [EEE] and comonomer incorporation increased with the longer chain of α-olefin and higher of ratio between ethylene/ α-olefin.
8. Melting temperature of copolymer tended to decrease with support increasing comonomer concentration and the continuous decrease in the crystallinity of the copolymer.

5.2 Recommendation

Copolymers should be further determined other main properties for any applications suce as molecular weight, molecular weight distribution, and mechanical properties. PS beads should be further polymerized in gas phase process more than slurry phase process.

REFERENCES

[1] Chem Market Assoc Inc (CMAI). World Polyolefins Analysis (2010).

[2] Chum, P. S.; Swogger, K. W. Olefin polymer technologies-History and recent progress at The Dow Chemical Company. Progress in Polymer Science 33 (2008): 797-819.

[3] Cano, J., and Kunz, K. How to synthesize a constrained geometry catalyst (CGC) Journal of Organometallic Chemistry 692 (2007): 4519-4527.

[4] Bensason, S., Minick, J., Moet, A., Chum, S., Hiltner, A., and Baer, E. Classification of homogeneous ethylene-octene copolymers based on comonomer content. Journal of Polymer Science Part B: Polymer Physics 34 (1996): 1301-1315

[5] Ali, E. M., Abasaeed, A. E., and Al-Zahrani, S. M. Optimization and control of industrial gas-phase ethylene polymerization reactors. Industrial & Engineering Chemistry Research 37 (1998): 3414-3423.

[6] Halterman, R.L. Synthesis and applications of chiral cyclopentadienylmetal complexes. Chemical Reviews 92 (1992): 965.

[7] Brintzinger, H., Beck, S., Leclerc, M., Stehling, U., and Roll, W. Reaction Mechanisms in Metallocene-Catalyzed Olefin Polymerization. Studies in Surface Science and Catalysis 89 (1994): 193-200.

[8] Bertrand, H., Cecile, B., Eric, C., Daniel, T., Alain, D., and Henri, C**.** Polymer support of single-site catalyst for heterogeneous olefin polymerization Progress in Polymer Science 36 (2011): 90.

[9] Roos, P., Meier, G. B., Samson, J. J. C., Weickert, G., and Westerterp, K. R. Gas phase polymerization of ethylene with a silica-supported metallocene catalyst: influence of temperature on deactivation. Macromolecular Rapid Communications 18 (1997): 319–324.

[10] Uozumi, T., Toneri, T., Soga, K., and Shiono, T. Copolymerization of ethylene and 1-octene with Cp^* $TiCl_3$ as catalyst supported on 3-aminopropyltrimethoxysilane treated SiO_2. Macromolecular Rapid Communications 18 (1997): 9–15.

[11] Soga, K., Kim, H. J., and Shiono, T. Highly isospecific SiO2-supported zirconocene catalyst activated by ordinary alkylaluminiums. Macromolecular Rapid Communications 15 (1994): 139–143.

[12] Klapper, M., and Fink, G. Via Immobilization of Alpha-Olefin Polymerization Catalysts. Tailor-Made Polymers (2008): 277–303.

[13] Nishida, H., Uozumi, T., Arai, T., and Soga, K. Polystyrene-supported metallocene catalysts for olefin polymerizations. Macromolecular Rapid Communications 16 (1995): 821-830.

[14] Koch, M., Stork, M., Klapper, M., and Mullen, K. Immobilization of Metallocenes through Noncovalent Bonding via MAO to a Reversibly Cross-Linked Polystyrene. Macromolecules 33 (2000): 7713-7717.

[15] Nenov, N., Koch, M., Klapper, M., and Mullen, K. PEO-functionalized polystyrene as polymeric support in metallocene catalysed olefin polymerisation. Polymer Bulletin 47 (2002): 391-398.

[16] Andrew, J. P. Handbook of Polyethylene.: Marcel Dekker, Inc., 2000.

[17] Kaminsky, W., and Laban A. Metallocene catalysis. Applied Catalysis A: General 222 (2001): 47–61.

[18] Scheirs, J., and Kaminsky, W. Metallocene-based Polyolefins, Preparation, Properties and Technology. Wiley Series in Polymer Science 1(1999).

[19] Alt, H. G., and Koppl, A. Effect of the Nature of Metallocene Complexes of Group IV Metals on Their Performance in Catalytic Ethylene and Propylene Polymerization. Chemical Reviews 100 (2000): 1205-1221.

[20] Brintzinger, H. H., Fischer, D., Mulhaupt, R., Rieger, B., and Waymouth, R. M. Stereospecific Olefin Polymerization with Chiral Matallocene Catalyts. Angewandte Chemie International Edition in English 34 (1995): 1143-1170.

[21] Coates, G. W. Control of Polyolefin Stereochemistry Using Single-Site Metal Catalysts. Chemical Reviews 100 (2000): 1223-1252.

[22] Coperet, C.; Chabanas, M.; Petroff, R.; Arroman, S., and Basset, J. M. Homogeneous and Heterogeneous Catalysis: Bridging the Gap through Surface Organometallic Chemistry. Angewandte Chemie International Edition 42 (2003): 156.

[23] Alt, H. G. Self-immobilizing catalysts and cocatalysts for olefin polymerization. Dalton Transactions 20 (2005): 3271-3276.

[24] Hao, P., Zhang, S.; Yi, J., Sun. W. H., and Mol, J. Morphology controlling of micrometer-sized mesoporous silica spheres assisted by polymers of polyethylene glycol and methyl cellulose. Microporous and Mesoporous Materials 115 (2008): 447-453.

[25] Quijada, R., Galland, G. B., and Mauler, R. S. The influence of the comonomer in the copolymerization of ethylene with α-olefins using $C_2H_4[ind]_2ZrCl_2$/methylaluminoxane as catalyst system. Macromolecular Chemistry and Physics 197(1996): 3091-3098.

[26] Benedikt, G. M., and Goodall, B. L. Macromolecule–metal complexes. Polymer International 49 (2000): 1024.

[27] Alt, H. G., and Koppl, A. Cocatalysts for Metal-Catalyzed Olefin Polymerization: Activators, Activation Processes, and Structure-Activity Relationships. Chemical Reviews 100 (2000): 1391-1434.

[28] Kaminsky, W. J. The discovery of metallocene catalysts and their present state of the art. Journal of Polymer Science Part A: Polymer Chemistry 42 (2004): 3911-3921.

[29] Ataf, A., Amin, B., Nasir, K., Shafiqullah, M., and Saqib, A. Zirconium complexes in homogeneous ethylene polymerization. Journal of Coordination Chemistry 64 (2011): 1815-1817.

[30] Wang, W., Fan, Z. Q., and Feng, L. X. Ethylene polymerization and ethylene/1-hexene copolymerization using homogeneous and heterogeneous unbridged bisindenyl zirconocene catalysts. European Polymer Journal 41 (2005): 2380-2387.

[31] Paninee Keawkrajang. Copolymerization of Ethylene/α-olefin on the Supported Zirconocene Catalyts. Master's Thesis, Department of Chemical Engineering, Facuty of Engineering, Chulalongkorn University, 2002.

[32] Ribeiro, M., Deffieux, A., and Portela, M. F. Supported Metallocene Complexes for Ethylene and Propylene Polymerizations: Preparation and Activity. Industrial & Engineering Chemistry Research 36 (1997): 1224-1237.

[33] Ciardelli, F., Altomare, A., and Michelotti, M. From homogeneous to supported metallocene catalysts. Catalyst Today 41(1998): 149-157.

[34] Kisren, M. O. Supported metallocene catalysts with MAO and boron activators. Topics in Catalyst 7 (1999): 89-95.

[35] Steinmertz,B., Tesche, B., Przybyla, C.,Zechlin, J., and Fink, G. Polypropylene growth on silica-supported matallocene catalysts: A microscopic study to explain kinetic behavior especially in early polymerization stages. Acta Polymerca 48 (1997): 392-399

[36] Jang YJ, Naundorf C, Klapper M, Mullen K. Study of the Fragmentation Process of Different Supports for Metallocenes by Laser Scanning Confocal Fluorescence Microscopy (LSCFM). Macromolecular Chemistry and Physics 206 (2005): 2027-2037.

[37] Huang, J., and Rempel, G. L. Ziegler-Natta catalysts for olefin polymerization: Mechanistic insights from metallocene systems. Progress in Polymer Science 20 (1995): 459-526.

[38] Pietikainen, P., and Seppala, J.V. Low Molecular Weight Ethylene/Propylene Copolymers. Effect of Process Parameters on Copolymerization with Homogeneous Cp_2ZrCl_2 Catalyst. Macromolecules 27 (1994): 1325-1328.

[39] Quijada, R., Galland, G. B., and Mauler, R. S.Using alkylaluminium activators to tailor short chain branching distributions of ethylene/1-hexene copolymers produced with in-situ supported metallocene catalysts**.** Macromolecular Chemistry and Physics 201 (2000): 2195-2202.

[40] Soga,K., and Kaminaka, M. Polymerization of propene with the heterogeneous catalyst system $Et[IndH_4]_2ZrCl_2/MAO/SiO_2$ combined with trialkylaluminium. Macromolecular Rapid Communications 13 (1992): 221-224.

[41] De Fatima, V., Marques, M., Conte, A., De Resende, F. C., and Chaves, E. G. Copolymerization of ethylene and 1-octene by homogeneous and different supported metallocene catalyst. Journal of Applied Polymer Science. 82 (2001): 724-730.

[42] Shan. C. L. P., Chu, K. J., Soares, J., and Penlidis, A. Ethylene/1-octene copolymerization studies with *in situ* supported metallocene catalysts: Effect of polymerization parameters on the catalyst activity and polymer microstructure. Jornal of Polymer Science Part A: Polymer Chemistry 40 (2002): 4426-4451.

[43] Shan. C. L. P., Chu, K. J., Soares, J., and Penlidis, A. Using alkylaluminium activators to tailor short chain branching distributions of ethylene/1-hexene copolymers produced with in-situ supported metallocene catalysts. Macromolecular Chemistry and Physics 201 (2000): 2195-2202.

[44] Yates, K. Polystyrene for Food Packging Applications. International Life Sciences Institute (2002): 5-6.

[45] Stork, M., Koch, M., Klapper, M., Müllen, K., Gregorius, H., and Rief, U. Ethylene polymerization using crosslinked polystyrene as support for zirconocene dichloride/methylaluminoxane. Macromol Rapid Commun 20 (1999): 210-213.

[46] Wang, W., Wang, L., Wang J., and Ma, Z. Study on Ethylene (Co)Polymerization and Its Kinetics Catalyzed by a Reversible Crosslinked Polystyrene-supported Metallocene Catalyst. Journal of Applied Polymer Science 97 (2005): 1632-1636.

[47] Wang, W., Wang, L., Dong, X., Sun, T. and Wang, J. Study on Copolymerization of Ethylene/1-Hexene Catalyzed by a Novel Polystyrene-Supported Metallocene Catalyst. Journal of Applied Polymer Science 102 (2006): 1574-1577.

[48] Hong, S. C.; Ban, H. T.; Kishi, N.; Jin, J.; Uozumi, T. and Soga, K. Ethene polymerization with a poly(styrene-co-divinylbenzene) beads supported rac-$Ph_2Si(Ind)_2ZrCl_2$ catalyst. Macromolecular Chemistry and Physics 199 (1998): 1393-1397.

[49] Hong, S. C., Teranishi, T., Soga, K. Investigation on the polymer particle growth in ethylene polymerization with PS beads supported rac-$Ph_2Si(Ind)_2ZrCl_2$ catalyst. Polymer 39 (1998): 7153-7157.

[50] Jang, Y. J., Naundorf, C., Klapper, M. and Mullen, K. Study of the Fragmentation Process of Different Supports for Metallocenes by Laser Scanning Confocal Fluorescence Microscopy (LSCFM). Macromolecular Chemistry and Physics 206 (2005): 2027-2037.

[51] Barrett, A. G. M. and De Miguel, Y. R. A well-defined metallocene catalyst supported on polystyrene beads. Chemical Communications 19 (1998): 2079-2080.

[52] Barrett, A. G. M. and De Miguel Y. R. Synthesis and characterization of a new polymer support for a metallocene catalyst. Tetrahedron 58 (2002): 3785-3792.

[53] Chan, M. C. W. et al. Polystyrene supports for vanadium ethylene polymerisation catalysts. Chemical Communications 16 (1998): 1673-1674.

[54] Gibson, V. C. and Reed, W. Supported Polymerization Catalysts. EP0816384. UK: Assigned to BP Chemicals Ltd. (1998).

[55] Ekrachan Chaichana. Study on Half-metallocene Catalyst for Linear Low Density Polyethylene. Master's Thesis, Department of Chemical Engineering, Facuty of Engineering, Chulalongkorn University, 2009.

[56] Wang, W.; Wang, L.; Wang J., and Ma, Z. Novel Polystyrene-Supported Zirconocene Catalyst for Olefin Polymerization and Its Catalytic Kinetics. Journal of Applied Polymer Science 43(2005): 2650-2656.

[57] Strack, P., and Lofgren, B. Thermal Properties of ethylene/long chain α-olefin copolymers produced by metallocenes. European Polymer Journal 38 (2002): 97-107

[58] Quijada, R., Galland, G.B., and Mauler, R.S. The influence of the comonomer in the copolymerization of ethylene with α-olefins using $C_2H_4[Ind]_2ZrCl_2$ methylaluminoxane as catalyst system. Macromolecular Chemistry and Physics 197 (1996): 3091-3098.

APPENDICES

APPENDIX A

Rate of ethylene consumption

Rate of ethylene consumption

Copolymerization conditions: [Al]/[Zr] = 5200, Temperature = 70 °C, 50 psi of ethylene pressure was applied.

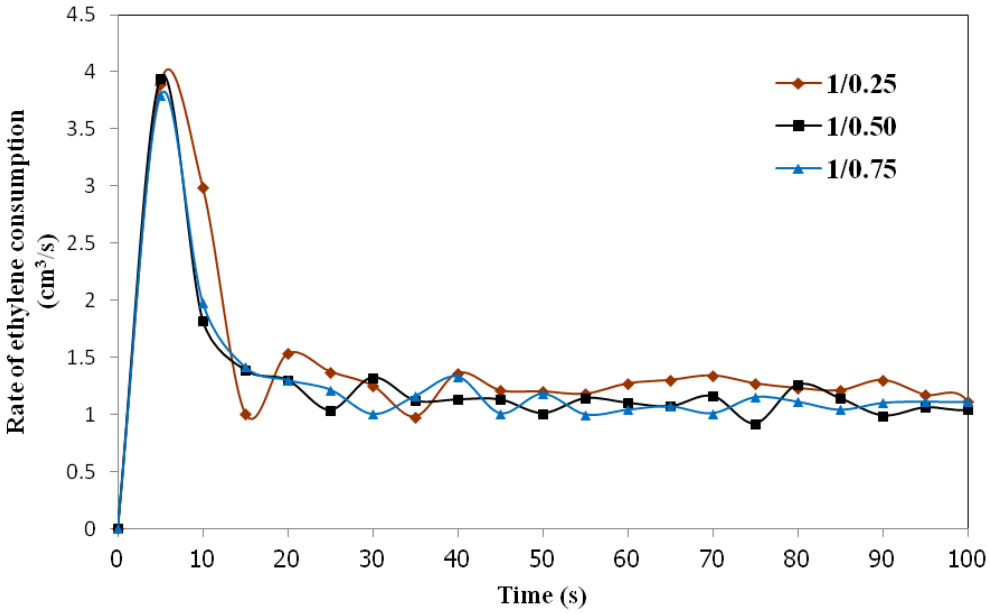

Figure A-1. Activity profiles for various ratios between ethylene/1-octene incopolymerization

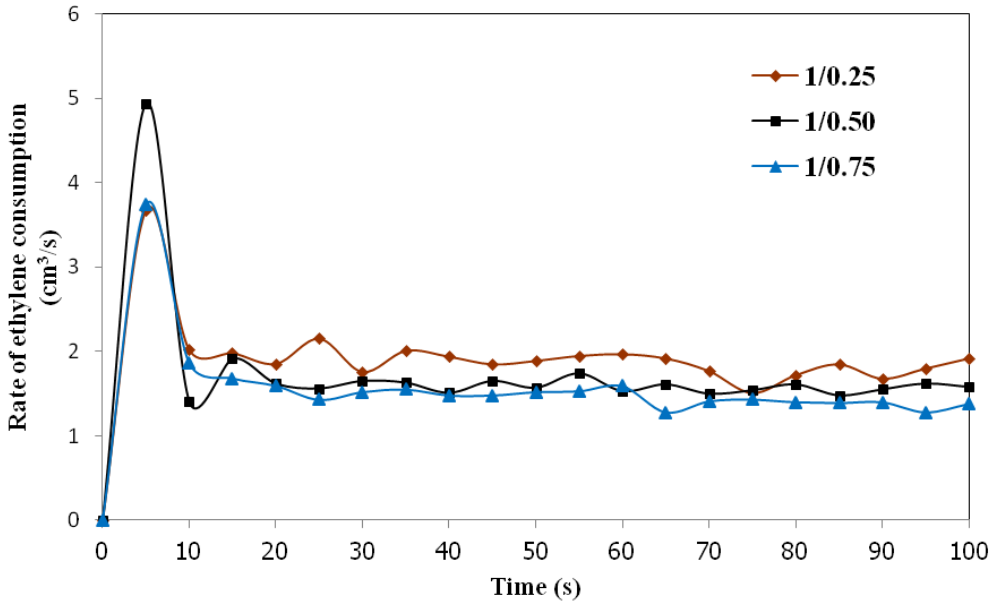

Figure A-2. Activity profiles for various ratios between ethylene/1-dodecene incopolymerization

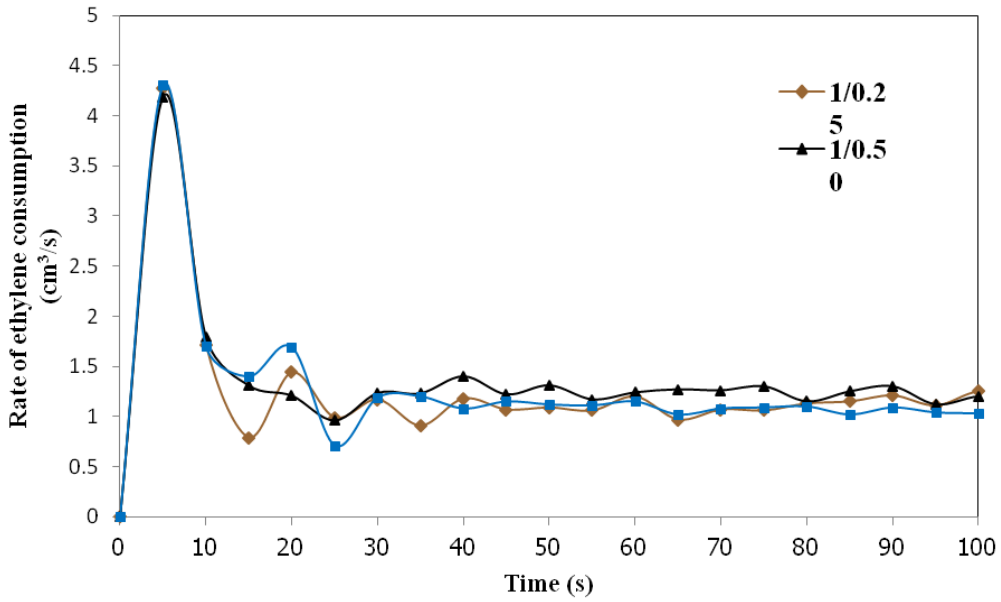

Figure A-3. Activity profiles for various ratios between ethylene/1-tetradecene incopolymerization

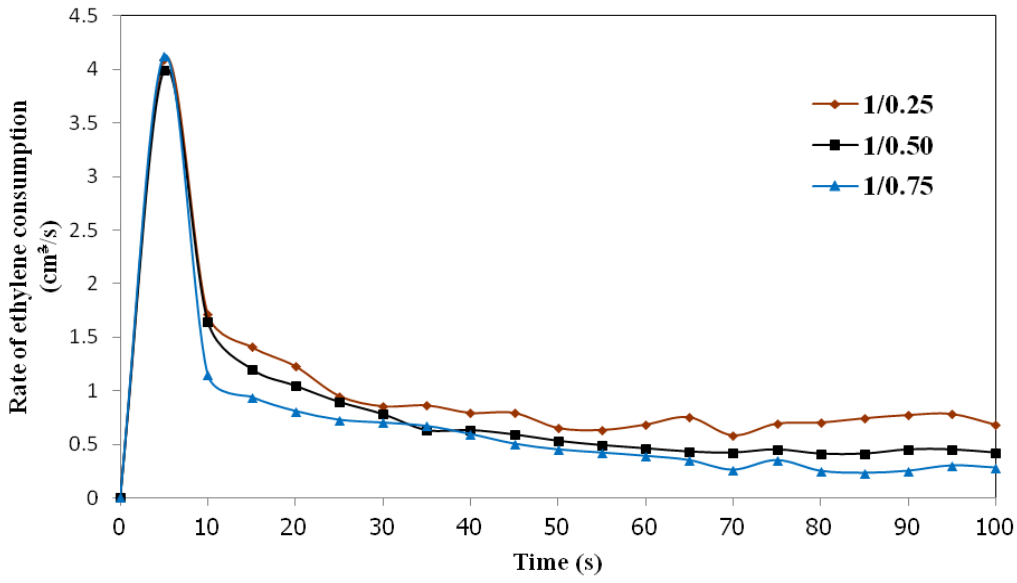

Figure A-4. Activity profiles for various ratios between ethylene/1-octadecene incopolymerization

APPENDIX B

^{13}C Nuclear magnetic resonance (^{13}C NMR)

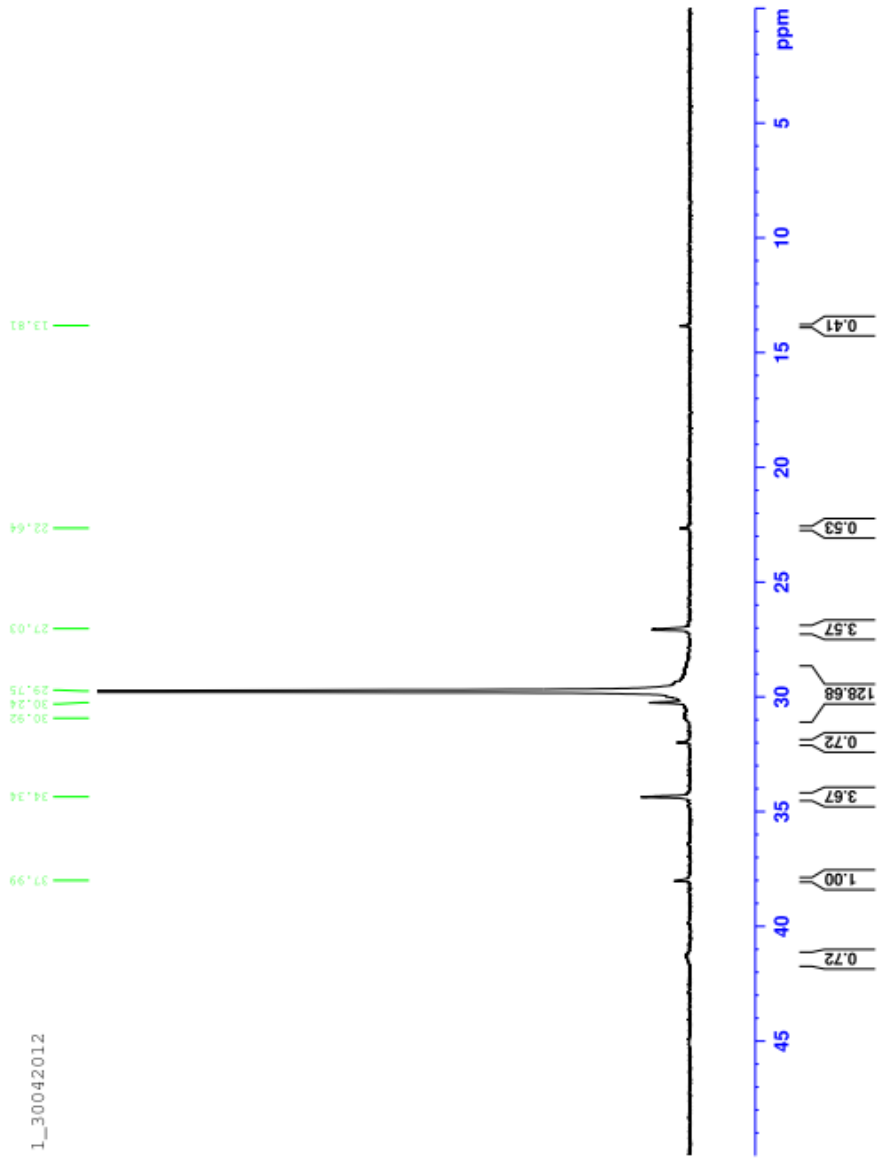

Figure B-1. ^{13}NMR spectra of ethylene/1-hexene copolymer at ratio 1:0.25

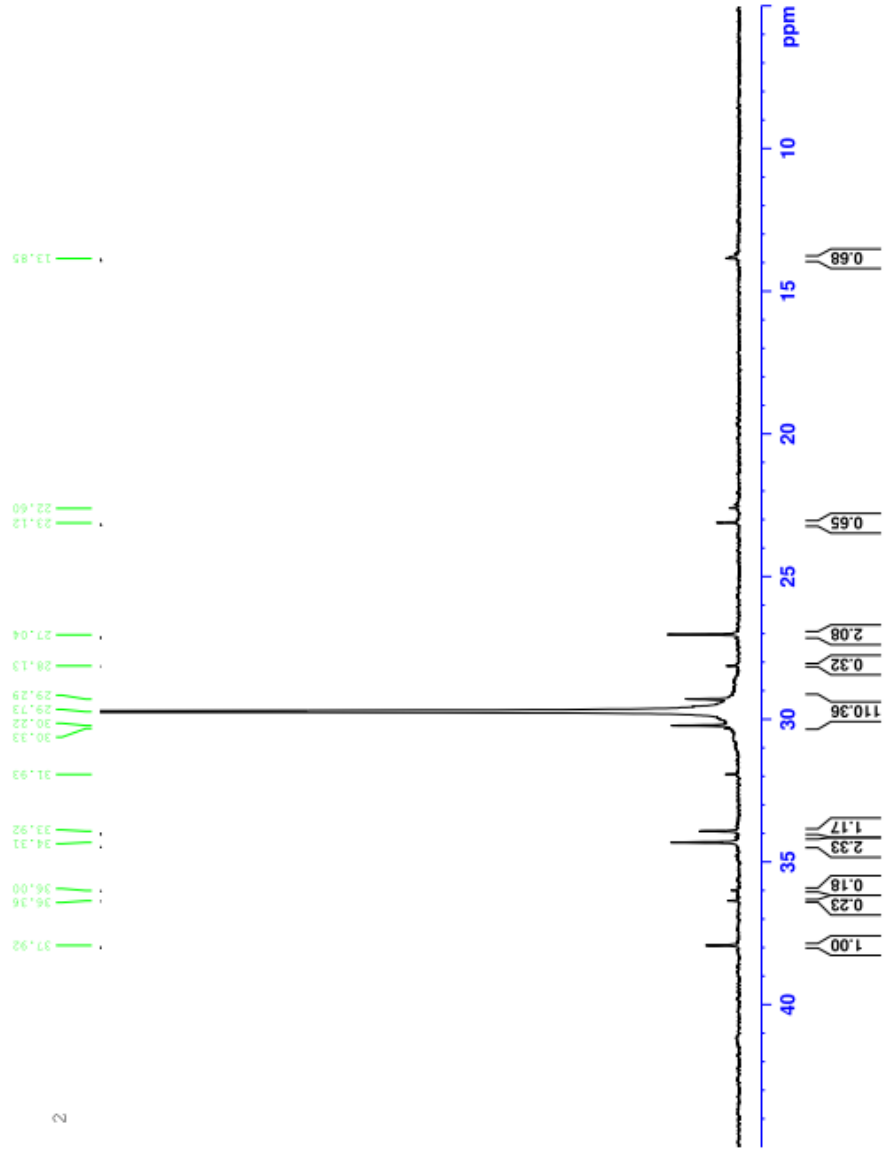

Figure B-2. ^{13}NMR spectra of ethylene/1-hexene copolymer at ratio 1:0.50

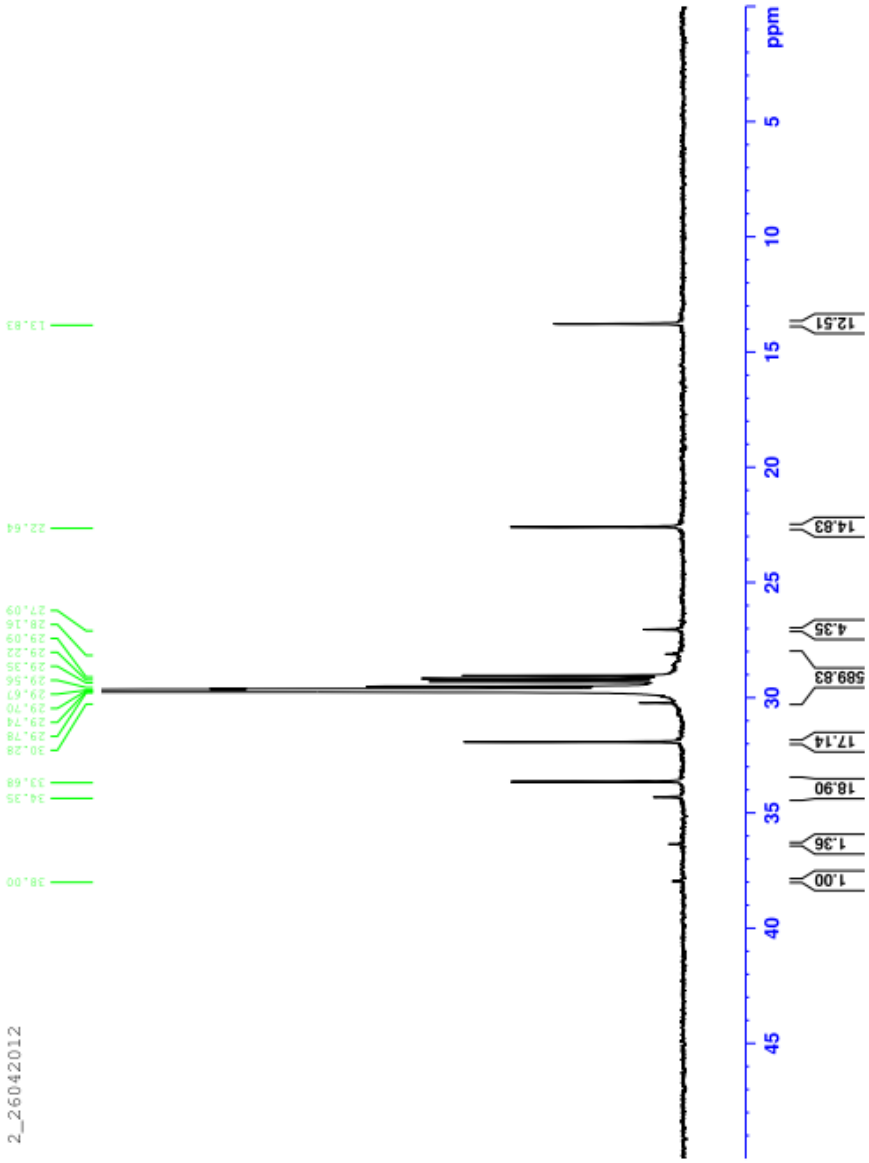

Figure B-3. ^{13}NMR spectra of ethylene/1-hexene copolymer at ratio 1:0.75

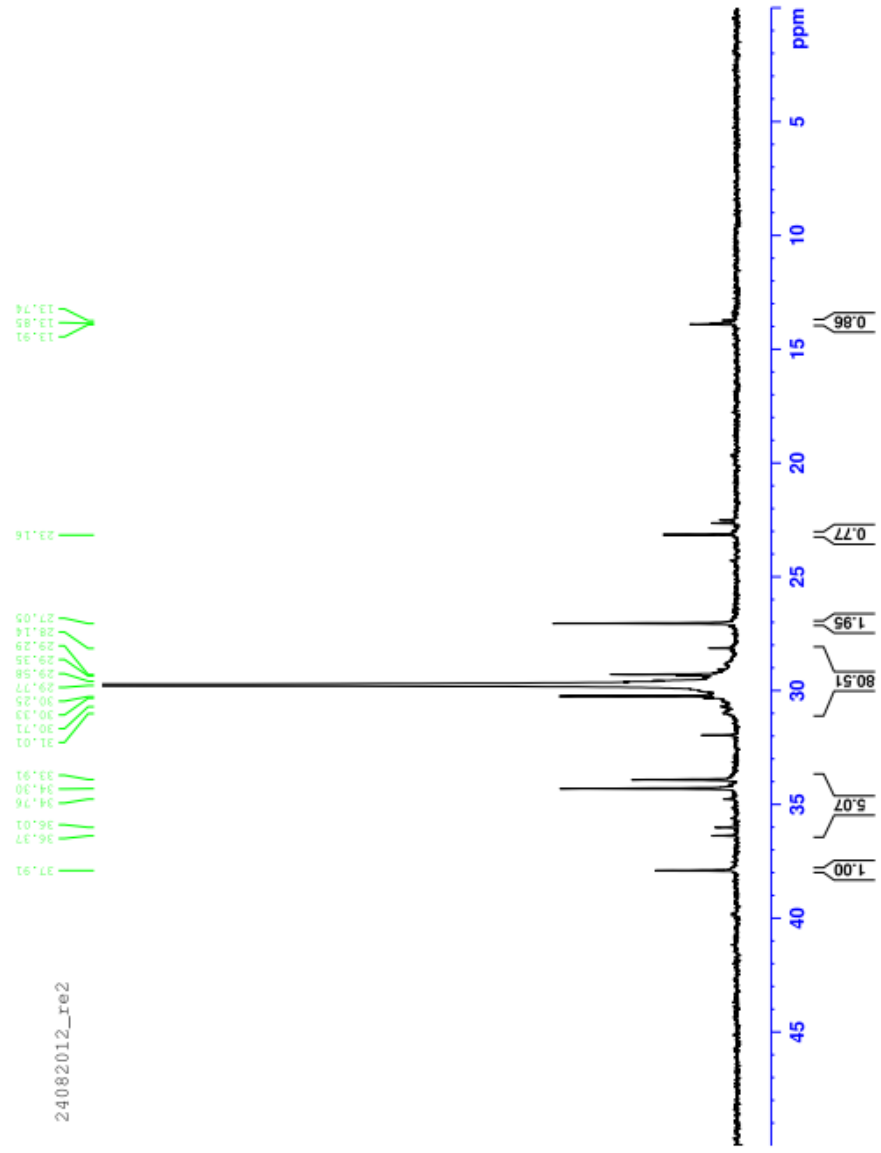

Figure B-4. ^{13}NMR spectra of ethylene/1-octene copolymer at ratio 1:0.25

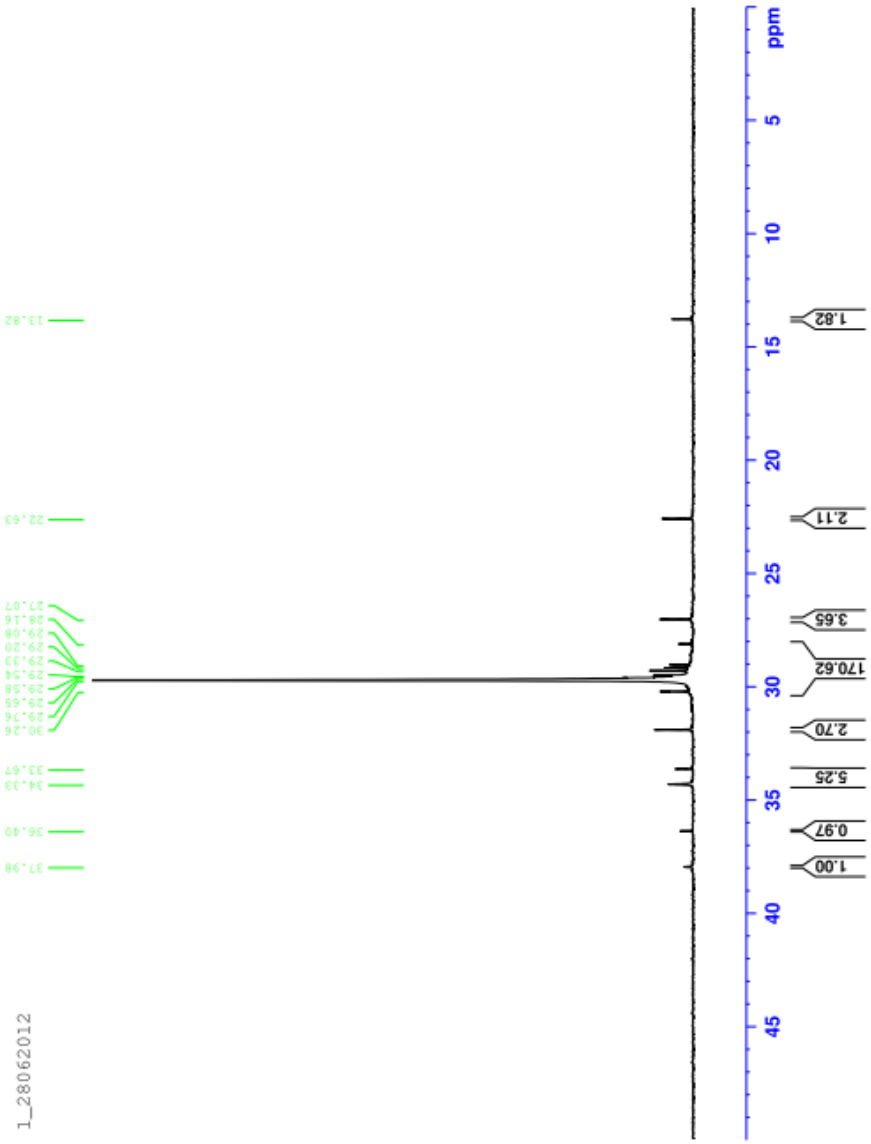

Figure B-5. ^{13}NMR spectra of ethylene/1-octene copolymer at ratio 1:0.50

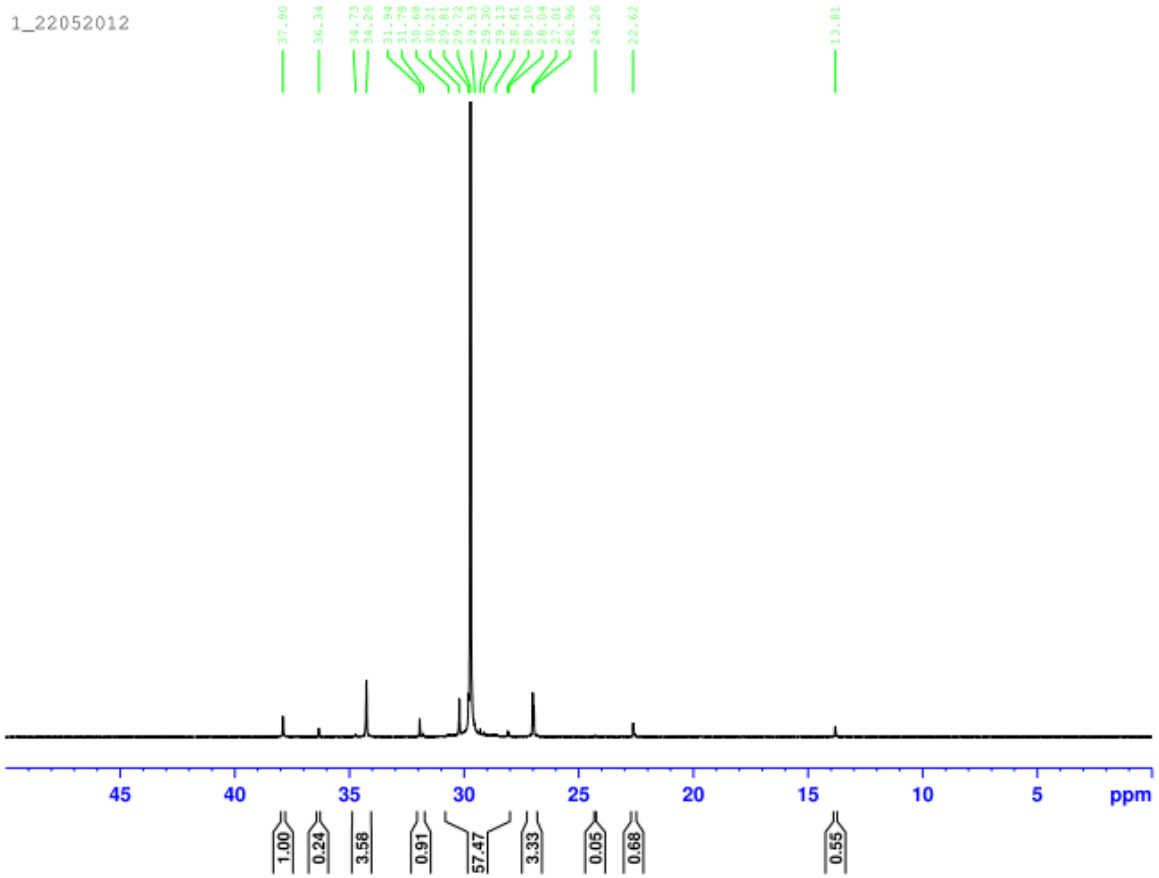

Figure B-6. ^{13}NMR spectra of ethylene/1-octene copolymer at ratio 1:0.75

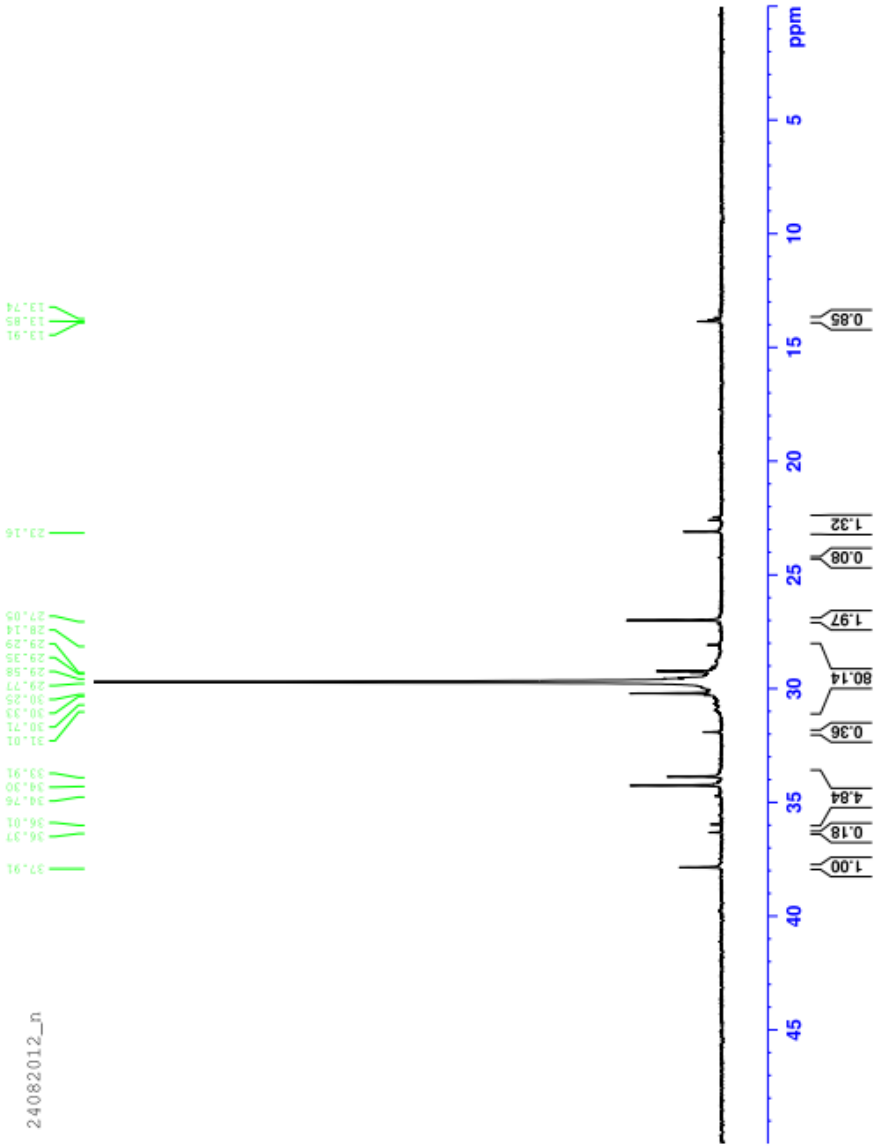

Figure B-7. ^{13}NMR spectra of ethylene/1-dodecene copolymer at ratio 1:0.25

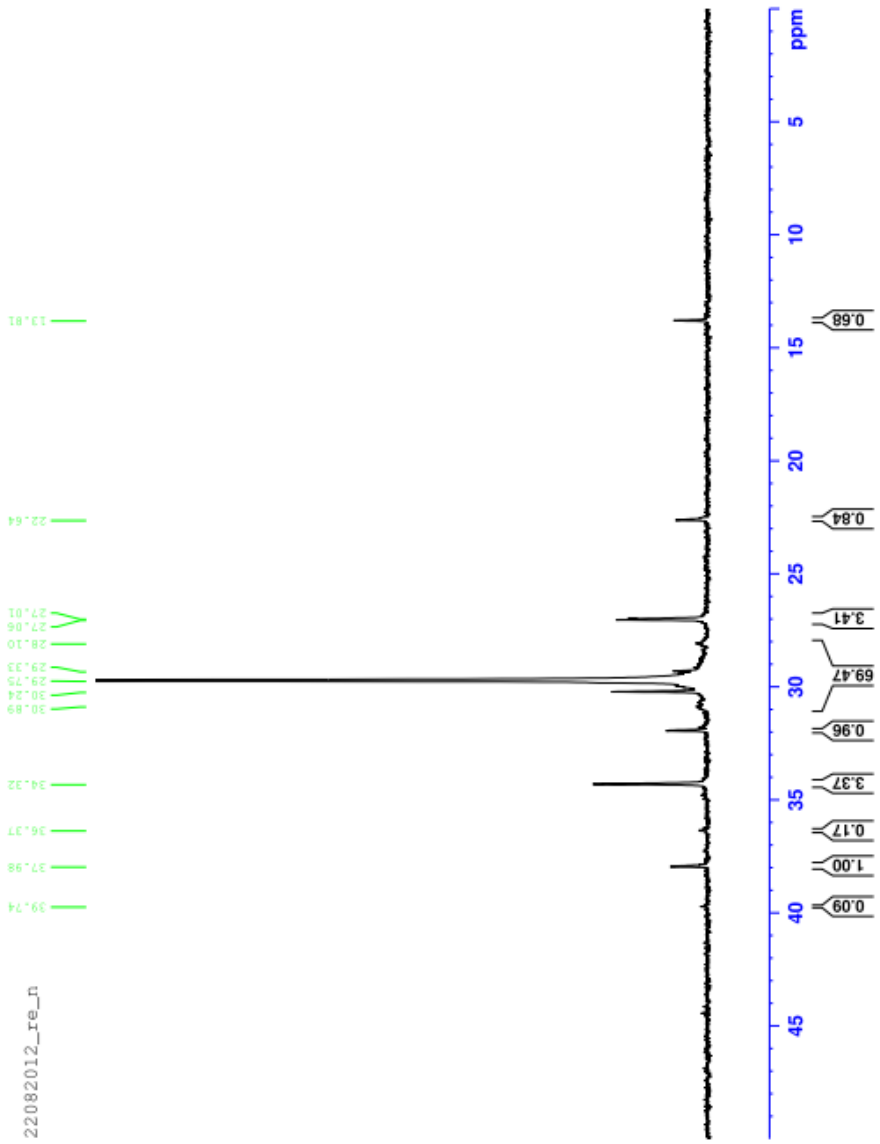

Figure B-8. ^{13}NMR spectra of ethylene/1-dodecene copolymer at ratio 1:0.50

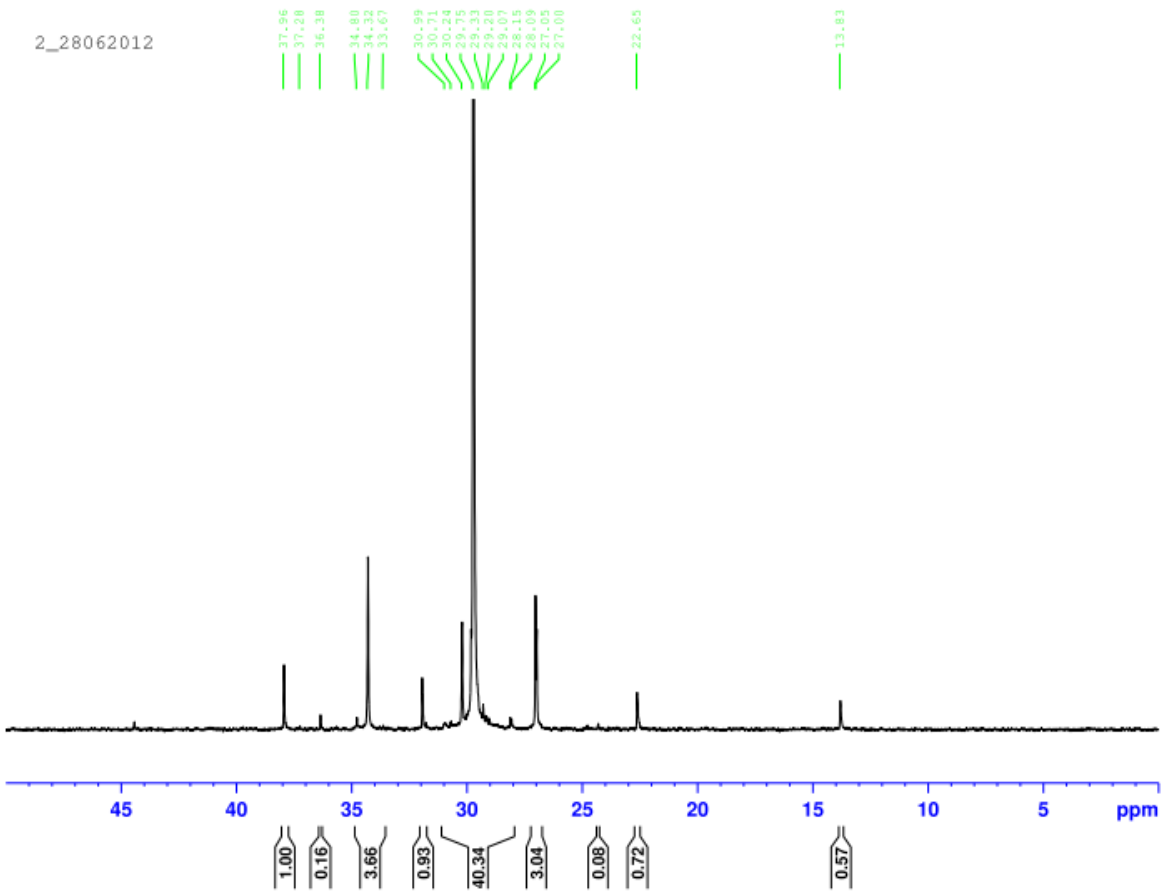

Figure B-9. ^{13}NMR spectra of ethylene/1-dodecene copolymer at ratio 1:0.75

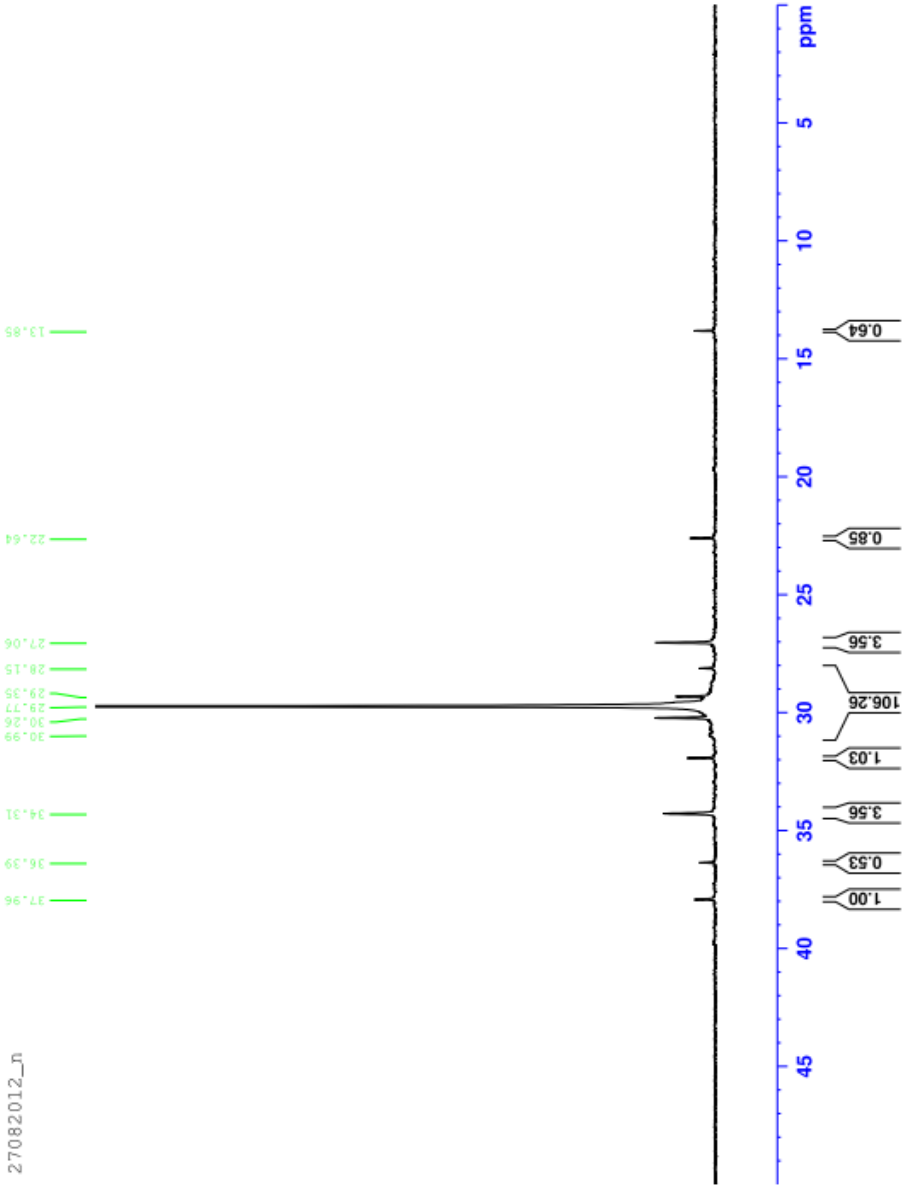

Figure B-10. ^{13}NMR spectra of ethylene/1-tetradecene copolymer at ratio 1:0.25

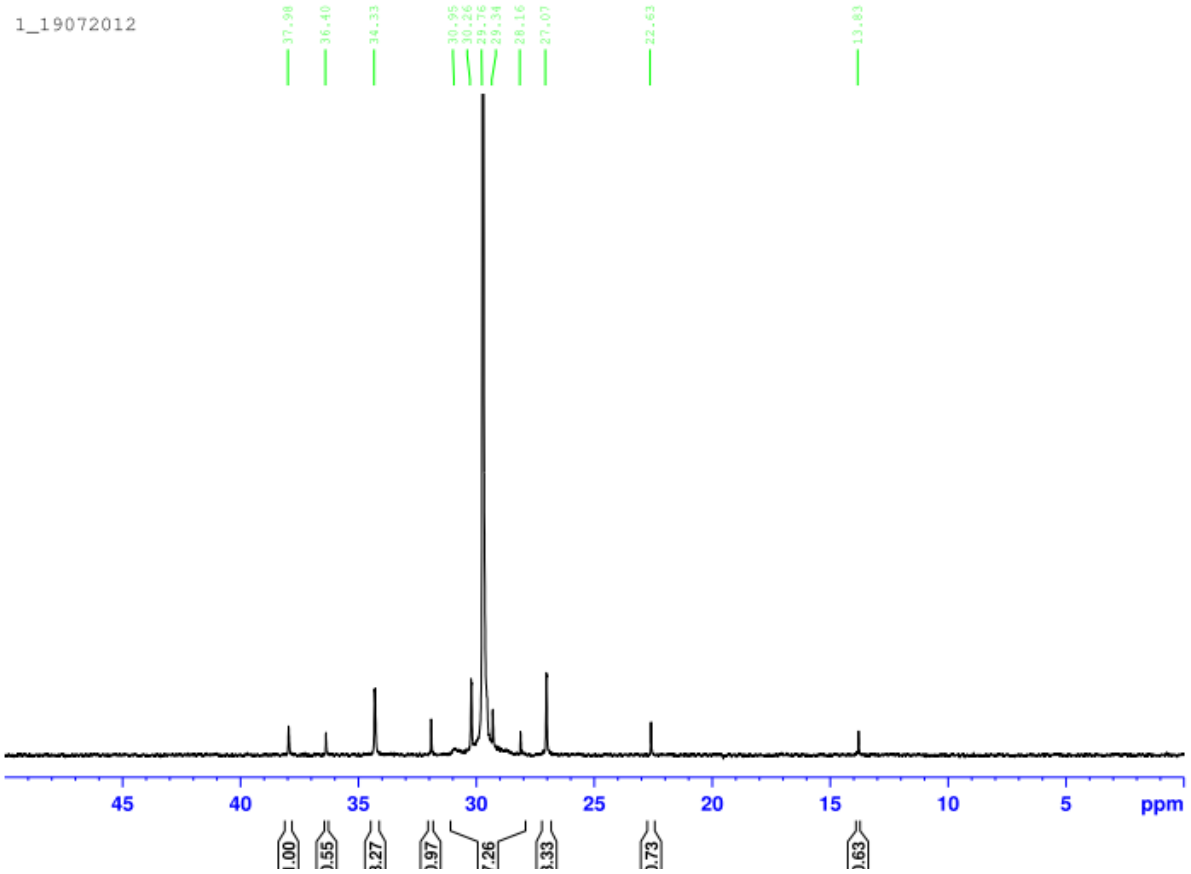

Figure B-11. ^{13}NMR spectra of ethylene/1-tetradecene copolymer at ratio 1:0.50

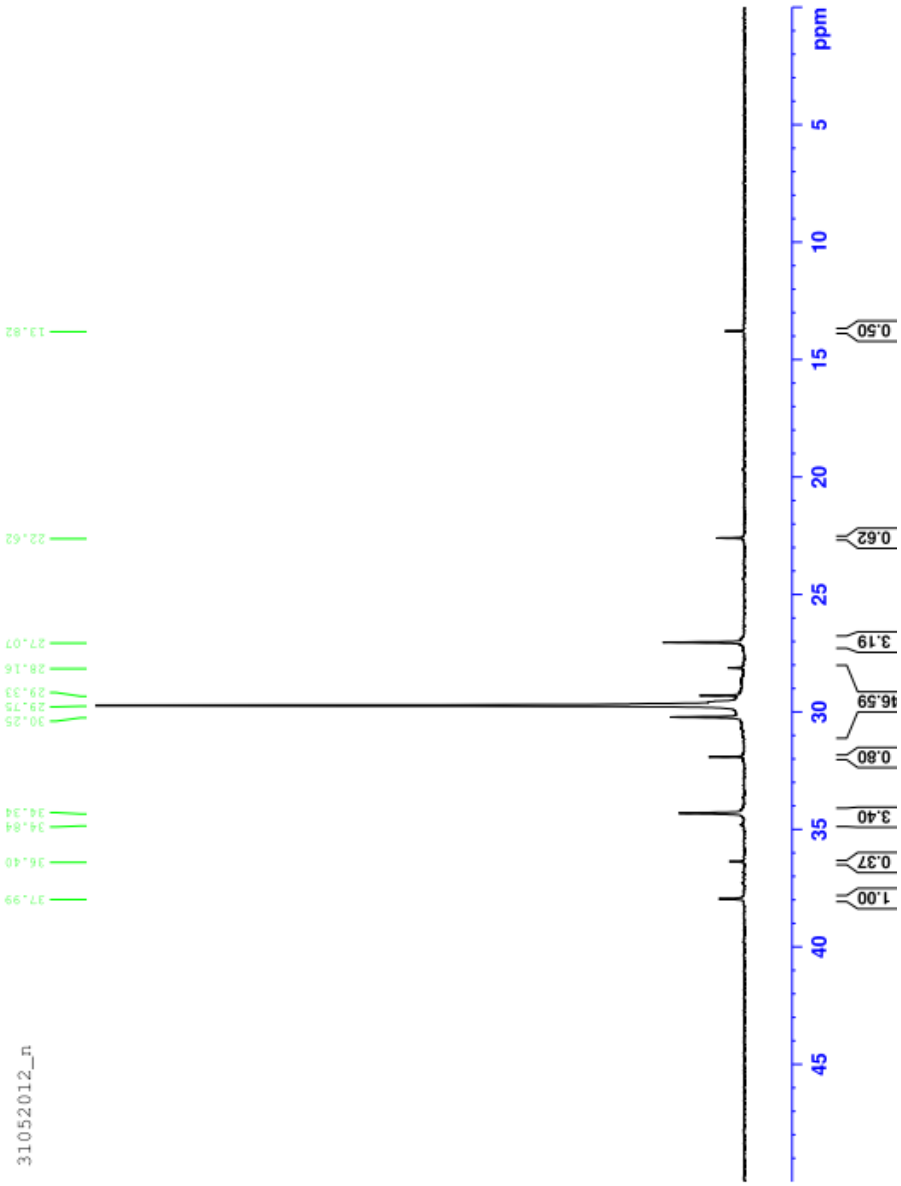

Figure B-12. ^{13}NMR spectra of ethylene/1-tetradecene copolymer at ratio 1:0.75

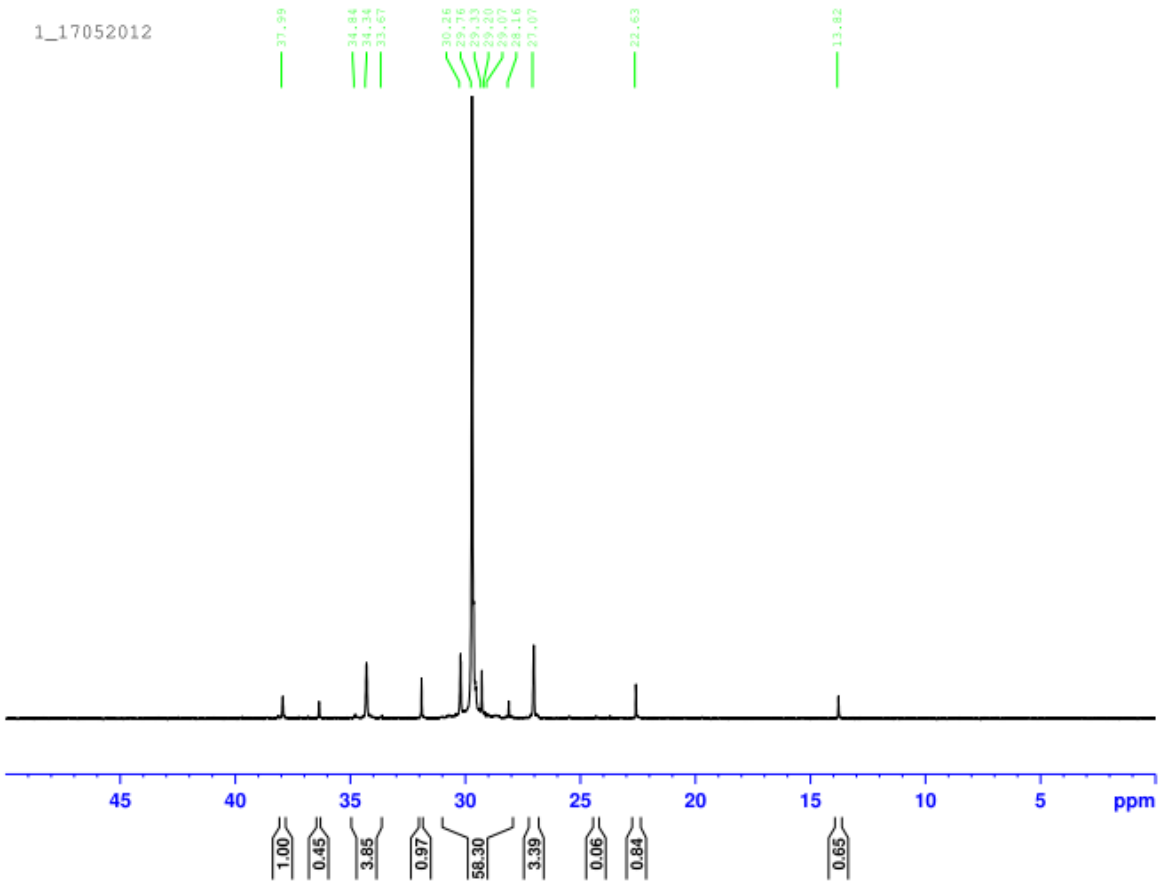

Figure B-13. ^{13}NMR spectra of ethylene/1-octraecene copolymer at ratio 1:0.25

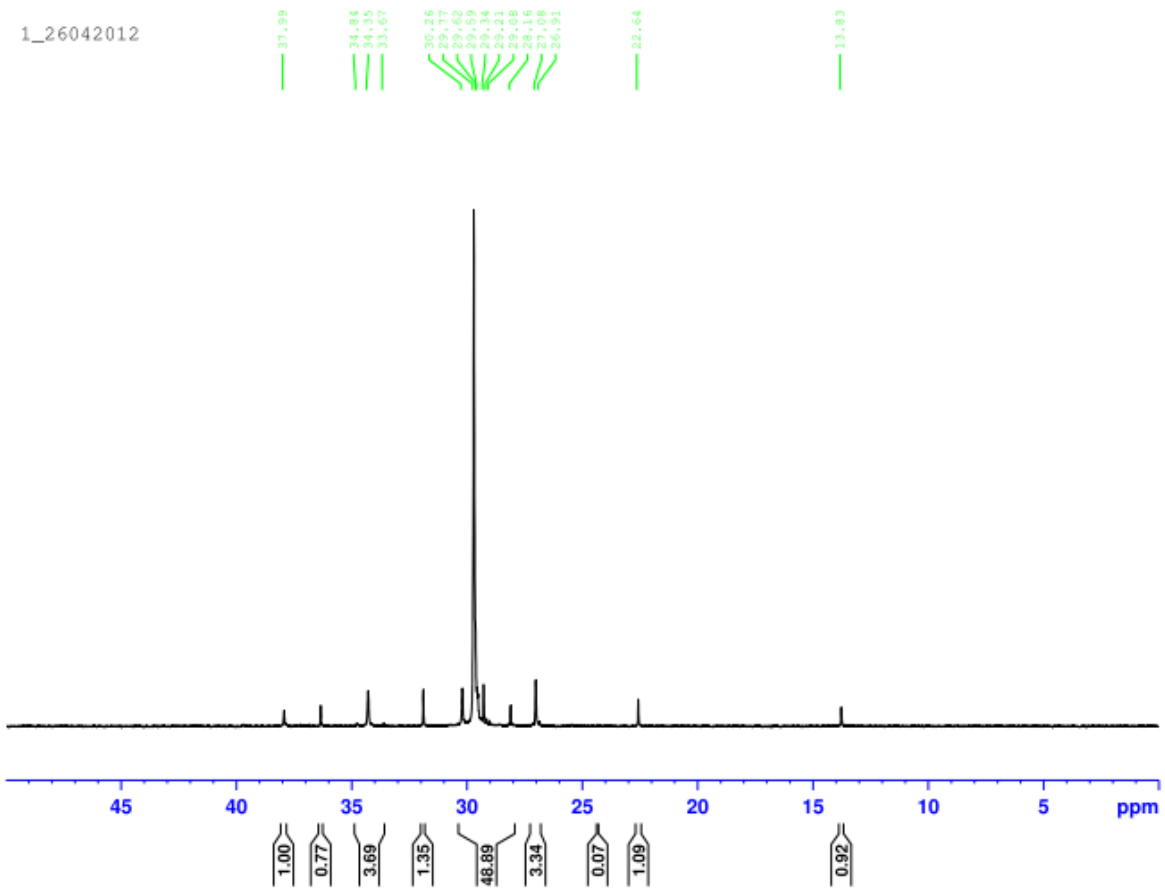

Figure B-14. ^{13}NMR spectra of ethylene/1-octraecene copolymer at ratio 1:0.50

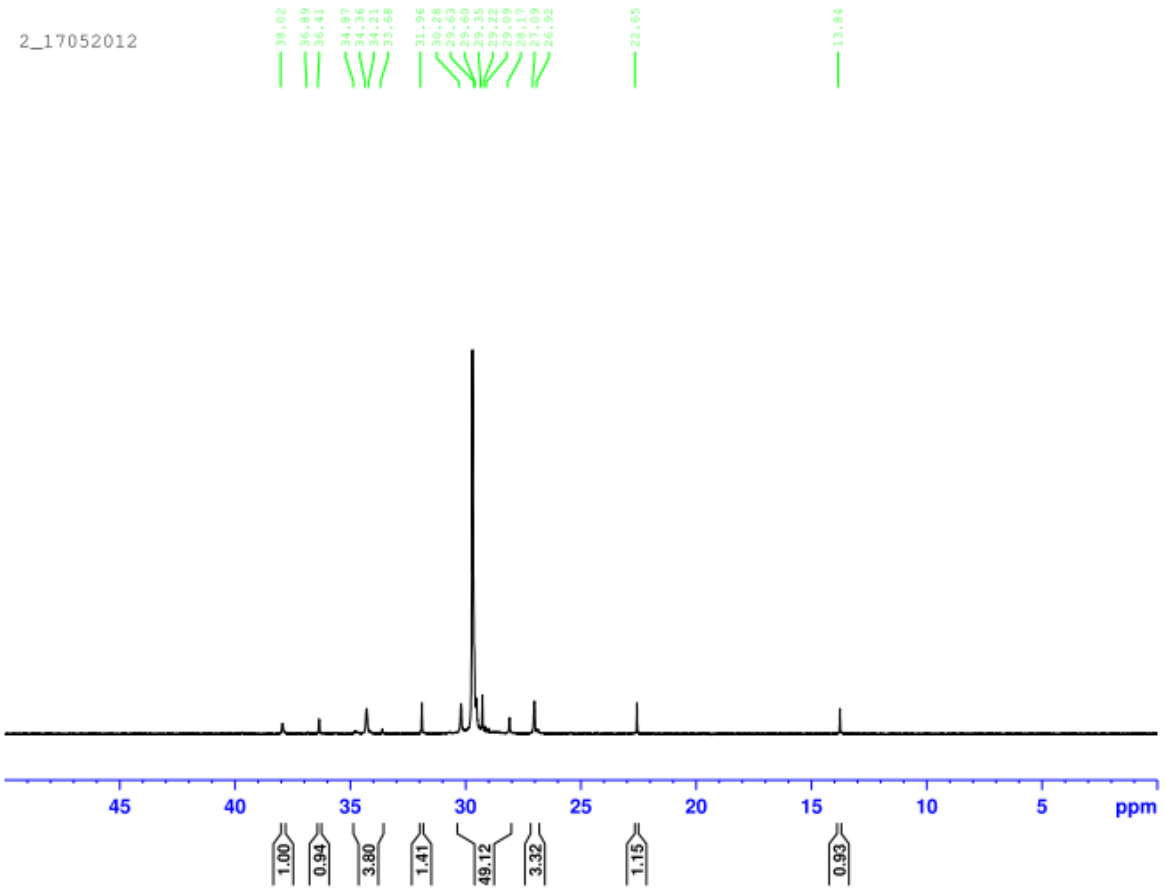

Figure B-15. ^{13}NMR spectra of ethylene/1-octraecene copolymer at ratio 1:0.75

APPENDIX C

Differential scanning calorimetry (DSC)

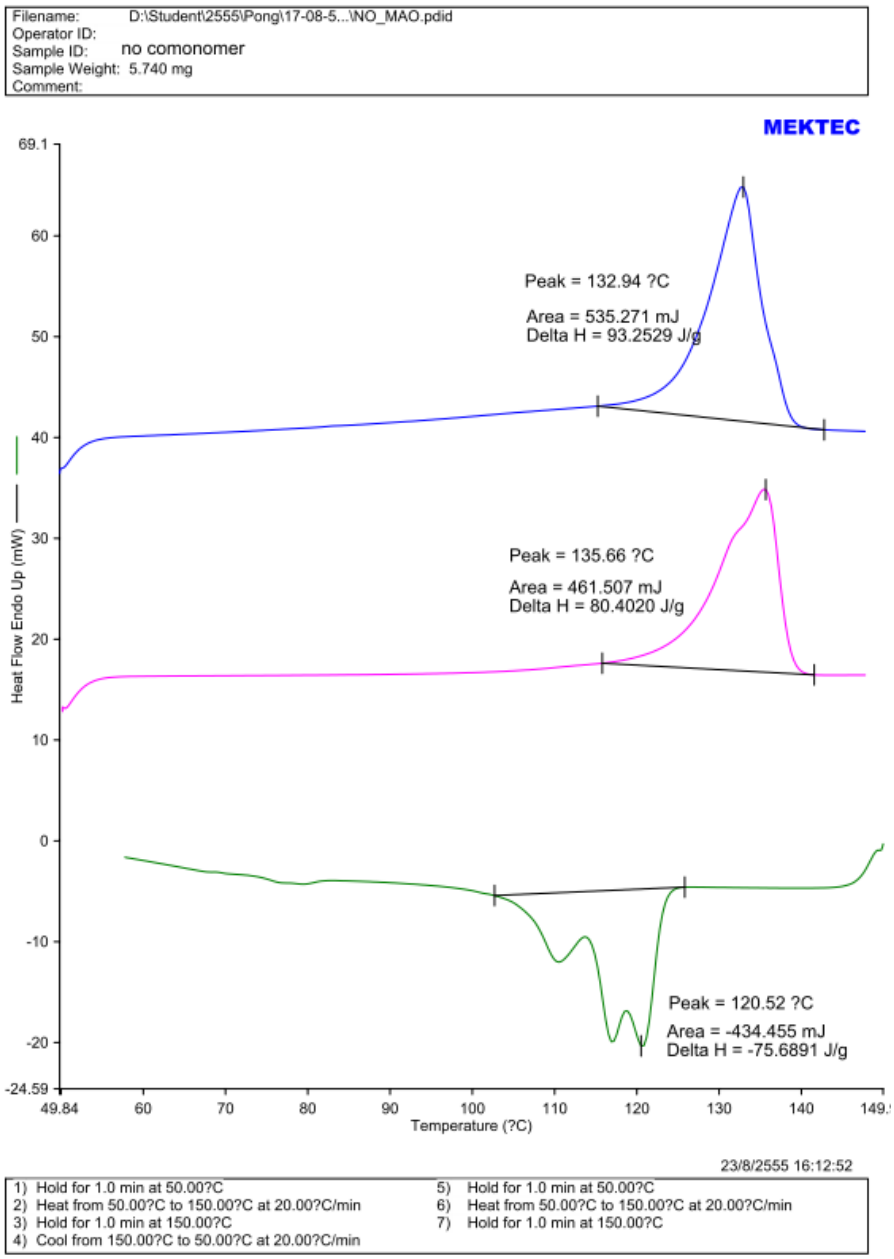

Figure C-1. DSC curve of polyethylene (no comonomer)

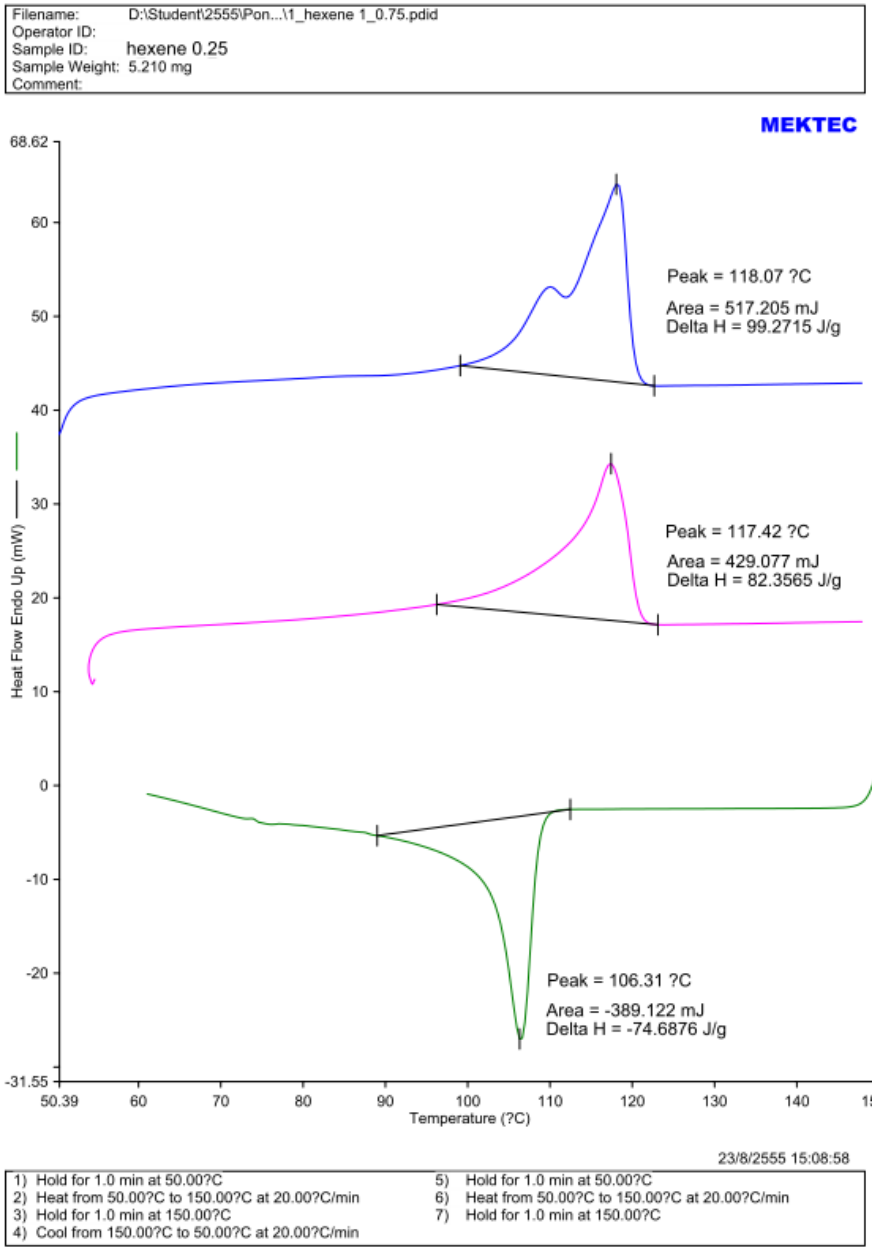

Figure C-2. DSC curve of ethylene/1-hexene copolymer at ratio 1:0.25

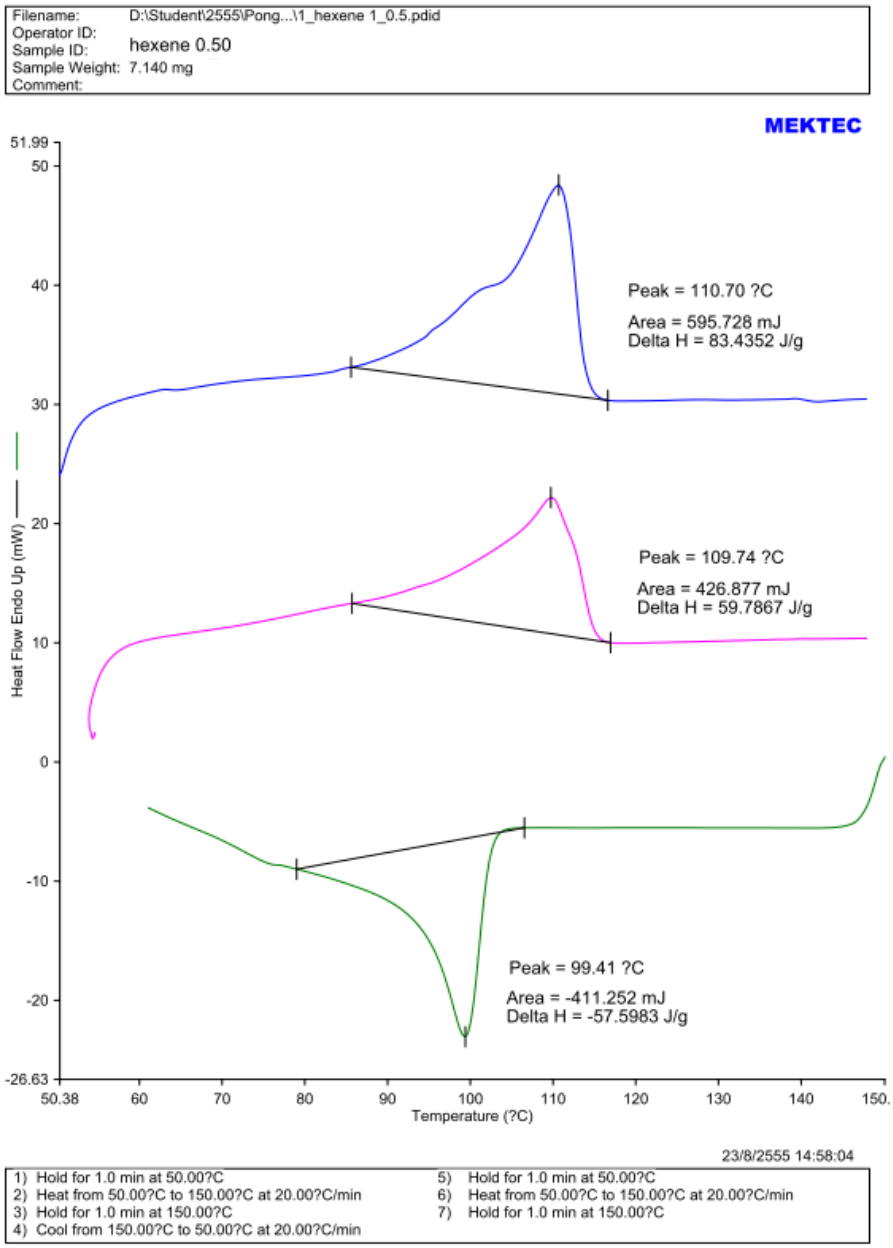

Figure C-3. DSC curve of ethylene/1-hexene copolymer at ratio 1:0.50

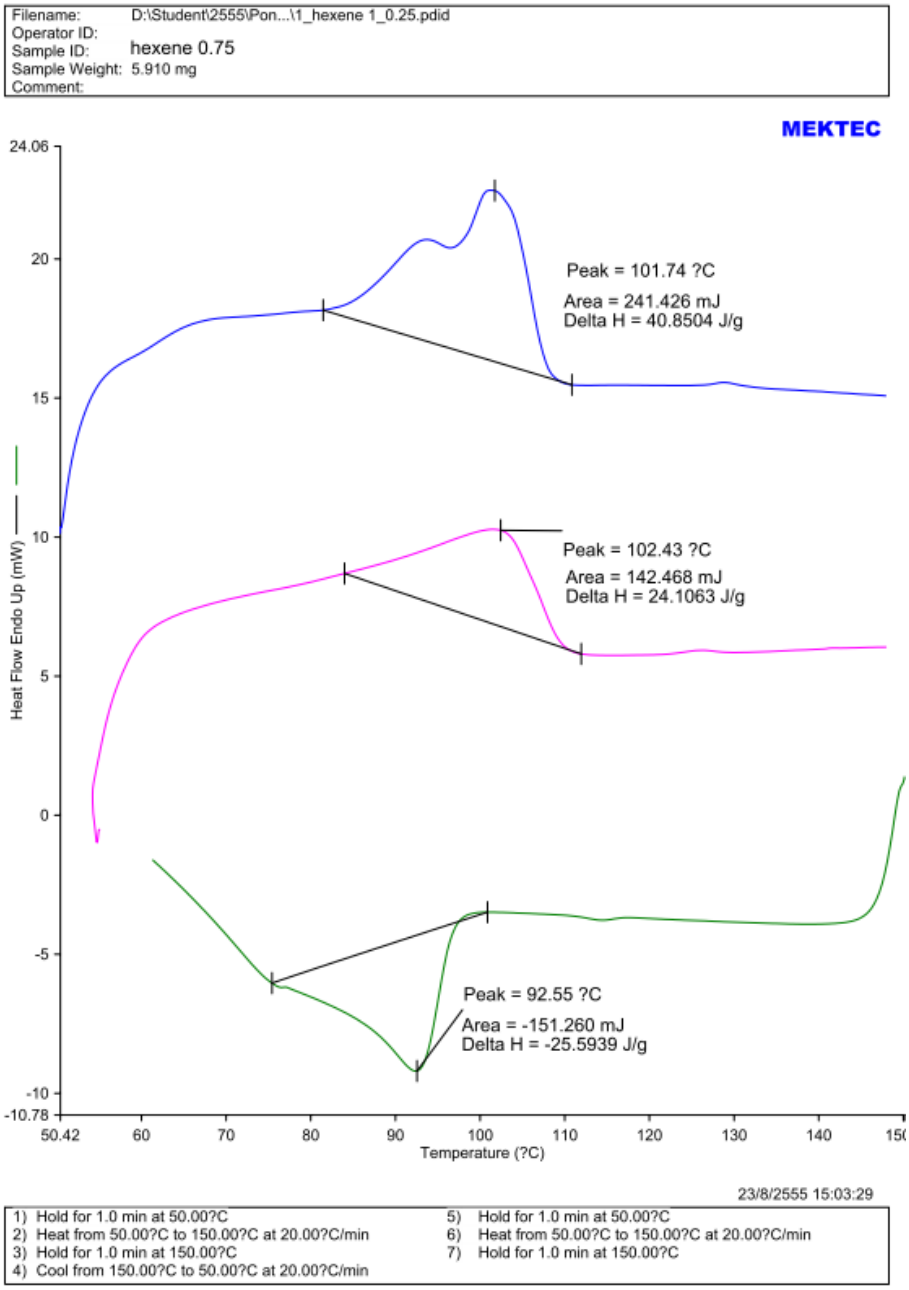

Figure C-4. DSC curve of ethylene/1-hexene copolymer at ratio 1:0.75

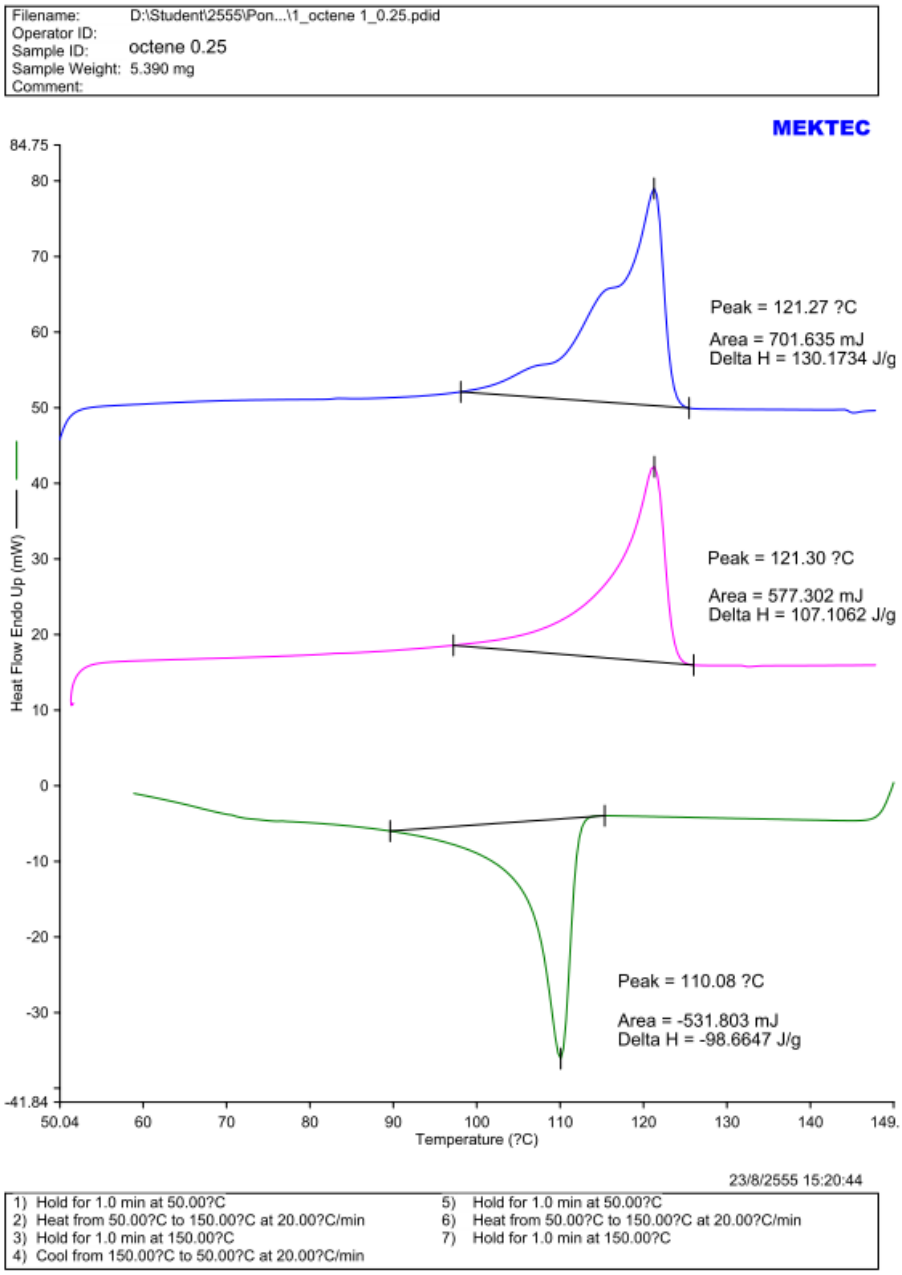

Figure C-5. DSC curve of ethylene/1-octene copolymer at ratio 1:0.25

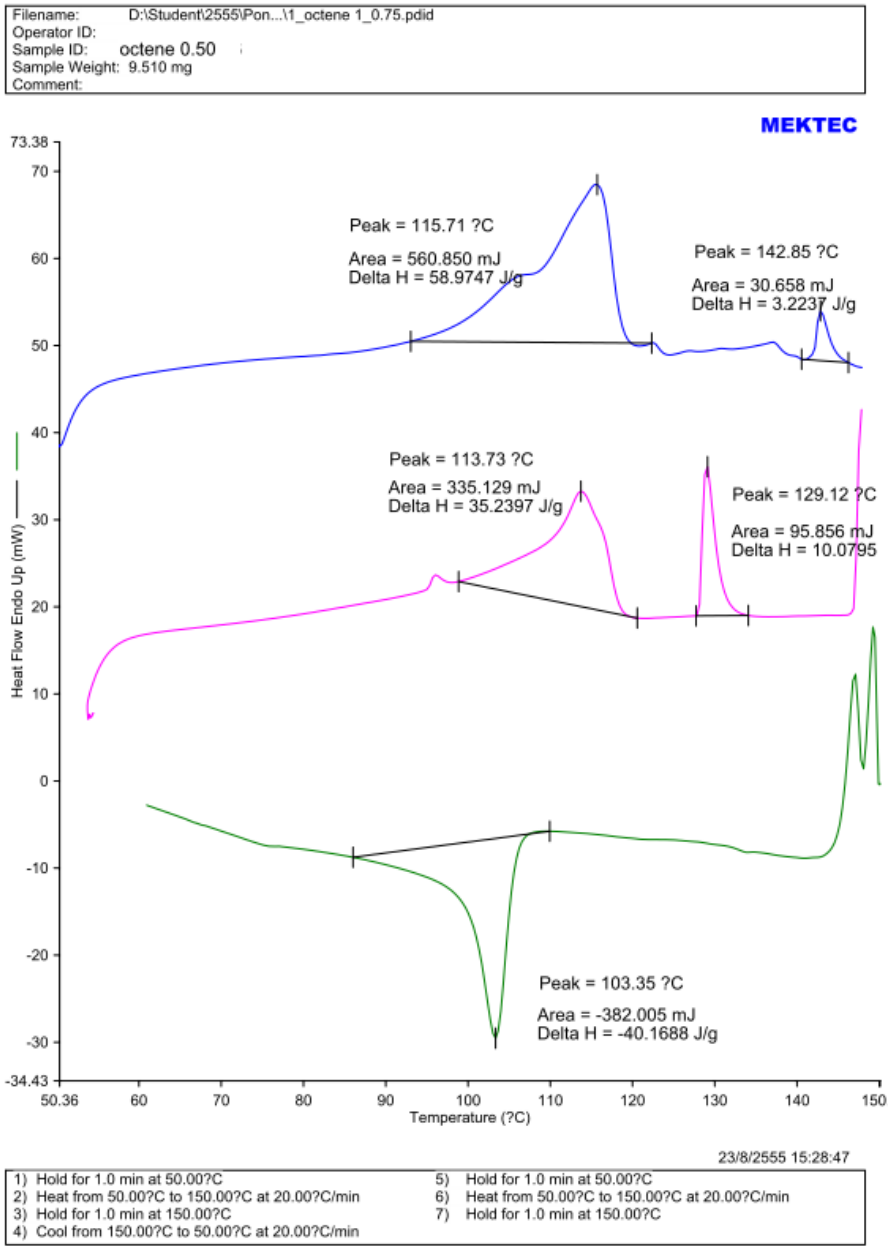

Figure C-6. DSC curve of ethylene/1-octene copolymer at ratio 1:0.50

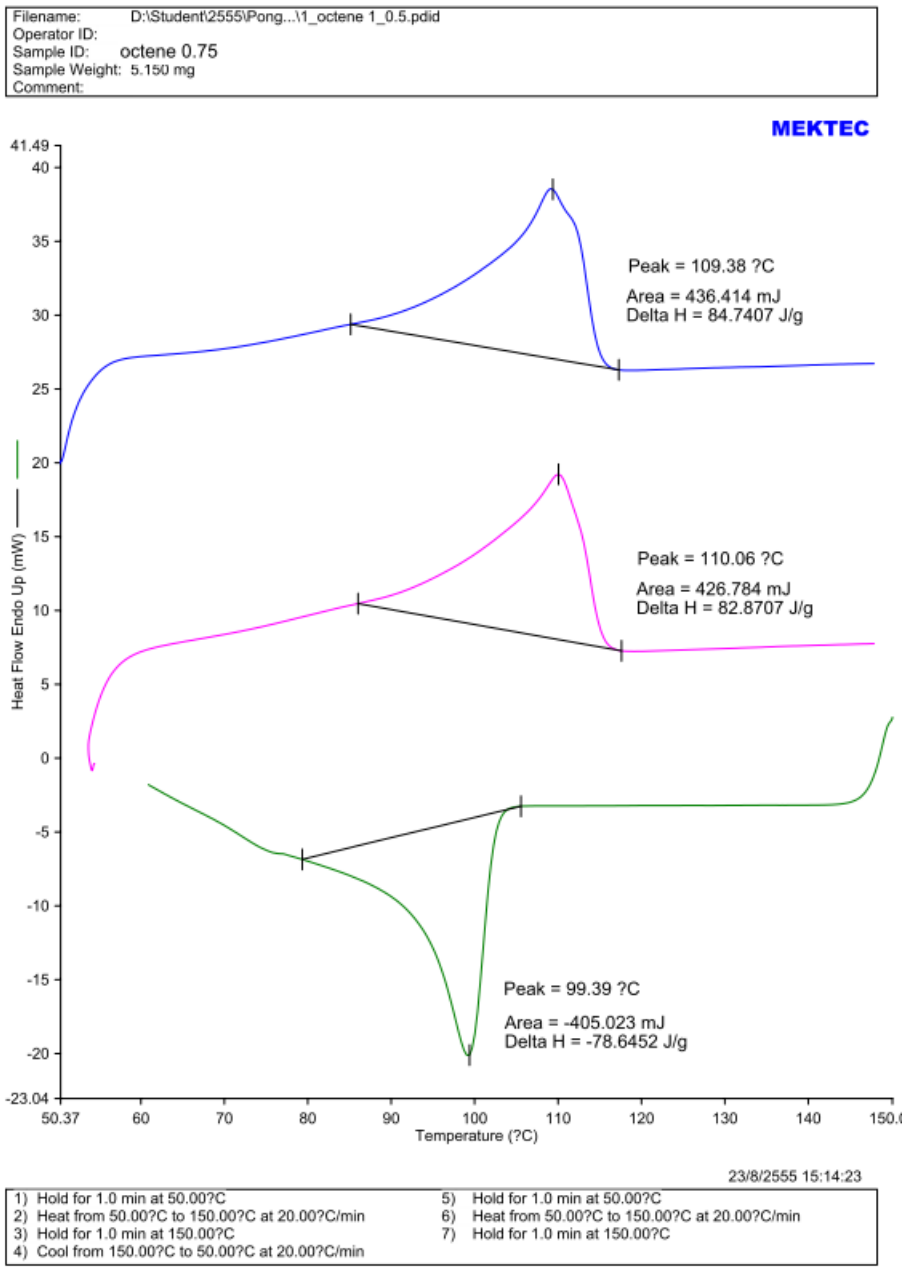

Figure C-7. DSC curve of ethylene/1-octene copolymer at ratio 1:0.75

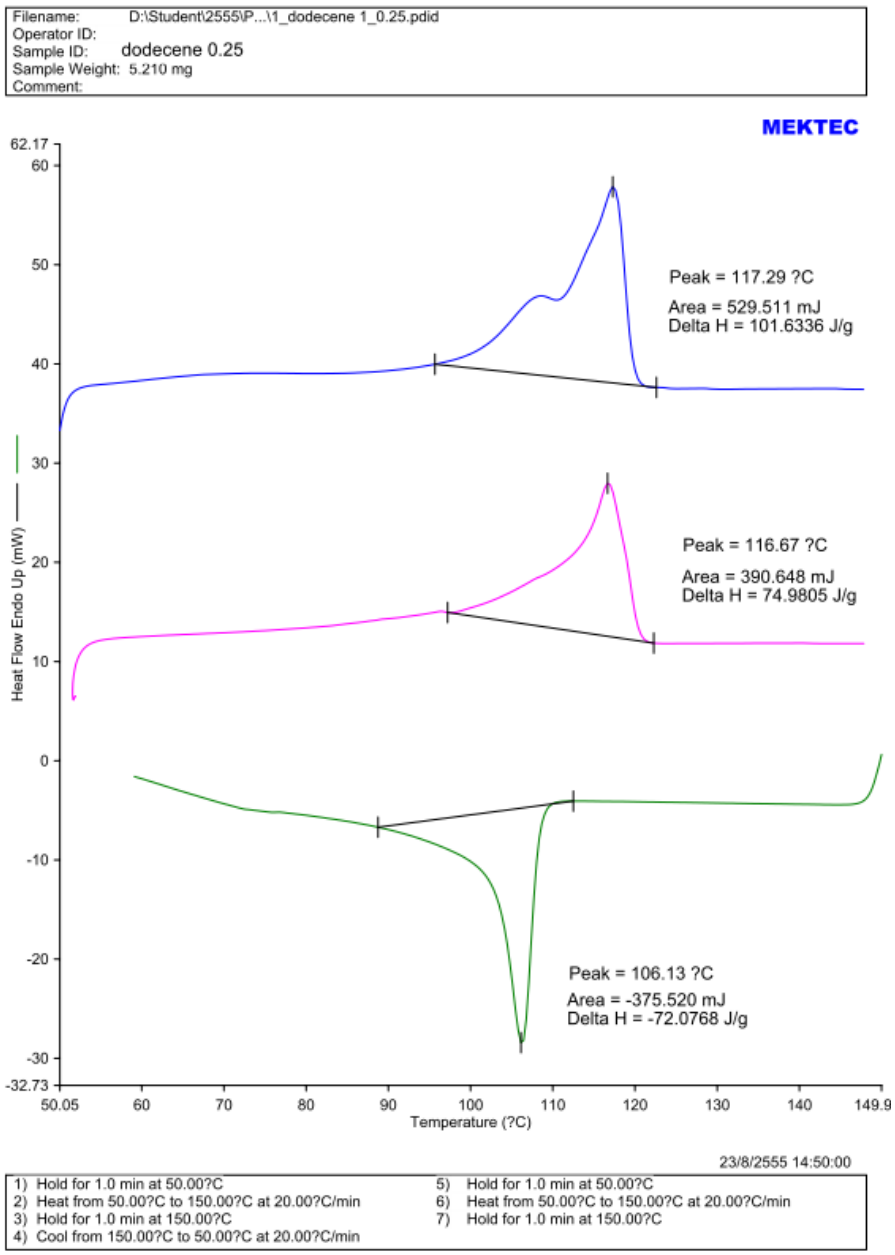

Figure C-8. DSC curve of ethylene/1-dodecene copolymer at ratio 1:0.25

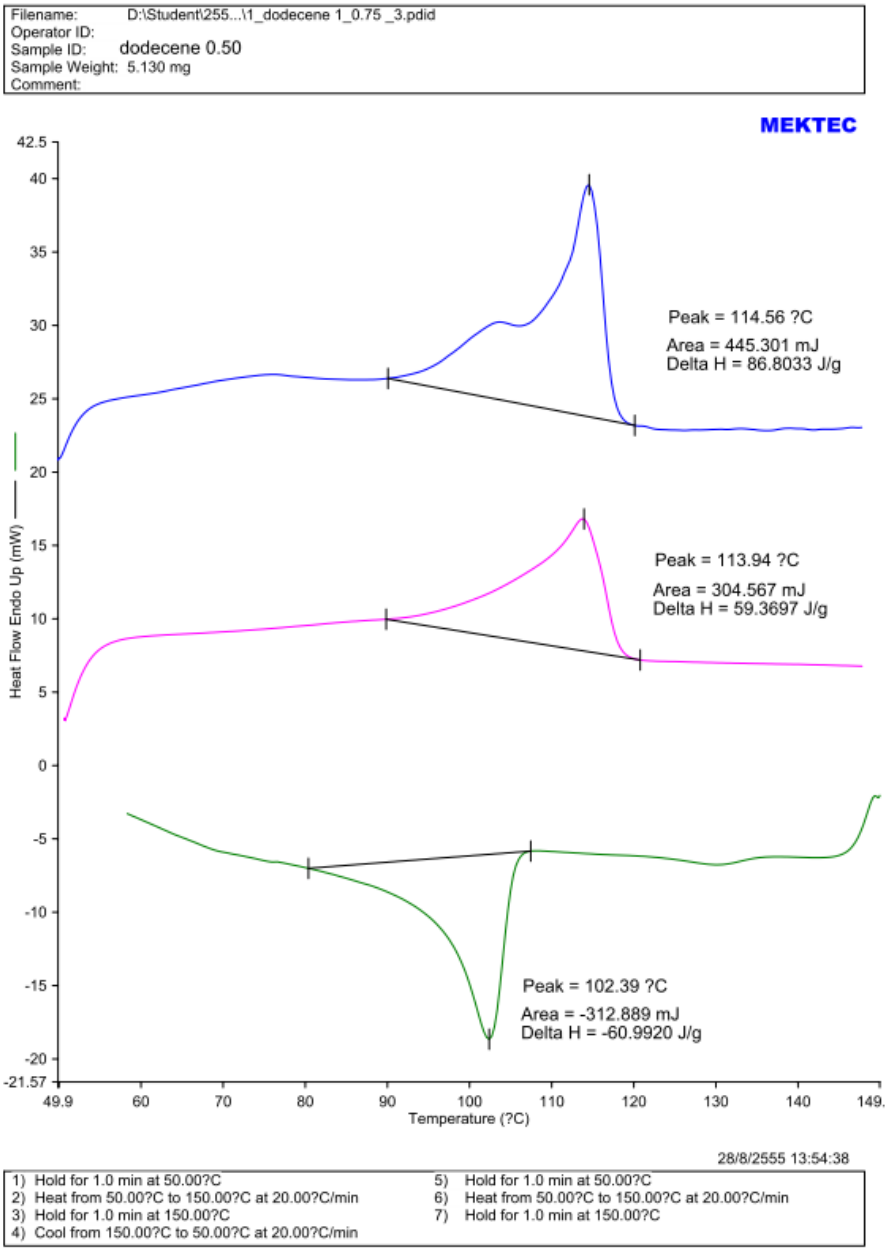

Figure C-9. DSC curve of ethylene/1-dodecene copolymer at ratio 1:0.50

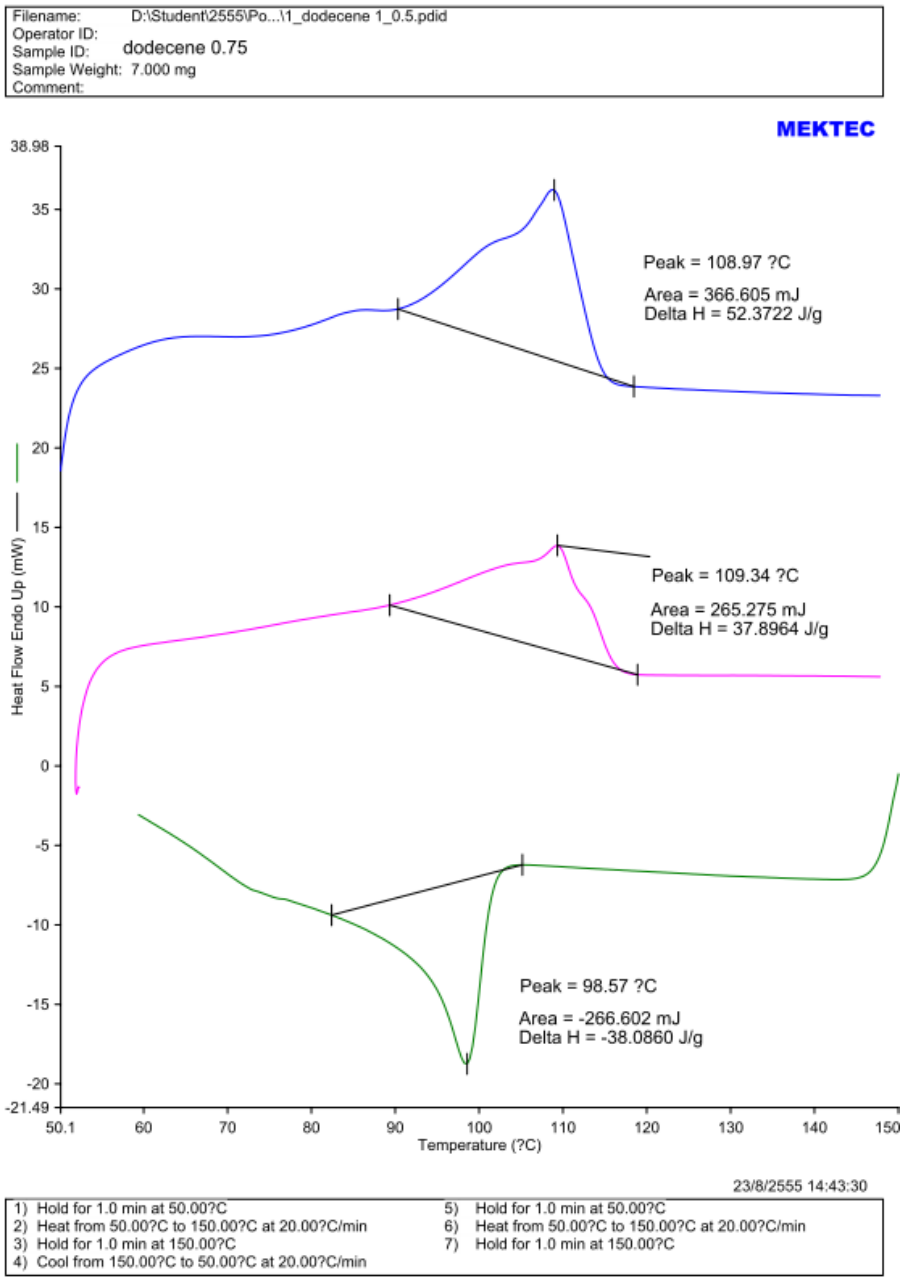

Figure C-10. DSC curve of ethylene/1-dodecene copolymer at ratio 1:0.75

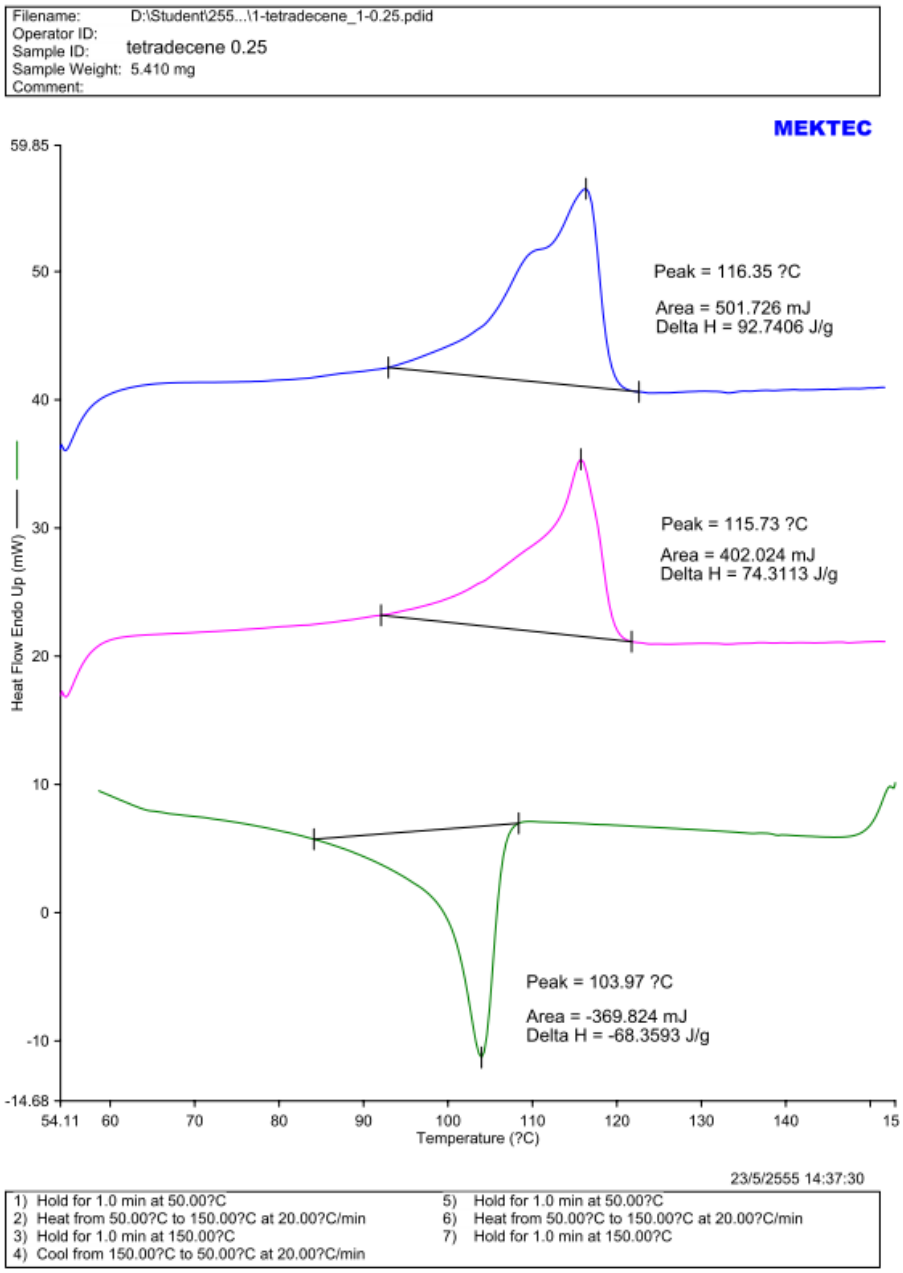

Figure C-11. DSC curve of ethylene/1-tetradecene copolymer at ratio 1:0.25

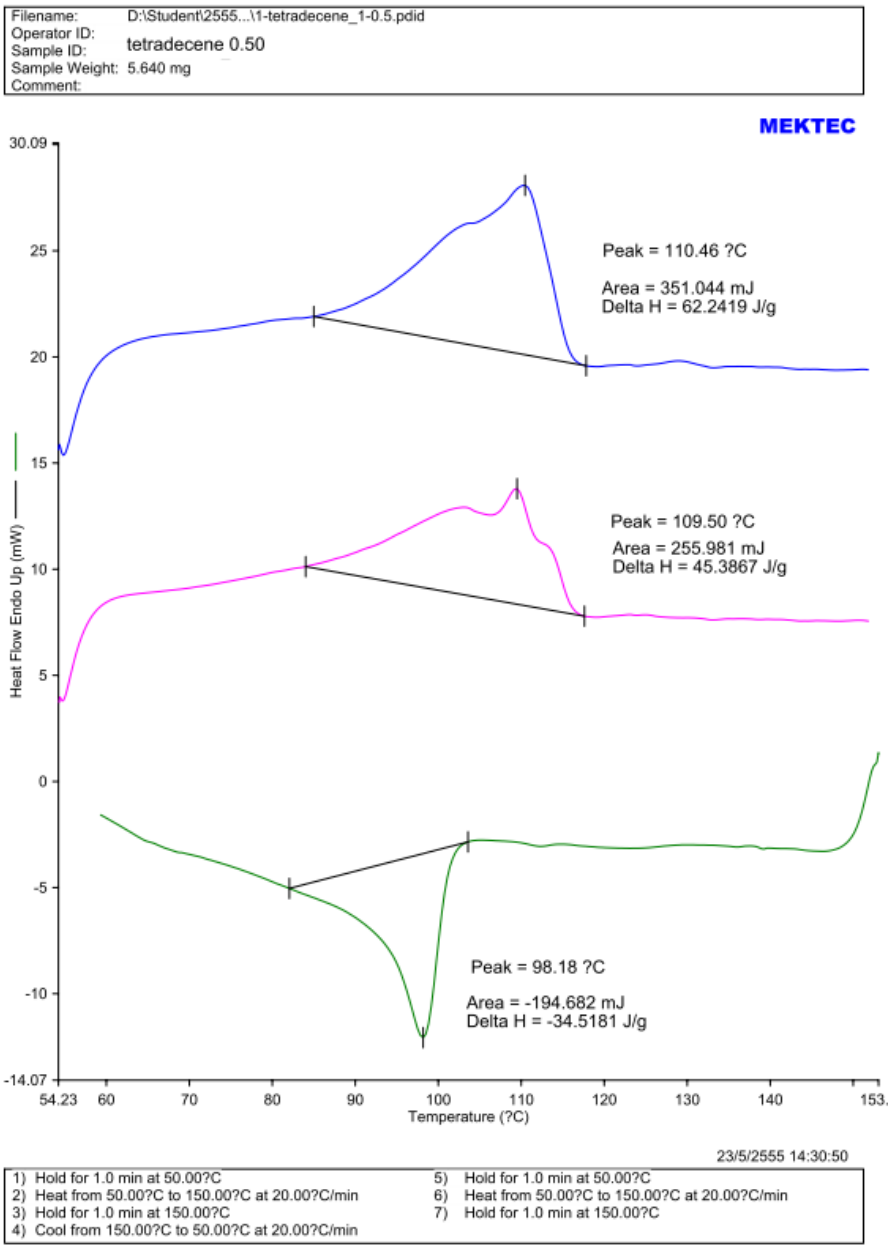

Figure C-12. DSC curve of ethylene/1-tetradecene copolymer at ratio 1:0.50

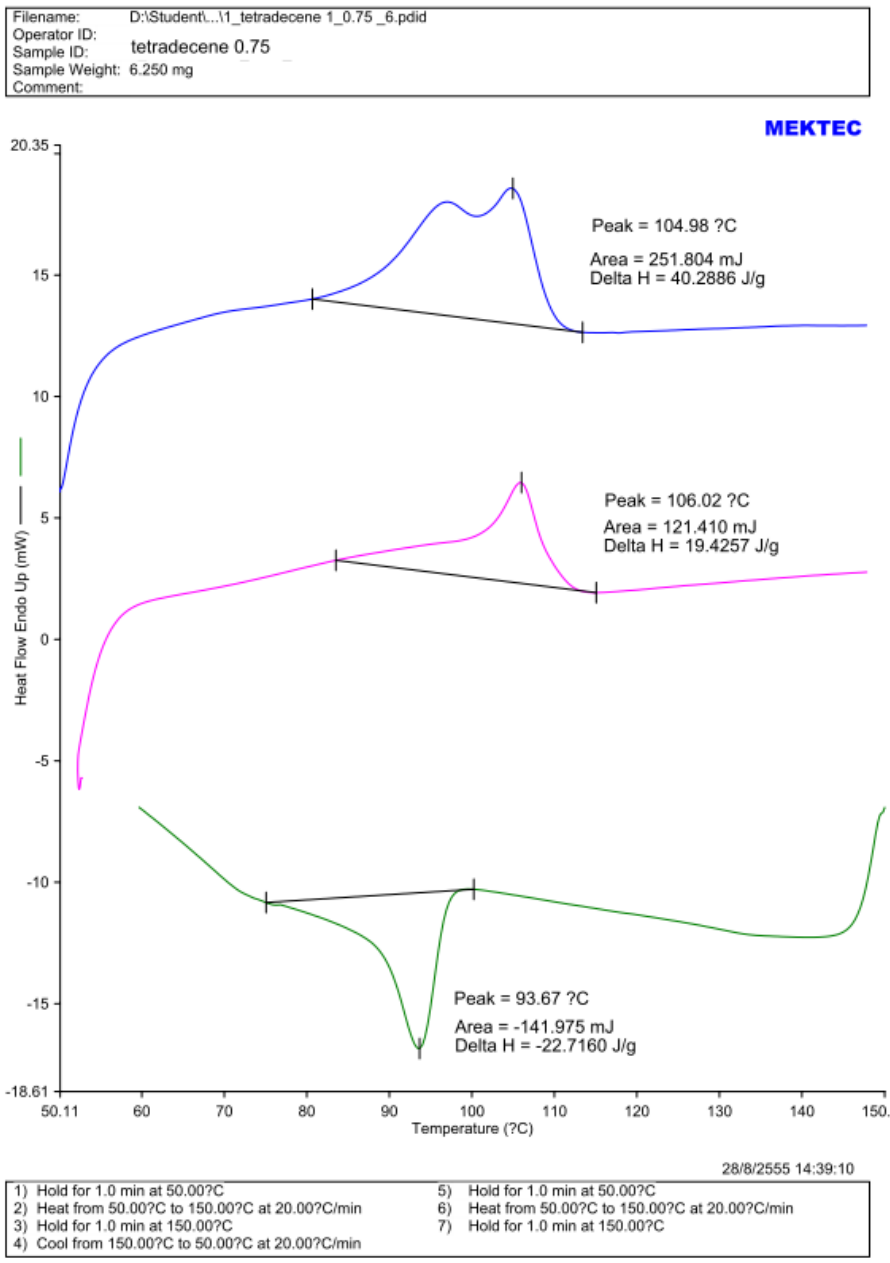

Figure C-13. DSC curve of ethylene/1-tetradecene copolymer at ratio 1:0.75

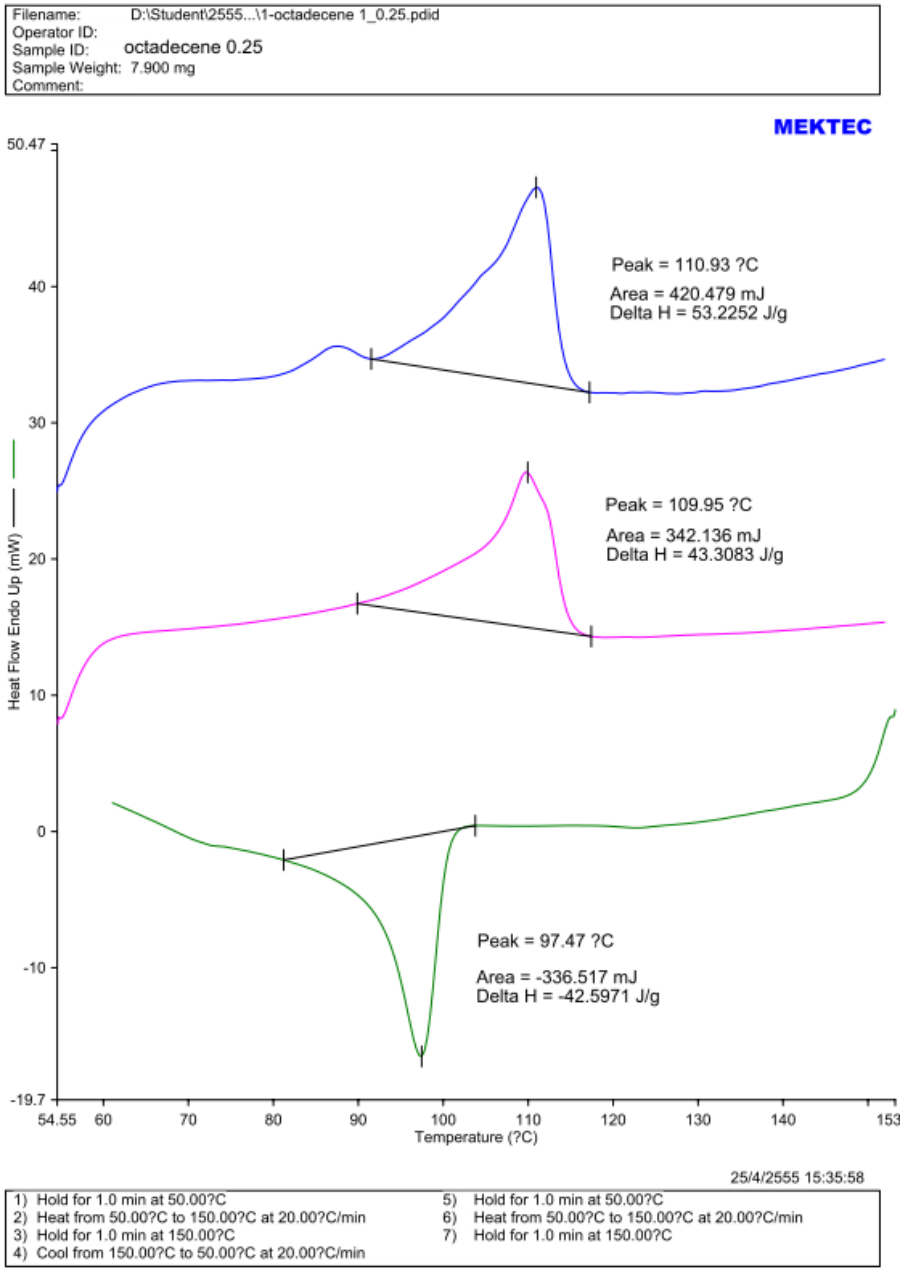

Figure C-14. DSC curve of ethylene/1-octadecene copolymer at ratio 1:0.25

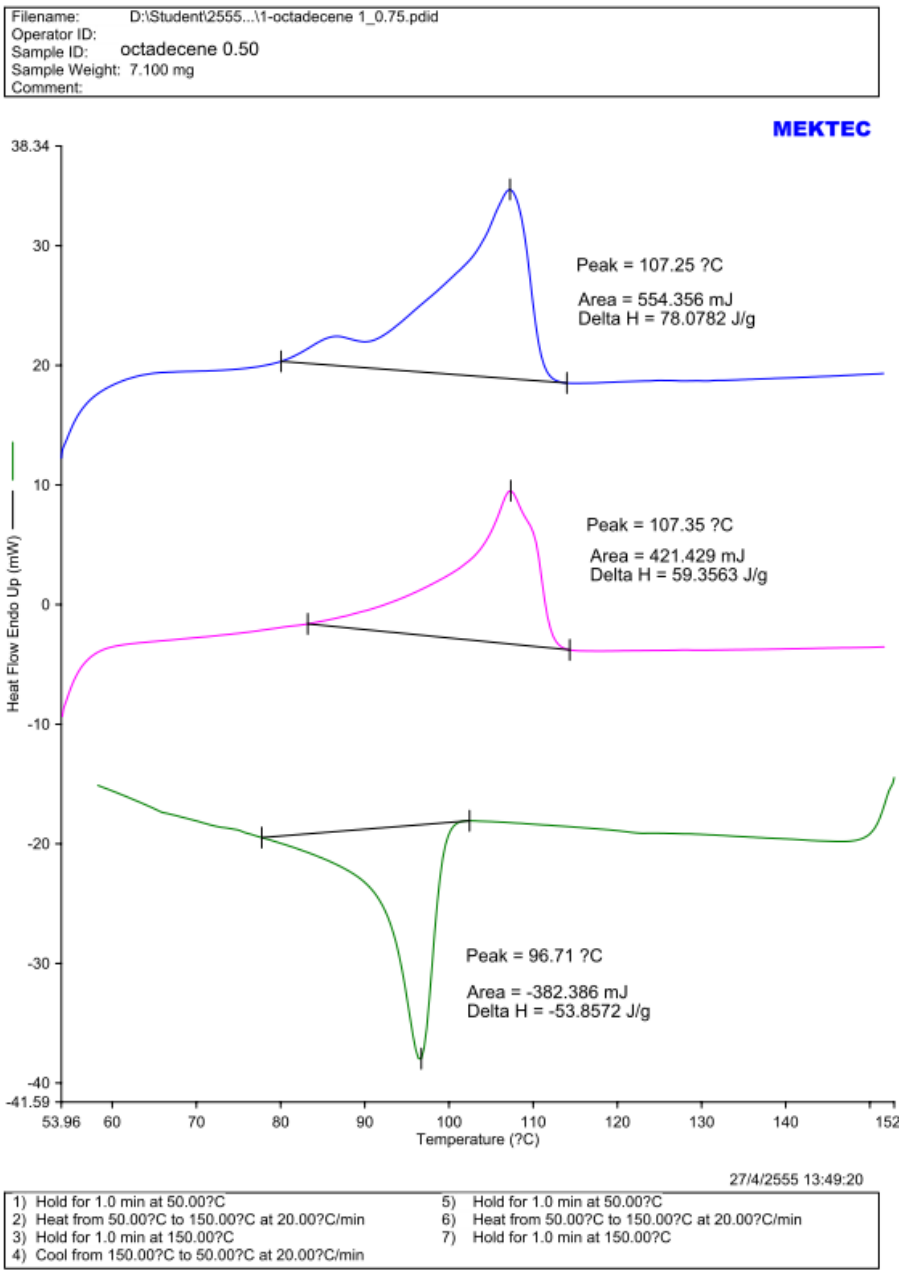

Figure C-15. DSC curve of ethylene/1-octadecene copolymer at ratio 1:0.50

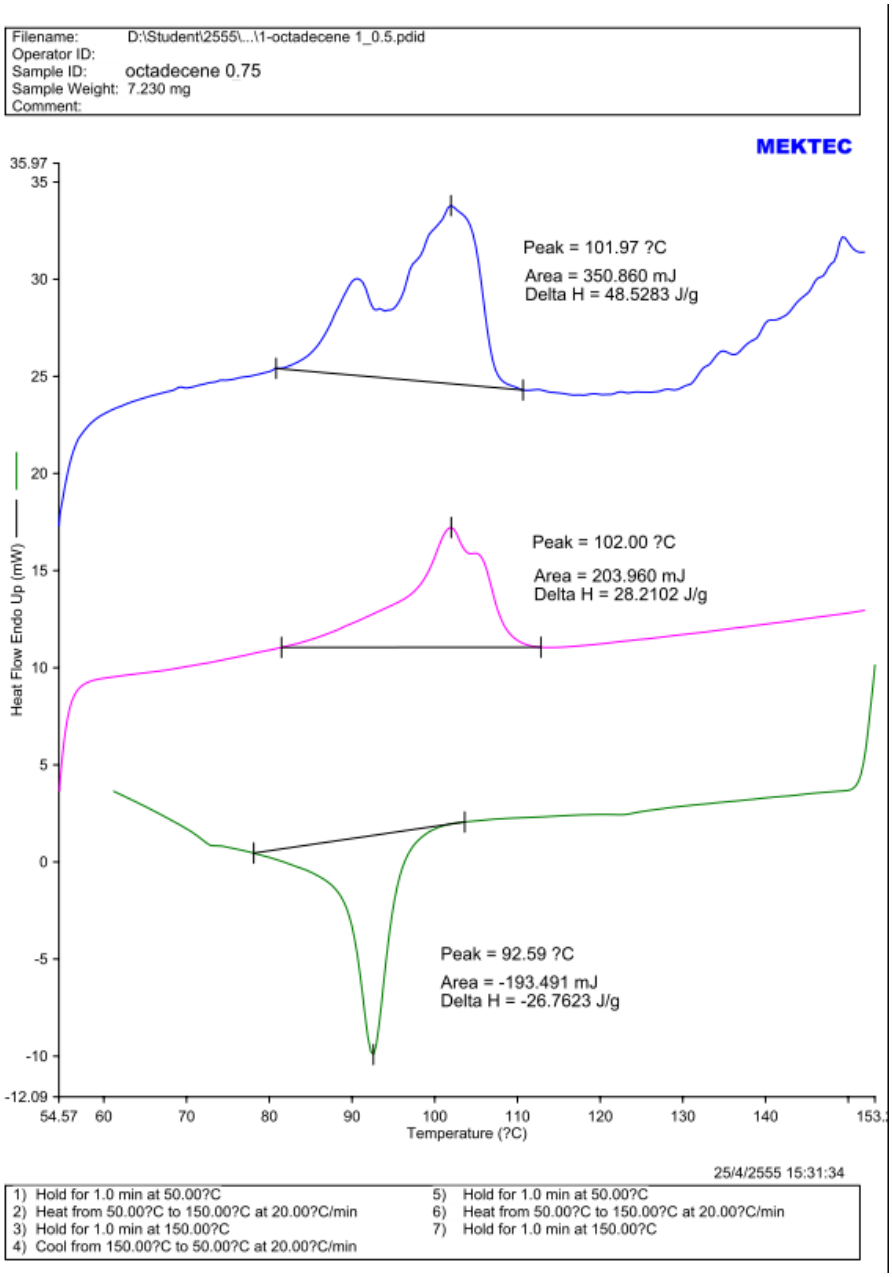

Figure C-16. DSC curve of ethylene/1-octadecene copolymer at ratio 1:0.75

APPENDIX D

Calculation of polymer properties

Calculation of polymer microstructure

Polymer microstructure and also triad distribution of monomer can be calculated according to the Galland G.B. [58] in the list of reference. The detail of calculation for ethylene/α-olefin copolymer was interpreted as follow.

1-Hexene

The integral area of ^{13}C-NMR spectrum in the specify range are listed.

T_A	=	39.5 - 42	ppm
T_B	=	38.1	ppm
T_C	=	33 - 36	ppm
T_D	=	28.5 - 31	ppm
T_E	=	26.5 – 27.5	ppm
T_F	=	24 - 25	ppm
T_G	=	23.4	ppm
T_H	=	14.1	ppm

Triad distribution was calculated as the followed formula.

k[HHH]	=	$2T_A - T_C + T_G + 2T_F + T_E$
k[EHH]	=	$2T_C - 2T_G - 4T_F - 2T_E - 2T_A$
k[EHE]	=	T_B
k[EEE]	=	$0.5T_D - 0.5T_G - 0.25T_E$
k[HEH]	=	T_F
k[HEE]	=	T_E

1-Octene, 1-Dodecene, 1-Tetradecene, and 1-Octacecene

The integral area of ^{13}C-NMR spectrum in the specify range are listed.

T_A	=	39.5 - 42	ppm
T_B	=	38.1	ppm
T_C	=	36.4	ppm
T_D	=	33 - 36	ppm
T_E	=	32.2	ppm
T_F	=	28.5 - 31	ppm
T_G	=	25.5 - 27.5	ppm
T_H	=	24 - 25	ppm
T_I	=	22 - 23	ppm
T_J	=	14 – 15	ppm

Triad distribution was calculated as the followed formula.

k[OOO]	=	$T_A - 0.5T_C$
k[EOO]	=	T_C
k[EOE]	=	T_B
k[EEE]	=	$0.5T_F - 0.25T_E - 0.25T_G$
k[OEO]	=	T_H
k[OEE]	=	$T_G - T_E$

VITAE

Mister Sompong Saetang was born in July 26th, 1988 in Suratthani, Thailand. He finished high school from Muang Suratthani School and received Bachelor's Degree in Chemical Engineering from the Faculty of Engineering, Prince of Songkla University in 2010. He subsequently completed the requirements for a Master's Degree in Chemical Engineering at the Department of Chemical Engineering, Faculty of Engineering, Chulalongkorn University in 2012.